

VLA Pointing  
Reference Pointing and the Pointing Model  
VLA Test Memorandum NO. 183

M.Kesteven

January 12, 1994

4

## 1 Introduction

The implementation of the "reference pointing mode" at the VLA has produced a significant improvement in the high-frequency imaging capability of the VLA. This note addresses some associated issues :

- a. Does reference pointing reduce the need for a good pointing model?
- b. Is a better pointing model needed? practical?
- c. Should reference pointing update the tilt rather than the collimation terms?
- d. Is second order reference pointing desirable?

I am very aware that VLA pointing is a well-trodden path, and I was anxious not to reinvent the wheel. But I felt that these two innovations - Q-band observations and reference pointing - may have altered the balance in some of the arguments.

The main points I wish to make are these:

- quality Q-band imaging will require pointing rms of  $\sim 4$  arcsecs.
- this will be hard to achieve with the current reference pointing.
- an enlarged pointing model, along with some changes to the pointing strategies will improve the prospects.
- with an enhanced pointing model, and with "over-the-top" operation disabled, it is possible to reduce the blind pointing rms from the current 5-20 arcsec range to a 5-10 arcsec range, at the quiet times.

In pursuing these questions I've had occasion to examine in detail some pointing data. Problems with specific antennas are identified.

A useful review of the VLA pointing problems can be found in Morris (1991) - Test memo. No. 182.

## 2 The Problem

Clearly, a model which predicts the antenna's pointing to high accuracy is preferable to a model with poor predictive ability. The question is the level of precision that is adequate.

Imaging at mm wavelengths is likely to involve sources which fill a sizeable fraction of the primary beam. This puts a serious constraint on the pointing tolerance: roughly, that a source component at the half-power not suffer more than 20 % (say) fluctuations because of the pointing errors. This translates to an rms of about 4 arcseconds at 43 GHz. (See Holdaway, 1990).

Reference pointing makes a great improvement; but its accuracy is predicated upon:

1. The accuracy of the previously determined collimation
2. The accuracy of the reference pointing
3. The validity range of the reference pointing

The reference pointing in effect provides a correction valid for a given azimuth, elevation, time and thermal stability. The quality of the pointing model determines the distance we can move from the reference position. Thus the quality of the model defines the range of reference sources available at any instant; it also defines how often we need to check the pointing.

4. The stability of the telescope

We can expect the antenna structure to vary with time; (for example at sunset and sunrise). This sets a further limit to the time between pointing checks.

5. Hysteresis

Antenna 7 shows clear signs of significant ( $\sim 15$  arcsec) hysteresis; a few others are suggestive. This could compromise the reference pointing since the target and reference sources are approached from different directions, and with the possibility of the sense reversing around transit.

### 3 Collimation

The collimation offset between the reference band and Q-band is defined by hardware, and might be expected to be stable. Movement of the feed towers is unlikely; furthermore, the cassegrain optics makes the pointing (collimation) fairly insensitive to movement of the tower. Incorrect rotation of the subreflector is a (remote) possibility.

A preliminary check indicated that the (X-Q) collimation does not change with elevation, but this needs to be checked more fully.

It seems therefore that, given time and patience, the collimation error could be rendered harmless.

To get an indication of the problems I examined the collimation data collected on december 10.

Table I shows a summary. For each (antenna, source) I compute the pointing differences:

RCP error = RCP(K-band) - RCP(X-band); LCP similarly. Then I compute the collimation and squints:

$$\text{collimation} = (\text{RCP} + \text{LCP}) / 2.0$$

$$\text{squint} = (\text{RCP} - \text{LCP}) / 2.0$$

Expressed this way, the squint and collimation rms should be comparable; that is, the squint rms gives a measure of the signal/noise contribution to the pointing error; the collimation rms will be larger only if other effects play a role: collimation which varies with time, azimuth or elevation; or short term pointing errors (such as wind or incorrect pointing model).

Table I shows the mean and rms for both collimation and squint for each antenna, and a summary (the average rms for each category) is given below, in Table II. The main message is that the collimation estimates are noisier than the squint - there are additional errors, but that these are small.

Table II

collimation		squint	
az rms (arcsec)	el rms (arcsec)	az rms (arcsec)	el rms (arcsec)
2.64	3.91	1.13	1.17

Obtaining collimations accurate to the sub-arcsecond level should therefore not

be a problem.

The data do raise a few interesting points, however:

In effect, these observations are a test of reference pointing in its optimum mode, with reference and target observations of the same source made within five minutes of each other. Errors in the pointing model enter only to the extent that the source coordinates (azimuth and elevation) have advanced in five minutes.

It seems that even in this mode, reference pointing is pressed to meet a 4 arcsec rms, even though these observations were made at night under calm conditions. This leaves little room to manoeuvre - every effort needs to be made to ensure that other sources of pointing error are kept to a minimum.

## 4 Reference Pointing

On November 30 we ran a check of the Q-band system as installed on antennas 4, 8 and 12. The data consisted of a number of X-Q cycles: four pointing observations at X-band, followed by about twenty minutes of Q-band pointing observations made in the reference pointing mode. The source was 3C84, observed from 21:17 to 1:42 (LST). The results are summarised in figures 1 to 3. Each figure shows, in the left hand panels the azimuth and elevation pointing errors; the right hand panels show the squint in azimuth and elevation. The X-band data are shown with a +, the Q-band with a o.

If all is well we expect to see the X-band points tracking the pointing errors (structural changes; incorrect pointing model); the Q-band data should cluster about a horizontal line, offset from zero by the collimation error. In the main that is the case, but some problems surfaced:

1. As with the collimation dataset discussed above, the squint rms is significantly less than the pointing observations, indicating the presence of additional pointing errors. We refer here to the rms within each scan.
2. A few X-band observations are wrong, and were detected as such by the on-line system and rejected from the reference position calculations. (see the data at 25.2, 26.8 and 27.2 UT). The data at 26.3 UT is incorrect, but slipped by the on-line traps, and so corrupted the following data - imposing a 10 arcsecond error. Ken Sowinski has identified this particular problem, and will strengthen the on-line checks.
3. The scan averages (at X-band) do not define a smooth curve - even allowing for the 4-5 arcsec rms within each scan. It would be interesting

to resolve the question: would we have seen this irregular curve if we had remained at X-band? Is it a consequence of switching frequencies?

4. The Q-band data ought to define a horizontal line; a saw-tooth would result if the pointing model were changing, but the long term trend should still be horizontal. The noise is too high to allow detection (or exclusion) of a saw-tooth, but there are hints that the trend is not horizontal. Further tests are recommended.

## 5 The pointing model

### 5.1 More parameters? The “n-theta” question

An alt-azimuth antenna has a basic set of 7 parameters in its model:

Description	VLA name	
Encoder zero points in azimuth and elevation	A7	E5
Collimation offset in azimuth	A6	
Gravitational sag with elevation		E3
Tilt of the azimuth axis	A1 and A2	
Non-perpendicularity of the axes	A5	

In addition, cyclic encoder errors are allowed for - that is, errors of the form  $\Delta Az = A3 * \cos(Az) + A4 * \sin(Az)$ . At the VLA these are the terms A3 and A4 (azimuth) and E3, E4 for elevation. (Since the gravitational sag is expected to have a cosine dependence, E3 is known as the “sag” term).

Experience indicates that these terms provide a fair description of the actual pointing, with RMS accuracies in the 5-20 arcsec range. This estimate comes from the pre-fit errors of the pointing runs - the histogram is shown in figure 4. Phil Hicks reports that the average rms for a pointing run (over all antennas) is about 10 arcsecs.

Earlier work (eg, Perley) had suggested that the model could be improved by the addition of the “n-theta” terms - that is, errors of the form:

$$\Delta Az = CA_n * \cos(nAz) + SA_n * \sin(nAz)$$

$$\Delta El = CE_n * \cos(nAz) + SE_n * \sin(nAz)$$

Failure to include the n-theta terms could affect the validity range of the model. For example, if the antenna had a 10 arcsec 3-theta component, then the refer-

ence source would need to be within 8 degrees of the target to maintain the 4 arcsec criterion.

I have looked for the “n-theta” signatures in the data from four recent runs. (September 11; September 29; October 30; December 1). I find a significant (and stable) “n-theta” component in about 20 antennas. The post-fit residuals, once these components are included, fall to the 5-10 arcsec range. The post-fit histograms are shown in figure 5.

Table III summarises the n-theta solutions for all antennas for the four sessions.

The n-theta terms probably relate to the azimuth bearing. As such, they could be expected to be reasonably stable - with changes indicating incipient troubles. The terms themselves are a convenient parameterisation of a complex function. While a fair improvement is obtained in the worst cases (antennas 17 and 23), it is not clear that this is the best formulation. Some effort into other formulations would be advisable.

[I have processed the data (the full set of pointing errors from each run) with my AT package. I claim no particular virtue or sophistication for this program; it is a simple package with which I am familiar, and one that I could manipulate without serious consequences elsewhere.]

## 5.2 Over-The-Top

I suspect that the structural engineers would deprecate this mode of observation, with the reversal of the gravitational distortions. There is a modest reduction in the residuals if the over-the-top data are excluded. A pointing model based entirely on “UNDER-the-top” data will provide adequate predictions for the (> 90) data, but there is a clear penalty in the residuals.

Is pointing accuracy important if the “over-the-top” sources are only phase reference sources? (It would be very imprudent to use an over-the-top source as pointing reference for a source under-the-top; it is wise to reorganize the schedule if the target is over-the-top).

About 25% of the sources observed in a pointing run are “over-the-top”.

## 6 Why do some antennas point so badly?

I have examined in detail the pre-fit and post-fit residual distributions for all antennas, concentrating on those for which the post-fit rms > 5 arcseconds (either az or el). There appear to be five categories of error:

1. Incorrect A4, E3 and/or E4

The present practice is to solve for a restricted set of parameters (tilt, collimation and encoder offsets :- A1, A2, A6, A7, E3 and E5); the remainder have not changed over the past two years. Several antennas have residual distributions which indicate that the “unsolved-for” parameters are no longer correct. Antennas 1 and 12 are perhaps the worst examples. Both have an almost linear  $\Delta E1$  vs  $E1$  dependence. A judicious combination of E3, E4 and E5 makes serious inroads into this error. See figure 6.

Both antennas also show a  $\Delta Az$  vs  $E1$  dependence; A5 (non-orthogonality of the axes) helps.

As both antennas have shown the same distribution of pre-fit residuals for the past four months, it is perhaps time for a grand re-evaluation of all the pointing terms.

2. Non-tilt  $\Delta E1$  vs  $Az$

In several antennas (#3, 6, 7, 15) we find a  $\Delta E1$  component of the form

$$\Delta E1 = E_1 \cos(Az) + E_2 \sin(Az)$$

The software expects such a dependence, but assigns it to tilt, and further expects a matching azimuth distribution. In these particular antennas the matching azimuth distribution is missing; the least squares algorithm can only reduce the elevation errors at the cost of increasing the azimuth errors. See figure 7.

Since the on-line software in fact allows for the possibility of splitting these 1-theta terms (A1 and A2 for azimuth, E1 and E2 for elevation), this complication could be resolved.

3. n-theta Components

In a number of antennas, but most noticeably in #17 and #23, both  $\Delta E1$  and  $\Delta Az$  vary with azimuth; enhancing the pointing model with a suitable set of n-theta components significantly improves the rms.

4. Hysteresis in Elevation

This is discussed in detail below. It is certainly present in antenna 7; it is likely in several others.

5. Real-time deterioration of the azimuth bearing

Antenna 9 appears to have suffered some mechanical trauma in October: we see an abrupt change in the tilt, 1-Az and 3-Az components. The problem is not due to a reconfiguration move: antenna 9 has been at pad W8 for the past five years.

An alternative explanation might be that the pad has shifted.

## 7 Hysteresis

This is clearly present in antenna 7. Figure 7 shows the post-fit residuals from the 1 December run. In the left hand panels the two symbols show:

open circle - the previous source was at a lower elevation.

filled circle - the previous source was at a higher elevation.

It is clear that the elevation residuals (top left) separate into two groups, with a separation of about 15 arcsec between the two means.

The right hand panels investigate the azimuth hysteresis.

Table IV summarises the hysteresis data for all antennas over the four sessions. Antenna 7 is the only unambiguous case; but the distribution of the errors over the entire array, for the last three observing runs is not random - it is possible that hysteresis at the 3 arcsec level is present in most antennas. (The 11 September run was made at dawn which lead to significantly higher elevation residuals).

A quick check on earlier pointing runs suggests that antenna 7's hysteresis has been present at the 15 arcsec level at least since april, 1992.

The hysteresis looks to depend on the direction of the drive, not its magnitude, provided the drive exceeds a threshold of about 10 degrees.

There is no evidence of hysteresis in azimuth (that is, neither  $\Delta El$  nor  $\Delta Az$  show hysteresis after drives in Az).

I don't imagine that the on-line system should concern itself with hysteresis. Other than to ensure that the worst antennas are not selected for Q-band operation, it is probably simply a fact of life. For high-dynamic imaging at K-band an observing strategy could be devised to minimize its impact.

## 8 Transient array-wide tilts

For each pointing run there is a specific tilt error which is common to all antennas. Figure 10 shows the scatter plots of the derived tilt parameters (A1,A2) for a number of pointing runs. In essentially every case the centroid is significantly offset from zero.

1. This test is not as clear cut as it could be since the plots also include the changes in the on-line A1,A2 values. I think the conclusions below are unchanged.



2. The effect is fairly stable on the time scale of an observing run (4 hours), but not stable over a month - compare the sequence 30 October, 14 November and 1 December.

I find it hard to imagine a physical mechanism for this effect, but since all the antennas show the same tilt the cause ought to be findable, and therefore correctable. This also may bear on the reference pointing strategy, discussed in section 10.4

3. It is possible that the effect is an artifact of the analysis, since the azimuth and time are tightly correlated. It might be wise to revise the source selection procedure in order to randomize the azimuth sequence. The importance of this is that it distinguishes between a stable environment during the run (ie, it really is a tilt) from one which is evolving during the run (ie, the azimuth and elevation are changing so as to mimic a tilt).
4. Following the philosophy that the pointing model should reflect, as far as possible, the stable antenna, relying on reference pointing to look after the transient problems, I suggest that the tilt common to all antennas be removed from the data prior to the analysis.
5. Pursuing further the question of correlation in the residuals over the entire array, I show in Figure 11 a typical example of the problem. The figure shows antenna 4 pre-fit data, plotted against the array mean. That is, for each source I calculate the mean residual, to be plotted against antenna 4's residuals, source by source. All antennas show a similar high correlation. Note also in figure 11 that the rapid excursion in elevation near 8:12 (UT) is present in the average:- they indicate that a fast response time is possible. An examination of the weather conditions at the time shows wind speeds (average) around 4 m/s, with peaks around 9 m/s at 8:12 (UT).

## 9 Second Order Reference Pointing

Suppose you wanted to make a high-dynamic range image at Q-band, and you had available a strong Q-band reference source. You might consider doing reference pointing at Q-band. The problem, however, is that the *ab initio* pointing may not be good enough for the pointing algorithm, operating at Q-band. (If, for example, the pointing error were 20 arcsecs or larger). Under these circumstances you might wish to reference point at X-band to get a good handle on the pointing errors, then using those results as a basis, refine the pointing at Q-band. This is the "second order reference pointing".

The current implementation does not permit this mode of operation, as there are a number of messy housekeeping problems to resolve.

The case for second order reference pointing is not strong: the situation described above is probably rare. It is desirable for holography.

## 10 Operational Considerations

### 10.1 Pointing Data

A number of pointing runs are disappointing in that the post-fit residuals are consistently higher than average, which suggests that the antennas were changing, adjusting to a new thermal environment, for example. The 11 September is one such case, as the observations extended over sunrise with a significant temperature gradient in the second half of the run. In these runs there is a pronounced correlation between the individual antenna's residuals and the array average.

Perhaps a more brutal editing is in order, allowing entire pointing runs to be discarded.

### 10.2 Treatment of long-term stable parameters

I suggest that more use could be made of the historical record. Some parameters such as inter-band collimation could be expected never to change, at least until the antenna is refurbished in the barn. Therefore the many collimation observations could be viewed as independent samples of the same item, and the data should be pooled. The main emphasis of the observations would become one of diagnosis - confirming that nothing has changed. If a change really has happened, it likely indicates a problem.

### 10.3 Is the current method of updating the pointing models optimum?

At present the operations group run pointing checks about once a month. The new pointing model for each antenna is then compared to the previous one, and where parameters differ significantly, they are replaced with the new value.

One might argue that as long as the antenna has remained at the same pad, the same model should apply. Put otherwise, one day's measurements are perhaps as likely as any other. The evidence tends to support this view: over the past

four months (for which data was readily accessible) the parameters appear to wander about a common value .. the pointing checks look more like tracking noise than any consistent trend. (In many cases a change after one session is followed by its negative the following session. Table V which summarises the A1-7 and E3-5 terms for the past 5 months shows several examples of this. This argument becomes stronger once the suspect observing sessions are identified: for example, after the 14 November run the tilt terms (A1,A2) were changed in 10 antennas by 0.2 arcmin, with the change reversed after the 1 December run).

Thus one might argue that an averaging, rather than a replacement might be a more suitable strategy.

Some time ago Barry Clark outlined a scheme along these lines; it would further separate the station-specific parameters from the antenna-specific parameters. Perhaps some variant of that scheme should be reconsidered. Once the predictable sources of change have been isolated, thresholds can be set to provide warnings when unexpected changes occur.

Barry's scheme slowly retired earlier observations unless a discontinuity occurred, at which point some block retirements took place. Given the prospect of antenna-pad specific components, (since the antennas are not all identical), it may be wise to confine all the parameters to a given configuration.

#### 10.4 Is the reference pointing strategy optimum?

The philosophy here is quite different. One can imagine that there is an underlying pointing model which is constant, with a smaller subset of parameters which change in time. The comment has been made that it is the tilt which is the real culprit.

Thus the question is whether the strategy of changing the collimation<sup>1</sup> terms is the optimum. (As opposed to having the virtue of simplicity). Some alternatives:

- a. At times of rapid temperature changes (eg, sunset and sunrise), one might bias the solution towards an axis shift, switching to collimation at other times.
- b. A background process might examine the last four or five reference pointings to determine if an axis tilt is more suitable than a simple collimation.

Some variant of these schemes would provide an additional check on rogue measurements.

Clearly any scheme, including the current version, must provide the astronomer

---

<sup>1</sup>These are the A6 and E5 terms of the pointing model, not the inter-band collimation

with a clear indication of what has been applied. The astronomer would also have to be provided with the option of some control if an intelligent scheme were activated. (This likely introduces enough complexity to kill the scheme).

An examination of six months or so of reference pointing data would be a useful start at addressing this question - I understand that Ken Sowinski is planning to log for posterity all reference pointing observations.

## 10.5 Recommendations

I believe that at present there is a requirement for an enhanced set of software tools for the operations group. They are currently doing an excellent job, but their task would be easier with a more powerful set of diagnostic and graphical tools.

Plots of residuals as a function of azimuth, elevation and time, triggered when the post-fit rms exceeds a threshold is desirable, as is the ability to retrieve and display past trends in in any selected parameter.

## 11 Summary and Conclusions

1. Reference pointing by itself may not provide the precision required for high-dynamic range imaging at Q-band.
2. An enlarged pointing model and a revised pointing strategy will provide some help.
3. With several years' worth of data available (1991-1993), it would be useful to re-evaluate the pointing model parameters - especially those that are excluded from the least squares solution.
4. Brutal discarding of unsatisfactory pointing runs - if the antennas are deforming during the observations, the data is useless, and should be thrown out. The problem is identifying the bad apples.
5. The origin of the array-wide transient tilts should be traced.
6. An investigation into the notoriously bad antennas (eg, antenna 7, with hysteresis; antenna 17, with large rapid azimuth-dependent errors) may provide insight into the mechanical problems which corrupt the pointing.
7. The diagnostic value of the pointing data should not be overlooked: something is wrong when the errors increase.

## Figure Captions

- figs. 1-3 The left hand panels show the azimuth and elevation residuals from the (X-Q) reference pointing experiment.  
(+) : X-band; (o) : Q-band in reference pointing mode.  
The right hand panels show the squint :  $(RCP-LCP)/2$
- fig. 4 Pre-fit pointing rms distribution, over all antennas, over four pointing runs in late 1993.
- fig. 5 Post-fit pointing rms distribution for the same four sessions.
- Symbols for figs. 6 to 10:  
In the left hand panels the filled circles are observations made after a DOWN drive in elevation; open circles are for UP drives.  
In the right hand panels the filled and open circles correspond to decreasing and increasing azimuth
- fig. 6 Pre- and Post-fit pointing summaries for antenna 1, Dec 1, 1993.  
Note the pronounced elevation dependence of both the Az and El errors. (top two panels on the left).
- fig. 7 Antenna 7. Two points of interest:  
(a). Hysteresis. There is a clear separation between the UP and the DOWN symbols in the El errors (panels 1 and 3 on the left). The effect is clearly present in both Pre- and Post-fit summaries.  
(b). Non-tilt El error. In fig. 7a (Pre-fit) we see that the  $\Delta El$  vs Az has a  $\sin(Az)$  dependence which is not matched in the  $\Delta Az$  vs Az. In fig. 7b we have an increased Az rms and the characteristic fan-shaped signature of a tilt error in  $\Delta Az$  vs El.
- fig. 8 Antenna 17. There is a serious ( $60''$ ) error, in both  $\Delta E$  and  $\Delta Az$  in the Az range 0 to 180. Note that the Az and El errors are comparable in amplitude and offset in Az which suggests a solid-body rocking of the azimuth structure.
- fig. 9 Antenna 23. Probably also an Az bearing signature, but the Az and El excursions are much steeper in onset, and they are also in phase.

- fig. 10 Scatter plot of the tilt parameters (A1,A2) derived in the different pointing runs.
- fig. 11 Antenna 4, 14 November session, showing the strong correlation between the the array average and this antenna. All antennas have a similar plot. The diagonal line in the last two panels is the (1:1) line, not a fit.

Table I

ant,	collimation	mean,	rms.	squint	mean,	rms.	pts		
1	3.34	3.46	0.22	5.37	2.30	1.22	-8.20	1.83	14
2	-3.44	3.08	3.49	3.28	2.62	1.02	-8.16	1.30	12
3	0.30	1.83	-3.34	2.74	2.67	0.65	-9.17	0.97	16
4	1.90	2.41	-1.29	5.02	1.61	1.16	-8.63	0.91	17
5	6.21	1.92	6.32	3.07	1.79	1.07	-9.24	1.02	17
6	-0.31	2.36	-0.19	2.84	1.73	1.02	-10.36	1.18	17
7	-2.16	2.54	-0.50	3.96	2.01	1.44	-9.25	1.15	16
8	2.84	2.31	2.14	3.48	1.99	0.64	-8.19	1.05	16
9	-0.45	3.40	-2.05	3.15	2.16	0.98	-7.94	0.96	17
10	2.64	2.84	-1.74	5.43	1.90	1.17	-9.42	0.94	17
11	0.67	2.91	-2.52	5.42	2.90	1.33	-9.38	2.19	15
12	3.31	2.70	-2.76	3.23	3.60	1.01	-8.83	1.14	17
13	1.50	2.50	6.99	3.04	1.94	1.06	-9.07	1.21	17
14	0.00	0.00	0.00	0.00	0.00	0.00	0.00	0.00	0
15	-0.08	3.46	-1.46	4.84	1.98	1.30	-8.11	0.97	16
16	0.78	2.00	-1.59	6.54	2.19	1.13	-7.71	0.95	17
17	-2.37	3.88	1.28	6.64	1.97	0.93	-10.20	2.10	17
18	-0.69	3.23	-2.78	3.16	1.54	1.18	-9.44	0.96	16
19	2.19	2.22	-1.68	2.82	2.05	1.04	-7.92	1.07	17
20	2.61	1.97	1.65	2.94	2.27	1.24	-8.77	1.34	15
21	1.63	3.22	-0.35	6.02	1.06	1.06	-8.21	0.92	17
22	0.55	2.77	-1.17	3.35	2.95	0.81	-8.25	0.79	14
23	2.91	2.01	2.45	3.43	2.54	1.79	-7.83	1.21	15
24	-2.09	3.72	0.97	3.44	2.67	1.17	-8.05	0.93	17
25	3.84	1.75	-1.34	1.96	1.13	0.76	-8.82	1.08	16
26	-1.07	3.25	2.48	3.61	1.69	1.74	-8.28	1.42	17
27	-2.57	1.38	-0.07	3.58	0.75	1.33	-7.94	1.04	17
28	6.05	2.19	-3.46	3.22	1.55	1.19	-8.97	0.84	17

AZ      RL      EL      RLRS  
 └──────────────────┘  
 collimation

AZ      EL  
 └──────────────────┘  
 Squint.

2.06    0.62    -8.68    0.72

collimation =  $[R_{err} + L_{err}] / 2$

squint =  $[R_{err} - L_{err}] / 2$

Dec 10 data.

K-band data referenced  
 to X-band.





Table III

- 1 -> file : vlax.sep11
- 2 -> file : vlax.sep29
- 3 -> file : vlax.oct30
- 4 -> file : vlax.dec1

ant	1-theta		2-th (az)		2-th (el)		3-th (az)		3-th (el)		Sa	Se
	C	S	C	S	C	S	C	S	C	S		
1 1	0.0	1.9	0.7	-0.7	-2.9	6.1	0.6	-1.1	3.8	3.6	10.7	9.9
1 2	2.3	-1.1	-2.3	0.5	-1.3	3.3	-2.2	-1.1	3.9	4.6	7.0	6.0
1 3	4.2	-4.0	-6.4	3.5	-3.8	5.2	-2.0	-3.6	4.5	0.0	6.9	7.0
1 4	4.4	-1.3	-3.2	2.7	-3.4	3.5	-2.0	-2.4	3.8	4.9	7.3	6.6
	2.7	-1.1	-2.8	1.5	-2.8	4.5	-1.4	-2.0	4.0	3.3	.....	mean
	1.8	2.1	2.5	1.7	1.0	1.2	1.2	1.0	0.3	2.0	.....	rms
2 1	6.7	8.8	-0.2	3.0	-0.4	5.4	3.4	-1.5	1.2	1.5	4.0	9.6
2 2	5.3	9.9	-0.3	1.6	0.9	3.9	3.1	-1.6	1.3	2.6	3.0	4.0
2 3	8.6	6.7	0.1	0.8	-2.0	3.9	2.6	-2.0	2.8	3.7	3.2	4.9
2 4	7.5	9.7	2.2	1.4	4.4	4.0	1.1	-0.6	1.1	0.5	2.9	5.3
	7.0	8.8	0.5	1.7	0.7	4.3	2.6	-1.4	1.6	2.1		
	1.2	1.3	1.0	0.8	2.4	0.6	0.9	0.5	0.7	1.2		
3 1	3.0	-2.9	1.9	-1.9	-1.1	2.8	-0.4	0.3	-0.3	3.2	3.9	7.5
3 2	-0.9	-1.2	3.2	-1.8	0.0	2.5	0.3	-0.1	0.3	2.3	3.0	4.7
3 3	-1.3	-1.7	-1.5	-0.3	-1.5	0.3	1.8	-1.1	1.0	3.2	3.1	5.7
3 4	-0.4	-1.3	-0.1	-3.5	0.4	1.8	0.4	-0.6	-0.5	3.9	4.2	5.5
	0.1	-1.8	0.9	-1.9	-0.5	1.9	0.5	-0.4	0.1	3.2		
	1.7	0.7	1.8	1.1	0.8	1.0	0.8	0.5	0.6	0.6		
4 1	7.9	-6.2	-7.7	-0.8	0.7	-3.3	-1.3	0.1	1.2	-1.8	4.2	8.5
4 2	0.4	-1.7	-3.9	1.0	1.3	-3.1	1.1	-0.5	0.0	1.2	3.8	3.4
4 3	0.4	-2.7	-4.2	5.1	0.5	-3.3	1.0	-2.0	-1.0	0.8	4.2	4.8
4 4	2.1	-2.5	-4.1	3.5	1.5	-2.5	1.9	-1.6	0.2	1.1	4.1	4.8
	2.7	-3.3	-5.0	2.2	1.0	-3.0	0.7	-1.0	0.1	0.3		
	3.1	1.7	1.6	2.3	0.4	0.3	1.2	0.8	0.8	1.2		
5 1	-13.7	2.1	-3.7	2.6	7.8	-3.9	-3.5	1.5	0.0	-3.6	3.0	7.3
5 2	-12.5	2.3	-1.3	0.7	5.7	-2.7	-1.7	1.0	-0.9	-2.5	2.9	3.9
5 3	-11.7	-1.0	-2.2	0.9	8.2	-3.2	1.6	0.9	-1.5	-0.4	2.9	4.1
5 4	-5.8	-3.4	-2.1	1.1	7.5	-2.1	-1.4	0.1	1.0	-3.0	3.2	4.4
	-10.9	0.0	-2.3	1.3	7.3	-3.0	-1.2	0.9	-0.4	-2.4		
	3.0	2.4	0.9	0.7	1.0	0.7	1.8	0.5	0.9	1.2		
6 1	3.6	-3.6	-1.0	0.7	-1.4	1.2	-3.6	-3.2	0.9	2.6	5.2	8.5
6 2	3.5	-2.5	-0.7	2.4	-0.8	1.4	-2.1	-2.6	1.5	3.9	4.4	5.4
6 3	1.2	-1.1	-0.1	3.8	-1.5	0.9	-2.9	-4.3	2.4	2.6	4.2	4.1
6 4	1.7	-3.7	-1.9	2.4	-0.5	2.3	-4.0	-3.1	2.0	1.5	4.9	4.4
	2.5	-2.7	-0.9	2.3	-1.0	1.5	-3.1	-3.3	1.7	2.6		
	1.1	1.0	0.6	1.1	0.4	0.5	0.7	0.6	-0.6	0.8		
7 1	5.1	-10.5	-4.1	-0.9	1.3	-7.8	-0.7	1.3	-3.1	6.6	5.5	12.9
7 2	-0.7	-8.4	-0.4	-0.2	2.0	-5.2	1.4	0.6	-3.1	4.5	4.6	12.6
7 3	-4.3	-8.1	-3.3	2.5	6.8	-10.1	3.0	-1.4	-6.8	11.1	4.6	12.8
7 4	-0.6	-9.9	-1.0	-1.6	1.4	-3.3	1.0	0.3	-0.6	3.2	5.5	14.5
	-0.1	-9.2	-2.2	-0.1	2.9	-6.6	1.1	0.2	-3.4	6.4		
	3.4	1.0	1.5	1.6	2.3	2.6	1.3	1.0	2.2	3.0		
8 1	-7.6	-2.9	-3.6	4.5	-10.5	-1.5	3.1	0.7	-0.6	2.5	6.1	9.7
8 2	-8.7	-2.1	-2.0	3.4	-9.2	-3.6	0.6	-1.0	-0.3	3.1	5.4	4.9
8 3	-7.5	-1.2	-6.3	2.2	-11.6	-0.3	0.3	0.5	-1.5	5.4	4.8	4.4
8 4	-7.9	-3.3	-1.6	3.4	-8.1	-1.9	2.4	-0.6	0.6	3.0	4.5	4.9

See  
section 6(s)

		-7.9	-2.4	-3.4	3.4	-9.9	-1.8	1.6	-0.1	-0.4	3.5		
		0.5	0.8	1.8	0.8	1.3	1.2	1.2	0.7	0.7	1.1		
9	1	1.4	8.0	3.7	3.2	4.9	4.6	4.5	-2.6	-2.5	6.4	7.0	7.9
9	2	1.0	5.8	2.4	2.7	6.0	4.6	-0.3	-1.1	-2.9	7.0	4.2	4.9
9	3	1.1	-12.7	-6.4	3.5	0.2	3.5	2.0	-3.9	0.2	15.3	7.2	9.7
9	4	3.9	-9.3	0.0	2.2	6.1	3.3	2.5	-2.5	-2.3	16.1	9.0	10.6
		1.9	-2.0	-0.1	2.9	4.3	4.0	2.2	-2.5	-1.9	11.2		
		1.2	9.1	3.9	0.5	2.4	0.6	1.7	1.0	1.2	4.5		
10	1	6.3	2.7	-2.9	3.2	0.0	4.2	-1.3	-1.0	1.4	5.8	4.6	7.3
10	2	6.3	0.1	-1.7	3.2	0.4	2.9	-1.0	-1.7	1.9	7.2	4.2	5.0
10	3	3.6	-1.9	-2.5	3.5	-3.7	2.5	-1.3	-2.0	1.0	8.1	3.9	5.1
10	4	6.0	-3.6	-3.5	3.8	1.2	2.4	-1.5	-1.6	2.7	5.8	4.8	5.2
		5.6	-0.7	-2.7	3.4	-0.5	3.0	-1.3	-1.6	1.7	6.7		
		1.1	2.3	0.7	0.2	1.9	0.7	0.2	0.4	0.6	1.0		
11	1	-1.2	4.1	-1.6	-1.7	0.2	-2.9	0.7	0.3	-4.3	6.3	2.6	5.9
11	2	-2.9	5.2	0.2	-1.1	2.1	-1.3	0.9	0.4	-4.2	8.7	2.9	5.6
11	3	-1.3	-4.5	-4.6	0.9	-1.5	5.9	1.4	-1.9	4.7	5.9	2.7	4.5
11	4	0.1	-3.5	-4.1	0.4	-1.9	3.6	0.9	-0.6	6.8	4.0	3.5	4.4
		-1.3	0.3	-2.5	-0.4	-0.3	1.3	1.0	-0.5	0.8	6.2		
		1.1	4.4	1.9	1.1	1.6	3.6	0.3	0.9	5.0	1.7		
12	3	-1.1	2.7	-4.4	0.5	-5.3	3.2	1.3	-0.6	1.5	7.5	2.5	4.6
12	4	-0.8	0.2	-3.8	1.4	-3.1	1.3	0.2	-1.5	-0.9	6.3	2.7	4.9
		-1.0	1.5	-4.1	0.9	-4.2	2.2	0.8	-1.0	0.3	6.9		
		0.1	1.2	0.3	0.5	1.1	1.0	0.6	0.4	1.2	0.6		
13	1	1.1	0.0	-2.7	-0.4	-3.2	-1.7	1.8	-2.0	-0.5	8.2	3.2	7.5
13	2	1.1	-1.6	-0.5	-0.5	0.3	-1.4	1.6	-1.7	-0.3	10.0	2.5	3.8
13	3	-2.9	0.4	0.0	0.6	-0.9	-0.9	1.3	-0.7	0.2	9.1	2.4	4.4
13	4	0.4	-1.7	0.0	-0.6	1.0	-2.0	2.4	-2.0	0.4	8.6	3.4	4.9
		-0.1	-0.7	-0.8	-0.2	-0.7	-1.5	1.8	-1.6	-0.1	9.0		
		1.7	0.9	1.1	0.5	1.6	0.4	0.4	0.5	0.4	0.7		
14	1	8.8	-2.2	-5.7	0.0	-3.8	-1.4	1.3	-1.0	-0.9	8.0	3.7	8.5
14	2	7.2	-1.3	-4.9	0.9	-0.6	-3.1	2.0	-1.7	0.5	6.6	3.1	5.0
		8.0	-1.8	-5.3	0.4	-2.2	-2.2	1.6	-1.3	-0.2	7.3		
		0.8	0.4	0.4	0.4	1.6	0.8	0.4	0.4	0.7	0.7		
15	1	0.8	1.0	-11.0	1.1	-1.6	-6.7	1.5	-1.5	0.9	2.9	5.6	8.0
15	2	-2.2	1.7	-8.9	0.9	1.7	-6.4	4.0	-3.7	1.0	4.7	5.6	5.3
15	3	-2.2	3.6	-8.8	1.6	0.1	-4.5	1.3	-1.5	-0.3	3.8	4.7	4.4
15	4	-0.3	1.6	-10.2	3.8	1.7	-5.8	3.7	-3.3	-0.5	3.6	5.4	4.9
		-1.0	2.0	-9.7	1.8	0.5	-5.9	2.6	-2.5	0.3	3.8		
		1.3	1.0	0.9	1.2	1.4	0.8	1.2	1.0	0.7	0.6		
16	1	-1.6	2.6	-2.1	-0.4	-0.4	-9.9	0.5	1.3	-3.2	0.3	3.6	8.4
16	2	-5.8	5.5	1.3	1.1	1.4	-7.0	0.3	2.0	-4.2	-1.0	2.9	6.8
16	3	-6.7	2.8	-2.6	1.7	1.9	-9.0	2.5	3.2	-1.5	-2.5	2.7	7.7
16	4	-3.8	5.2	1.2	-1.4	1.9	-6.2	0.8	1.0	-4.2	-0.5	3.0	8.0
		-4.5	4.0	-0.5	0.3	1.2	-8.0	1.1	1.9	-3.3	-0.9		
		2.0	1.3	1.8	1.2	0.9	1.5	0.9	0.8	1.1	1.0		
17	1	5.8	2.0	7.1	0.5	-1.6	10.2	-6.0	1.4	3.9	-2.1	7.6	7.2
17	2	-1.8	3.0	9.1	1.3	-1.0	10.0	-2.7	1.8	2.8	-1.6	6.6	4.8
17	4	0.8	2.1	8.6	-1.7	-3.0	10.2	-4.4	3.1	4.4	-1.0	6.1	4.7
		1.6	2.4	8.3	0.0	-1.9	10.1	-4.4	2.1	3.7	-1.6		

		3.2	0.4	0.8	1.3	0.8	0.1	1.4	0.7	0.7	0.5		
18	1	8.6	-2.9	-5.2	-4.4	8.5	-4.5	-9.7	-0.7	2.3	-5.8	8.3	13.9
18	2	7.4	-7.6	-5.8	-4.8	2.2	-7.7	-5.8	0.4	1.8	-1.3	8.1	9.2
18	3	6.3	-7.1	-7.6	-0.6	2.5	-8.7	-7.8	-1.9	0.1	-0.8	8.9	9.5
18	4	4.4	-2.7	-2.1	-3.4	4.0	-2.8	-6.9	-1.0	3.2	-4.4	8.4	9.4
		6.7	-5.1	-5.2	-3.3	4.3	-5.9	-7.5	-0.8	1.9	-3.1		
		1.5	2.3	2.0	1.6	2.5	2.4	1.4	0.8	1.1	2.1		
19	1	2.5	-4.6	-5.3	2.5	-1.9	3.3	1.1	0.1	0.4	6.3	3.0	8.2
19	2	1.2	-2.2	-3.1	3.2	-0.7	1.9	1.3	0.6	0.1	7.2	3.5	5.0
19	3	1.1	-2.3	-6.0	2.2	-1.0	1.4	1.3	1.4	-2.3	6.3	3.9	4.4
19	4	0.9	-2.5	-2.4	2.4	-0.2	2.3	0.7	-0.2	-0.5	5.8	2.8	5.0
		1.4	-2.9	-4.2	2.6	-0.9	2.2	1.1	0.5	-0.6	6.4		
		0.6	1.0	1.5	0.4	0.6	0.7	0.2	0.6	1.1	0.5		
20	1	7.6	-5.6	-3.5	-1.4	1.4	-0.6	-1.6	-2.0	2.1	2.6	6.0	9.6
20	2	5.1	-6.9	-3.0	-1.7	1.1	-0.8	-1.7	-0.6	2.0	3.2	4.3	4.8
20	3	6.7	-6.5	-5.7	-2.0	3.3	-2.2	-0.7	0.0	1.9	4.0	2.2	3.3
20	4	4.5	-4.9	-1.5	-0.8	2.5	-2.9	-3.3	-1.0	4.4	1.6	3.7	5.0
		6.0	-6.0	-3.4	-1.5	2.1	-1.6	-1.8	-0.9	2.6	2.8		
		1.2	0.8	1.5	0.4	0.9	1.0	1.0	0.7	1.1	0.9		
21	1	4.6	-2.6	-8.6	4.1	-4.5	3.2	0.3	-0.6	-1.5	8.7	4.1	7.7
21	2	4.2	-2.0	-7.9	4.1	-2.9	3.0	-1.2	-0.2	-0.9	7.7	3.6	5.4
21	3	2.8	0.3	-9.2	0.4	-4.6	3.1	-1.8	0.7	-0.1	7.2	3.3	5.1
21	4	2.9	-1.4	-7.9	2.3	-1.8	2.7	-2.3	-0.3	-0.3	6.9	3.9	5.5
		3.6	-1.4	-8.4	2.7	-3.5	3.0	-1.3	-0.1	-0.7	7.6		
		0.8	1.1	0.5	1.5	1.2	0.2	1.0	0.5	0.5	0.7		
22	1	0.1	-0.2	-4.2	1.3	-1.1	6.6	0.3	-1.5	-0.2	6.3	4.6	9.5
22	2	-1.1	-3.1	-3.5	1.5	2.5	3.3	-1.5	-2.1	1.0	6.7	4.1	4.8
22	3	9.6	-11.9	-7.6	1.8	4.2	-0.6	-1.3	0.3	1.4	-2.6	4.8	5.6
22	4	4.7	-7.4	-3.9	1.9	4.7	-1.8	-4.9	1.9	4.3	-1.7	3.9	6.2
		3.3	-5.7	-4.8	1.6	2.6	1.9	-1.9	-0.3	1.6	2.2		
		4.2	4.4	1.6	0.2	2.3	3.3	1.9	1.6	1.7	4.4		
23	1	2.2	-0.3	3.0	-8.1	9.6	19.8	-10.9	1.1	7.9	-6.1	9.0	10.4
23	2	-0.1	4.4	7.1	-6.1	7.9	15.1	-4.3	-1.4	8.0	-3.9	9.6	5.9
23	3	-1.0	4.2	6.8	-4.9	2.5	20.5	-3.3	-5.2	9.2	-3.5	10.1	8.3
23	4	-1.4	1.1	5.1	-7.2	6.7	19.2	-9.1	-1.1	10.7	-3.7	8.2	7.1
		-0.1	2.3	5.5	-6.6	6.7	18.7	-6.9	-1.6	8.9	-4.3		
		1.4	2.0	1.6	1.2	2.6	2.1	3.2	2.3	1.1	1.1		
24	1	-0.1	3.2	2.8	-0.4	8.0	2.9	-4.0	3.3	0.1	-7.6	4.3	6.5
24	2	-1.0	2.4	4.6	1.0	8.0	2.6	-1.5	2.5	1.0	-6.9	4.3	5.4
24	3	-1.5	1.7	1.6	0.4	5.8	2.3	0.3	2.1	0.0	-7.5	3.3	4.6
24	4	-0.8	0.6	4.7	-0.3	6.2	3.0	-2.8	1.7	1.7	-6.9	3.5	4.8
		-0.8	2.0	3.4	0.2	7.0	2.7	-2.0	2.4	0.7	-7.2		
		0.5	1.0	1.3	0.6	1.0	0.3	1.6	0.6	0.7	0.3		
25	1	3.4	-2.9	-4.2	-1.9	-0.7	0.0	-2.8	0.0	-0.6	7.2	3.1	7.7
25	2	0.5	-0.4	-1.2	0.3	0.0	0.3	-2.4	0.3	-0.8	8.7	2.3	4.0
25	3	-1.6	1.4	-2.1	1.3	-1.9	-1.6	-2.1	-0.6	-1.5	6.8	2.5	4.0
25	4	-0.6	1.9	-0.2	2.8	0.7	0.1	-3.0	0.8	-0.5	6.8	2.1	3.5
		0.4	0.0	-1.9	0.6	-0.5	-0.3	-2.6	0.1	-0.9	7.4		
		1.9	1.9	1.5	1.7	1.0	0.8	0.4	0.5	0.4	0.8		
26	1	5.0	-2.0	-1.2	-2.3	-0.3	-1.9	-2.3	-1.2	-1.9	4.9	2.7	7.1
26	2	0.8	1.9	1.1	-0.6	2.0	-0.9	-1.7	-0.3	-2.0	6.9	2.3	4.3
26	3	-1.0	2.7	-0.7	-0.9	-0.7	-0.9	-1.8	0.4	-1.6	5.0	2.2	2.9

26	4	-0.5	0.6	0.9	-1.0	1.0	-0.5	-0.3	-0.8	-1.8	6.0	3.4	3.6
		1.1	0.8	0.0	-1.2	0.5	-1.0	-1.5	-0.5	-1.8	5.7		
		2.4	1.8	1.0	0.7	1.1	0.5	0.7	0.6	0.2	0.8		
27	1	2.7	-9.0	-2.9	-1.5	-2.3	1.8	-0.3	-0.6	0.4	4.0	4.3	6.9
27	2	0.6	-5.6	-0.3	0.5	-1.3	0.6	-1.3	-0.5	0.6	6.4	4.0	4.4
27	3	0.6	-7.2	-4.0	2.0	-0.4	0.9	-1.7	-1.3	0.1	7.3	3.8	4.3
27	4	1.2	-5.6	-0.4	1.9	1.0	2.0	-1.3	-1.1	0.1	6.1	4.4	3.9
		1.3	-6.8	-1.9	0.7	-0.8	1.3	-1.1	-0.9	0.3	5.9		
		0.9	1.4	1.6	1.4	1.2	0.6	0.5	0.4	0.2	1.2		
28	1	5.9	3.9	-1.6	1.6	-4.4	3.3	-0.4	-2.4	-0.5	5.5	5.5	8.3
28	2	3.1	5.8	-1.5	1.4	-2.4	2.0	-0.9	-0.9	0.5	4.4	3.5	4.6
28	3	4.5	7.9	-1.9	-0.9	-3.0	3.3	-0.4	-1.7	2.3	4.1	2.7	5.7
28	4	-0.3	5.1	-2.6	2.9	-1.1	2.4	-1.3	-1.1	1.1	3.3	4.1	5.8
		3.3	5.7	-1.9	1.2	-2.7	2.8	-0.8	-1.5	0.9	4.3		
		2.3	1.5	0.4	1.4	1.2	0.6	0.4	0.6	1.0	0.8		

Data logged to summary.log

Table IV

Hysteresis								
ant	Elevation		Azimuth					
1	-0.86	+/- 2.93	-4.55	+/- 3.05	..	sept.	11	
1	-5.00	+/- 1.51	0.77	+/- 1.91	..	sept.	29	
1	-3.30	+/- 2.53	-1.99	+/- 2.66	..	oct	30	
1	-3.66	+/- 1.56	-0.65	+/- 1.78	..	dec	1	
2	3.90	+/- 2.53	-1.04	+/- 1.01				
2	-1.13	+/- 1.06	0.08	+/- 0.84				
2	0.01	+/- 1.56	-1.36	+/- 1.19				
2	-3.62	+/- 1.20	0.53	+/- 0.70				
3	4.31	+/- 1.93	-0.78	+/- 1.05				
3	0.86	+/- 1.30	0.56	+/- 0.83				
3	1.71	+/- 2.34	-0.09	+/- 1.21				
3	-2.03	+/- 1.33	0.57	+/- 1.03				
4	7.66	+/- 1.98	-1.74	+/- 1.05				
4	0.30	+/- 0.93	-1.60	+/- 1.04				
4	1.02	+/- 2.21	-1.86	+/- 1.55				
4	-3.51	+/- 1.06	-1.27	+/- 0.97				
5	5.57	+/- 1.76	-0.48	+/- 0.76				
5	0.36	+/- 1.03	-0.26	+/- 0.79				
5	-0.55	+/- 1.72	-0.28	+/- 1.10				
5	-3.83	+/- 0.94	-0.35	+/- 0.76				
6	4.31	+/- 2.15	-2.28	+/- 1.35				
6	-1.14	+/- 1.40	-2.45	+/- 1.16				
6	-0.46	+/- 1.30	-1.98	+/- 1.53				
6	-3.08	+/- 0.99	-0.95	+/- 1.16				
7	-12.47	+/- 2.98	0.13	+/- 1.38				
7	-14.52	+/- 2.86	0.04	+/- 1.29				
7	-16.48	+/- 3.97	-1.71	+/- 1.67				
7	-17.46	+/- 2.80	0.42	+/- 1.31				
8	5.07	+/- 2.49	-2.98	+/- 1.54				
8	0.93	+/- 1.27	0.47	+/- 1.45				
8	-1.29	+/- 1.62	-0.46	+/- 1.79				
8	-2.80	+/- 1.09	0.16	+/- 1.10				
9	3.44	+/- 2.10	-1.21	+/- 1.79				
9	-5.09	+/- 1.16	0.38	+/- 1.18				
9	-5.77	+/- 3.68	-3.99	+/- 2.61				
9	-8.97	+/- 2.34	-0.04	+/- 2.17				
10	3.47	+/- 1.87	-1.55	+/- 1.17				
10	-0.64	+/- 1.29	-1.43	+/- 1.17				
10	-2.37	+/- 1.63	-2.16	+/- 1.38				
10	-2.82	+/- 1.17	-0.93	+/- 1.15				
11	3.11	+/- 1.47	-0.81	+/- 0.65				
11	-0.15	+/- 1.51	-0.77	+/- 0.79				
11	0.92	+/- 1.76	-1.44	+/- 1.02				
11	-0.12	+/- 1.11	0.29	+/- 0.89				
12	0.00	+/- 0.00	0.00	+/- 0.00				
12	0.00	+/- 0.00	0.00	+/- 0.00				
12	-1.39	+/- 1.59	-1.14	+/- 0.92				
12	-1.62	+/- 1.16	-0.36	+/- 0.64				
13	0.49	+/- 2.01	-1.16	+/- 0.79				
13	-3.37	+/- 0.90	-0.28	+/- 0.69				
13	-2.40	+/- 1.63	-0.72	+/- 0.88				
13	-3.84	+/- 1.03	0.33	+/- 0.80				

14	3.60 +/-	2.13	-1.22 +/-	0.94
14	-0.84 +/-	1.32	-0.85 +/-	0.86
14	0.00 +/-	0.00	0.00 +/-	0.00
14	0.00 +/-	0.00	0.00 +/-	0.00
15	4.75 +/-	1.93	-0.78 +/-	1.41
15	0.52 +/-	1.41	0.08 +/-	1.51
15	0.88 +/-	1.74	-4.05 +/-	1.68
15	-0.22 +/-	1.19	0.52 +/-	1.37
16	4.65 +/-	2.25	0.20 +/-	1.00
16	0.13 +/-	1.85	-0.90 +/-	0.79
16	4.39 +/-	2.61	-0.56 +/-	1.00
16	-5.57 +/-	1.89	-0.57 +/-	0.76
17	2.35 +/-	1.85	-1.17 +/-	1.92
17	-2.23 +/-	1.27	0.33 +/-	1.80
17	0.00 +/-	0.00	0.00 +/-	0.00
17	0.86 +/-	1.12	0.21 +/-	1.47
18	3.03 +/-	3.66	0.79 +/-	2.09
18	-1.61 +/-	2.44	-1.25 +/-	2.22
18	0.46 +/-	2.87	-2.37 +/-	3.27
18	-4.00 +/-	2.15	-2.20 +/-	2.00
19	3.05 +/-	2.14	-1.36 +/-	0.75
19	-2.61 +/-	1.26	-2.07 +/-	0.93
19	-0.13 +/-	1.36	-1.75 +/-	1.48
19	-4.65 +/-	1.07	0.18 +/-	0.71
20	2.61 +/-	2.41	1.35 +/-	1.51
20	-3.55 +/-	1.19	0.49 +/-	1.20
20	-0.69 +/-	1.55	1.38 +/-	0.84
20	-3.98 +/-	1.10	0.46 +/-	0.93
21	1.80 +/-	2.01	-0.33 +/-	1.06
21	-1.37 +/-	1.41	-0.63 +/-	1.01
21	0.23 +/-	2.01	-1.67 +/-	1.16
21	-2.28 +/-	1.27	-0.18 +/-	0.95
22	0.35 +/-	2.71	-1.44 +/-	1.25
22	-3.37 +/-	1.19	0.11 +/-	1.15
22	-0.96 +/-	3.46	-1.29 +/-	2.03
22	-7.67 +/-	1.27	-0.26 +/-	1.01
23	4.14 +/-	2.81	1.21 +/-	2.43
23	-3.20 +/-	1.53	1.98 +/-	2.68
23	0.03 +/-	2.97	0.66 +/-	3.65
23	-1.94 +/-	1.68	1.46 +/-	2.14
24	2.07 +/-	1.66	0.16 +/-	1.13
24	-2.98 +/-	1.38	-0.31 +/-	1.15
24	-0.31 +/-	1.77	-0.63 +/-	1.24
24	-3.49 +/-	1.04	0.40 +/-	0.82
25	2.93 +/-	2.02	-1.47 +/-	0.78
25	-2.02 +/-	1.05	-0.38 +/-	0.62
25	1.67 +/-	1.71	-2.88 +/-	0.81
25	-2.58 +/-	0.76	0.50 +/-	0.54
26	1.78 +/-	1.81	-2.08 +/-	0.64
26	-4.03 +/-	1.04	-0.01 +/-	0.62
26	-0.64 +/-	1.21	-0.56 +/-	0.79
26	-2.22 +/-	0.79	-0.26 +/-	0.81
27	3.62 +/-	1.74	-0.79 +/-	1.09
27	0.84 +/-	1.15	-1.21 +/-	1.13
27	-1.00 +/-	1.75	-2.53 +/-	1.34

27	-0.82 +/- 0.87	-0.56 +/- 1.04
28	1.36 +/- 2.17	-3.40 +/- 1.34
28	-2.41 +/- 1.23	-1.84 +/- 0.96
28	-3.40 +/- 2.42	-1.92 +/- 0.99
28	-6.54 +/- 1.20	-1.61 +/- 1.00





Table V

vlax.apr17.92  
vlax.feb20.93  
vlax.jun29.93  
vlax.jul21.93  
vlax.sep11.93  
vlax.sep29.93  
vlax.oct30.93  
vlax.nov14.93  
vlax.dec1.93  
vlax.dec29.93

A1 to A7; E3 to E5; Rotx corrections; Pad

1	-0.17	-0.16	-0.18	0.01	0.10	-3.01	42.00	-0.09	1.21	0.06	0.17	0.77	W14
1	0.32	0.62	-0.18	0.01	0.10	-3.01	40.32	-0.09	1.21	0.06	0.17	0.77	OUT
1	-0.47	-0.15	-0.18	0.01	0.10	-2.68	41.32	0.90	1.21	-0.15	0.17	0.77	N16
1	-0.47	-0.15	-0.18	0.01	0.10	-2.68	41.32	0.90	1.21	-0.15	0.17	0.77	N16
1	-0.47	-0.15	-0.18	0.01	0.10	-2.68	41.32	0.90	1.21	-0.15	0.17	0.77	N16
1	-0.24	-0.15	-0.18	0.01	0.10	-2.68	41.32	0.90	1.21	-0.15	0.17	0.77	N16
1	0.69	-0.15	-0.18	0.01	0.10	-2.68	41.32	0.90	1.21	0.56	0.17	0.77	N05
1	0.81	-0.45	-0.18	0.01	0.10	-2.50	36.15	0.90	1.21	0.56	0.17	0.77	N05
1	0.81	-0.45	-0.18	0.01	0.10	-2.50	36.15	0.90	1.21	0.56	0.17	0.77	N05
1	0.81	-0.29	-0.18	0.01	0.10	-2.50	35.76	0.90	1.21	-0.50	0.17	0.77	N05
2	-0.58	-0.45	-0.22	-0.09	0.15	0.29	0.87	0.39	0.39	-7.59	0.06	0.10	N02
2	-1.19	-0.90	-0.22	-0.09	0.15	0.29	1.61	0.27	0.39	-7.75	0.06	0.10	N16
2	-0.07	0.88	-0.22	-0.09	0.15	0.29	2.11	0.46	0.39	-7.64	0.06	0.10	W04
2	-0.07	0.88	-0.22	-0.09	0.15	0.29	2.11	0.46	0.39	-7.64	0.06	0.10	W04
2	-0.15	0.88	-0.22	-0.09	0.15	0.19	1.81	0.46	0.39	-7.76	0.06	0.10	W04
2	-0.15	0.95	-0.22	-0.09	0.15	0.19	1.81	0.46	0.39	-7.76	0.06	0.10	W04
2	-0.15	0.95	-0.22	-0.09	0.15	0.19	1.81	0.46	0.39	-7.76	0.06	0.10	W04
2	-0.15	0.85	-0.22	-0.09	0.15	0.19	1.81	0.46	0.39	-7.63	0.06	0.10	W04
2	-0.15	0.85	-0.22	-0.09	0.15	0.19	1.81	0.46	0.39	-7.63	0.06	0.10	W04
2	-0.15	0.97	-0.22	-0.09	0.15	0.19	1.81	0.46	0.39	-7.63	0.06	0.10	W04
3	-0.03	0.21	0.04	-0.15	-0.07	-0.68	-3.91	0.65	0.00	3.04	0.02	0.72	W04
3	1.43	-0.88	0.04	-0.15	-0.07	-0.65	-6.80	0.61	0.00	3.42	0.02	0.72	W20
3	0.23	0.10	0.04	-0.15	-0.07	-0.65	-5.87	0.71	0.00	3.03	0.02	0.72	W02
3	0.23	0.10	0.04	-0.15	-0.07	-0.65	-5.87	0.71	0.00	3.03	0.02	0.72	W02
3	0.23	0.10	0.04	-0.15	-0.07	-0.65	-5.87	0.71	0.00	3.03	0.02	0.72	W02
3	0.23	0.17	0.04	-0.15	-0.07	-0.65	-5.87	0.71	0.00	3.28	0.02	0.72	W02
3	0.16	0.17	0.04	-0.15	-0.07	-0.65	-5.87	0.71	0.00	3.15	0.02	0.72	W02
3	0.16	0.10	0.04	-0.15	-0.07	-0.65	-6.07	0.71	0.00	3.15	0.02	0.72	W02
3	0.16	0.10	0.04	-0.15	-0.07	-0.65	-6.07	0.71	0.00	3.15	0.02	0.72	W02
3	0.16	0.15	0.04	-0.15	-0.07	-0.65	-6.07	0.71	0.00	3.06	0.02	0.72	W02
4	0.62	0.77	-0.06	0.08	-0.50	-2.88	-2.87	0.31	0.28	-2.53	0.14	0.14	E14
4	-0.48	-0.62	-0.06	0.08	-0.50	-2.90	-4.84	0.27	0.28	-2.51	0.14	0.14	E04
4	-0.48	-0.56	-0.06	0.08	-0.50	1.17	-4.79	0.27	0.28	-2.89	0.14	0.14	E04
4	-0.48	-0.61	-0.06	0.08	-0.50	1.17	-4.79	0.27	0.28	-2.89	0.14	0.14	E04
4	-0.48	-0.61	-0.06	0.08	-0.50	1.30	-4.79	0.27	0.28	-2.89	0.14	0.14	E04
4	-0.48	-0.61	-0.06	0.08	-0.50	1.30	-4.79	0.27	0.28	-2.89	0.14	0.14	E04
4	-0.54	-0.61	-0.06	0.08	-0.50	1.30	-4.92	0.27	0.28	-2.89	0.14	0.14	E04
4	-0.54	-0.72	-0.06	0.08	-0.50	1.30	-4.92	0.27	0.28	-2.89	0.14	0.14	E04
4	-0.54	-0.61	-0.06	0.08	-0.50	1.30	-4.92	0.27	0.28	-2.89	0.14	0.14	E04
4	-0.54	-0.61	-0.06	0.08	-0.50	1.30	-4.92	0.27	0.28	-2.89	0.14	0.14	E04
5	0.38	0.42	0.16	0.05	-0.62	1.12	-2.74	-0.21	-0.28	1.86	0.17	0.47	E10
5	-0.78	0.01	0.16	0.05	-0.62	1.17	-1.74	0.27	-0.28	2.24	0.17	0.47	E16
5	0.02	0.32	0.16	0.05	-0.62	1.17	-2.25	0.43	-0.28	2.01	0.17	0.47	E08
5	0.02	0.16	0.16	0.05	-0.62	1.17	-2.25	0.43	-0.28	2.01	0.17	0.47	E08
5	0.11	0.24	0.16	0.05	-0.62	1.17	-2.25	0.43	-0.28	2.01	0.17	0.47	E08
5	0.11	0.24	0.16	0.05	-0.62	1.17	-2.25	0.43	-0.28	2.01	0.17	0.47	E08
5	0.11	0.24	0.16	0.05	-0.62	1.17	-2.38	0.30	-0.28	2.11	0.17	0.47	E08
5	0.11	0.24	0.16	0.05	-0.62	1.17	-2.38	0.30	-0.28	2.22	0.17	0.47	E08
5	0.11	0.24	0.16	0.05	-0.62	1.17	-2.38	0.30	-0.28	2.22	0.17	0.47	E08
5	0.15	0.29	0.16	0.05	-0.62	1.17	-2.58	0.30	-0.28	2.22	0.17	0.47	E08

6	0.48	0.73	-0.06	-0.02	-0.24	0.70	2.46	0.29	0.01	1.80	-0.96	0.85	N12
6	2.60	-3.32	-0.06	-0.02	-0.24	0.70	3.59	0.28	0.01	1.80	-0.96	0.85	N24
6	-0.41	-0.34	-0.06	-0.02	-0.24	0.70	7.35	0.28	0.01	1.80	-0.96	0.85	N06
6	-0.41	-0.34	-0.06	-0.02	-0.24	0.70	7.35	0.28	0.01	1.80	-0.96	0.85	N06
6	-0.41	-0.34	-0.06	-0.02	-0.24	0.70	7.35	0.28	0.01	1.80	-0.96	0.85	N06
6	-0.30	-0.34	-0.06	-0.02	-0.24	0.59	7.35	0.28	0.01	1.94	-0.96	0.85	N06
6	-0.36	-0.34	-0.06	-0.02	-0.24	0.68	7.35	0.28	0.01	1.82	-0.96	0.85	N06
6	-0.26	-0.34	-0.06	-0.02	-0.24	0.68	7.15	0.28	0.01	1.82	-0.96	0.85	N06
6	-0.47	-0.34	-0.06	-0.02	-0.24	0.68	7.15	0.28	0.01	1.82	-0.96	0.85	N06
6	-0.32	-0.34	-0.06	-0.02	-0.24	0.68	7.15	0.28	0.01	1.82	-0.96	0.85	OUT
7	0.23	0.32	0.04	0.00	-0.85	0.90	0.02	0.39	0.31	-1.41	-0.49	0.15	E18
7	-0.24	0.29	0.04	0.00	-0.85	0.90	1.10	0.29	0.31	-1.47	-0.49	0.15	E32
7	0.59	0.16	0.04	0.00	-0.85	0.90	1.45	0.29	0.31	-1.47	-0.49	0.15	E14
7	0.70	0.16	0.04	0.00	-0.85	0.90	1.45	0.29	0.31	-1.47	-0.49	0.15	E14
7	0.09	0.53	0.04	0.00	-0.85	0.90	-1.21	0.29	0.31	-1.47	-0.49	0.15	E05
7	0.09	0.53	0.04	0.00	-0.85	0.90	-1.21	0.29	0.31	-1.47	-0.49	0.15	E05
7	0.09	0.53	0.04	0.00	-0.85	0.90	-1.21	0.29	0.31	-1.47	-0.49	0.15	E05
7	0.09	0.53	0.04	0.00	-0.85	0.90	-1.21	0.29	0.31	-1.47	-0.49	0.15	E05
7	-0.18	0.53	0.04	0.00	-0.85	0.90	-1.21	0.29	0.31	-1.47	-0.49	0.15	E05
7	0.04	0.53	0.04	0.00	-0.85	0.90	-1.21	0.29	0.31	-1.63	-0.49	0.15	E05
8	-0.99	-0.32	0.13	0.21	-0.67	-0.48	-15.01	0.28	0.29	-0.58	0.09	0.10	N10
8	0.11	0.21	0.13	0.21	-0.67	-0.51	-23.52	0.28	0.29	-1.17	0.09	0.10	W16
8	0.20	0.20	0.13	0.21	-0.67	-0.51	-23.89	0.28	0.29	-1.17	0.09	0.10	W16
8	0.20	0.20	0.13	0.21	-0.67	-0.51	-23.89	0.28	0.29	-1.17	0.09	0.10	W16
8	0.00	-0.53	0.13	0.21	-0.67	-0.51	-17.01	0.28	0.29	-1.17	0.09	0.10	W07
8	0.19	-0.53	0.13	0.21	-0.67	-0.51	-17.01	0.28	0.29	-1.17	0.09	0.10	W07
8	0.02	-0.45	0.13	0.21	-0.67	-0.51	-17.01	0.28	0.29	-1.27	0.09	0.10	W07
8	0.02	-0.45	0.13	0.21	-0.67	-0.51	-17.01	0.28	0.29	-1.27	0.09	0.10	W07
8	0.02	-0.32	0.13	0.21	-0.67	-0.51	-17.01	0.28	0.29	-1.27	0.09	0.10	W07
8	0.02	-0.47	0.13	0.21	-0.67	-0.51	-17.01	0.28	0.29	-1.17	0.09	0.10	W07
9	1.11	-0.22	-0.01	0.01	-0.35	0.88	1.79	0.51	0.59	-1.33	-1.35	0.26	W08
9	1.30	-0.26	-0.01	0.01	-0.35	0.88	1.77	0.51	0.59	-1.33	-1.35	0.26	W08
9	1.25	-0.18	-0.01	0.01	-0.35	0.88	1.96	0.51	0.59	-1.33	-1.35	0.26	W08
9	1.25	-0.18	-0.01	0.01	-0.35	0.88	2.18	0.51	0.59	-1.33	-1.35	0.26	W08
9	1.25	-0.18	-0.01	0.01	-0.35	0.88	2.18	0.51	0.59	-1.33	-1.35	0.26	W08
9	1.25	-0.18	-0.01	0.01	-0.35	0.88	2.18	0.51	0.59	-1.33	-1.35	0.26	W08
9	1.25	-0.18	-0.01	0.01	-0.35	0.88	2.18	0.51	0.59	-1.33	-1.35	0.26	W08
9	1.63	-0.18	-0.01	0.01	-0.35	0.88	2.18	0.51	0.59	-1.33	-1.35	0.26	W08
9	1.63	-0.18	-0.01	0.01	-0.35	0.88	2.18	0.51	0.59	-1.33	-1.35	0.26	W08
9	1.63	-0.18	-0.01	0.01	-0.35	0.88	1.91	0.51	0.59	-1.33	-1.35	0.26	W08
10	-0.41	0.62	0.02	-0.12	0.05	-0.66	7.83	0.43	0.17	-0.47	-0.26	0.56	W06
10	-0.40	0.69	0.02	-0.12	0.05	-0.54	1.51	0.43	0.17	-0.31	-0.26	0.56	W24
10	-0.61	0.73	0.02	-0.12	0.05	-0.54	8.47	0.43	0.17	-0.43	-0.26	0.56	W06
10	-0.61	0.73	0.02	-0.12	0.05	-0.54	8.47	0.43	0.17	-0.43	-0.26	0.56	W06
10	-0.61	0.64	0.02	-0.12	0.05	-0.54	8.29	0.43	0.17	-0.53	-0.26	0.56	W06
10	-0.61	0.73	0.02	-0.12	0.05	-0.54	8.29	0.43	0.17	-0.35	-0.26	0.56	W06
10	-0.61	0.73	0.02	-0.12	0.05	-0.54	8.29	0.43	0.17	-0.35	-0.26	0.56	W06
10	-0.61	0.64	0.02	-0.12	0.05	-0.54	8.02	0.43	0.17	-0.35	-0.26	0.56	W06
10	-0.61	0.64	0.02	-0.12	0.05	-0.54	8.02	0.43	0.17	-0.35	-0.26	0.56	W06
10	-0.54	0.64	0.02	-0.12	0.05	-0.54	8.02	0.43	0.17	-0.35	-0.26	0.56	W06
11	-0.56	-0.34	-0.06	-0.02	0.12	0.55	-0.21	0.35	-0.26	3.04	-5.00	0.04	W12
11	0.79	-1.20	-0.06	-0.02	0.12	0.55	2.50	0.35	-0.26	2.14	-5.00	0.04	N28
11	-0.65	-0.61	-0.06	-0.02	0.12	0.55	0.88	0.35	-0.26	3.02	-5.00	0.04	N10
11	-0.65	-0.61	-0.06	-0.02	0.12	0.55	0.88	0.22	-0.26	3.02	-5.00	0.04	N10
11	-0.65	-0.61	-0.06	-0.02	0.12	0.55	0.88	0.22	-0.26	3.02	-5.00	0.04	N10
11	-0.53	-0.66	-0.06	-0.02	0.12	0.55	0.88	0.22	-0.26	3.13	-5.00	0.04	N10
11	0.23	-1.48	-0.06	-0.02	0.12	0.55	-1.78	0.22	-0.26	3.13	-5.00	0.04	N01
11	0.41	-1.33	-0.06	-0.02	0.12	0.55	-1.93	0.22	-0.26	3.13	-5.00	0.04	N01
11	0.41	-1.33	-0.06	-0.02	0.12	0.55	-1.93	0.22	-0.26	3.13	-5.00	0.04	N01
11	0.36	-1.33	-0.06	-0.02	0.12	0.55	-1.93	0.22	-0.26	3.13	-5.00	0.04	N01
12	0.64	0.50	-0.04	-0.04	-0.59	0.77	0.90	0.44	0.85	-2.43	-3.40	0.16	W18
12	-0.29	0.06	-0.04	-0.04	-0.59	0.77	2.37	0.29	0.85	-2.44	-3.40	0.16	W04
12	-0.29	0.26	-0.04	-0.04	-0.59	0.77	1.82	0.43	0.85	-2.44	-3.40	0.16	E12

12	-0.29	0.05	-0.04	-0.04	-0.59	0.77	1.82	0.28	0.85	-2.44	-3.40	0.16	E12
12	-0.29	0.05	-0.04	-0.04	-0.59	0.77	1.82	0.28	0.85	-2.44	-3.40	0.16	OUT
12	-0.29	0.05	-0.04	-0.04	-0.59	0.77	1.82	0.28	0.85	-2.44	-3.40	0.16	OUT
12	-0.94	-0.55	-0.04	-0.04	-0.59	0.77	0.20	0.57	0.85	-2.44	-3.40	0.16	W09
12	-0.85	-0.55	-0.04	-0.04	-0.59	0.77	0.01	0.57	0.85	-2.26	-3.40	0.16	W09
12	-0.85	-0.55	-0.04	-0.04	-0.59	0.77	-0.20	0.57	0.85	-2.26	-3.40	0.16	W09
13	-1.27	0.17	0.03	-0.04	-0.30	1.45	-11.00	0.44	0.69	-1.98	3.40	0.20	N18
13	0.72	-0.27	0.03	-0.04	-0.30	1.39	-12.56	0.28	0.69	-1.85	3.40	0.20	N72
13	-1.06	-0.56	0.03	-0.04	-0.30	1.39	-13.94	0.43	0.69	-2.02	3.40	0.20	N18
13	-0.99	-0.46	0.03	-0.04	-0.30	1.39	-13.70	0.43	0.69	-2.02	3.40	0.20	N18
13	-0.99	-0.46	0.03	-0.04	-0.30	1.39	-13.94	0.43	0.69	-2.02	3.40	0.20	N18
13	-0.89	-0.46	0.03	-0.04	-0.30	1.39	-13.94	0.43	0.69	-1.92	3.40	0.20	N18
13	0.62	-0.05	0.03	-0.04	-0.30	1.39	-17.05	0.43	0.69	-1.92	3.40	0.20	N07
13	0.92	-0.17	0.03	-0.04	-0.30	1.39	-17.05	0.43	0.69	-1.79	3.40	0.20	N07
13	0.75	-0.17	0.03	-0.04	-0.30	1.39	-17.05	0.43	0.69	-1.79	3.40	0.20	N07
13	0.87	-0.13	0.03	-0.04	-0.30	1.39	-17.05	0.43	0.69	-1.90	3.40	0.20	N07
14	-0.05	-0.79	-0.06	-0.05	-0.34	1.57	-10.40	0.42	0.34	-2.75	-3.00	0.11	E02
14	5.50	-2.07	-0.06	-0.05	-0.34	1.57	-6.69	0.47	0.34	-2.83	-3.00	0.11	W36
14	1.01	0.18	-0.06	-0.05	-0.34	1.57	-8.41	0.47	0.34	-2.83	-3.00	0.11	W18
14	1.01	0.18	-0.06	-0.05	-0.34	1.57	-8.28	0.47	0.34	-2.83	-3.00	0.11	W18
14	-0.69	-0.84	-0.06	-0.05	-0.34	1.57	-7.81	0.47	0.34	-2.83	-3.00	0.11	W09
14	-0.69	-0.84	-0.06	-0.05	-0.34	1.57	-7.81	0.47	0.34	-2.83	-3.00	0.11	W09
14	-0.76	-0.84	-0.06	-0.05	-0.34	1.57	-8.00	0.47	0.34	-2.83	-3.00	0.11	OUT
14	-0.76	-0.84	-0.06	-0.05	-0.34	1.57	-8.00	0.47	0.34	-2.83	-3.00	0.11	OUT
14	-0.76	-0.84	-0.06	-0.05	-0.34	1.57	-8.00	0.47	0.34	-2.83	-3.00	0.11	OUT
14	0.50	-0.42	-0.06	-0.05	-0.34	1.57	-4.31	0.47	0.34	-2.38	-3.00	0.11	N06
15	-1.27	0.17	-0.05	0.15	0.08	0.25	-6.40	0.22	0.15	0.55	-0.14	0.13	OUT
15	0.30	0.72	-0.05	0.15	0.08	0.30	-5.11	0.17	0.15	0.39	-0.14	0.13	N32
15	0.44	-0.01	-0.05	0.15	0.08	0.30	-7.38	0.17	0.15	0.27	-0.14	0.13	N14
15	0.57	-0.01	-0.05	0.15	0.08	0.30	-7.38	0.17	0.15	0.27	-0.14	0.13	N14
15	0.57	-0.01	-0.05	0.15	0.08	0.30	-7.38	0.17	0.15	0.27	-0.14	0.13	N14
15	0.65	-0.01	-0.05	0.15	0.08	0.30	-7.38	0.17	0.15	0.44	-0.14	0.13	N14
15	-2.56	-0.01	-0.05	0.15	0.08	0.30	-9.85	0.17	0.15	0.44	-0.14	0.13	N03
15	-1.74	-0.17	-0.05	0.15	0.08	0.30	-9.61	0.17	0.15	0.44	-0.14	0.13	N03
15	-1.93	-0.17	-0.05	0.15	0.08	0.30	-9.61	0.17	0.15	0.44	-0.14	0.13	N03
15	-1.80	-0.07	-0.05	0.15	0.08	0.30	-9.61	0.17	0.15	0.44	-0.14	0.13	N03
16	0.59	-1.24	-0.01	0.10	-0.19	-0.20	-2.38	0.35	0.36	-1.44	-3.40	0.52	E06
16	0.11	-0.05	-0.01	0.10	-0.19	-0.20	-3.11	0.23	0.36	-1.46	-3.40	0.52	E12
16	0.11	-0.06	-0.01	0.10	-0.19	-0.20	-3.11	0.23	0.36	-1.36	-3.40	0.52	OUT
16	0.11	-0.06	-0.01	0.10	-0.19	-0.20	-3.11	0.23	0.36	-1.36	-3.40	0.52	OUT
16	0.22	-0.92	-0.01	0.10	-0.19	-0.20	-1.33	0.23	0.36	-1.36	-3.40	0.52	E03
16	0.33	-0.92	-0.01	0.10	-0.19	-0.20	-1.33	0.43	0.36	-1.36	-3.40	0.52	E03
16	0.23	-0.85	-0.01	0.10	-0.19	-0.20	-1.50	0.43	0.36	-1.36	-3.40	0.52	E03
16	0.23	-0.85	-0.01	0.10	-0.19	-0.20	-1.50	0.43	0.36	-1.21	-3.40	0.52	E03
16	0.23	-0.85	-0.01	0.10	-0.19	-0.20	-1.50	0.43	0.36	-1.21	-3.40	0.52	E03
16	0.23	-0.85	-0.01	0.10	-0.19	-0.20	-1.70	0.43	0.36	-1.33	-3.40	0.52	E03
17	0.67	-0.85	-0.15	-0.07	0.16	1.42	-2.17	0.27	0.18	-1.92	0.39	0.91	N04
17	-0.16	-0.85	-0.15	-0.07	0.16	1.43	-3.98	0.30	0.18	-1.82	0.39	0.91	E36
17	0.93	-0.52	-0.15	-0.07	0.16	1.43	-4.97	0.30	0.18	-2.06	0.39	0.91	E18
17	0.93	-0.72	-0.15	-0.07	0.16	1.43	-4.78	0.30	0.18	-2.06	0.39	0.91	E18
17	-2.87	2.51	-0.15	-0.07	0.16	1.43	-2.96	0.30	0.18	-2.06	0.39	0.91	E09
17	-2.73	2.63	-0.15	-0.07	0.16	1.43	-2.76	0.30	0.18	-2.06	0.39	0.91	E09
17	-2.73	2.63	-0.15	-0.07	0.16	1.43	-2.76	0.30	0.18	-2.06	0.39	0.91	E09
17	-2.73	2.63	-0.15	-0.07	0.16	1.43	-2.76	0.30	0.18	-2.06	0.39	0.91	E09
17	-3.14	2.63	-0.15	-0.07	0.16	1.43	-3.50	0.30	0.18	-2.06	0.39	0.91	E09
17	-2.79	2.63	-0.15	-0.07	0.16	1.43	-3.30	0.30	0.18	-2.06	0.39	0.91	E09
18	-0.40	0.83	-0.02	0.08	-0.22	0.08	-0.02	0.31	0.40	-1.65	0.10	0.24	E12
18	0.04	0.09	-0.02	0.08	-0.22	0.07	1.04	0.22	0.40	-1.82	0.10	0.24	E24
18	0.12	-0.49	-0.02	0.08	-0.22	0.07	1.04	0.22	0.40	-1.82	0.10	0.24	E06
18	0.12	-0.71	-0.02	0.08	-0.22	0.07	1.39	0.22	0.40	-1.82	0.10	0.24	E06
18	0.12	-0.59	-0.02	0.08	-0.22	0.07	1.13	0.22	0.40	-1.82	0.10	0.24	E06
18	0.12	-0.70	-0.02	0.08	-0.22	0.07	1.13	0.22	0.40	-1.82	0.10	0.24	E06

18	0.12	-0.70	-0.02	0.08	-0.22	0.07	1.13	0.22	0.40	-1.82	0.10	0.24	E06
18	0.12	-0.81	-0.02	0.08	-0.22	0.07	1.13	0.22	0.40	-1.82	0.10	0.24	E06
18	-0.14	-0.56	-0.02	0.08	-0.22	0.07	1.13	0.22	0.40	-1.82	0.10	0.24	E06
18	0.13	-0.72	-0.02	0.08	-0.22	0.07	0.84	0.22	0.40	-1.82	0.10	0.24	E06
19	0.34	-0.55	-0.05	0.01	0.01	1.21	2.70	0.42	0.43	-0.40	-0.66	0.85	N06
19	0.41	-0.98	-0.05	0.01	0.01	1.21	1.13	0.42	0.43	-0.37	-0.66	0.85	N04
19	0.39	-0.87	-0.05	0.01	0.01	1.21	0.96	0.42	0.43	-0.44	-0.66	0.85	N04
19	0.47	-0.87	-0.05	0.01	0.01	1.21	1.12	0.42	0.43	-0.44	-0.66	0.85	N04
19	0.47	-0.87	-0.05	0.01	0.01	1.21	0.96	0.42	0.43	-0.44	-0.66	0.85	N04
19	0.47	-0.87	-0.05	0.01	0.01	1.21	0.96	0.42	0.43	-0.28	-0.66	0.85	N04
19	0.47	-0.87	-0.05	0.01	0.01	1.21	0.96	0.42	0.43	-0.43	-0.66	0.85	N04
19	0.47	-0.99	-0.05	0.01	0.01	1.21	0.96	0.42	0.43	-0.33	-0.66	0.85	N04
19	0.29	-0.99	-0.05	0.01	0.01	1.21	0.96	0.42	0.43	-0.33	-0.66	0.85	N04
19	0.44	-0.93	-0.05	0.01	0.01	1.21	0.84	0.42	0.43	-0.33	-0.66	0.85	N04
20	0.02	0.68	0.07	0.01	0.12	0.22	-1.58	0.34	0.38	-4.74	2.50	0.48	W10
20	0.70	-0.63	0.07	0.01	0.12	0.19	-6.72	0.27	0.38	-4.76	2.50	0.48	E28
20	0.63	-0.93	0.07	0.01	0.12	0.19	-9.57	0.27	0.38	-4.86	2.50	0.48	E10
20	0.72	-1.02	0.07	0.01	0.12	0.19	-9.57	0.27	0.38	-4.86	2.50	0.48	E10
20	0.83	-0.46	0.07	0.01	0.12	0.19	-6.08	0.27	0.38	-4.50	2.50	0.48	E01
20	0.83	-0.46	0.07	0.01	0.12	0.19	-6.08	0.27	0.38	-4.50	2.50	0.48	E01
20	0.83	-0.46	0.07	0.01	0.12	0.19	-6.08	0.27	0.38	-4.50	2.50	0.48	E01
20	0.83	-0.56	0.07	0.01	0.12	0.19	-6.31	0.27	0.38	-4.50	2.50	0.48	E01
20	0.83	-0.56	0.07	0.01	0.12	0.19	-6.31	0.27	0.38	-4.50	2.50	0.48	E01
20	0.83	-0.56	0.07	0.01	0.12	0.19	-6.31	0.27	0.38	-4.50	2.50	0.48	E01
21	-0.03	-1.35	0.03	-0.10	-0.38	0.11	-1.00	0.50	0.21	-1.73	-0.61	0.23	E04
21	0.48	-0.61	0.03	-0.10	-0.38	0.16	0.38	0.53	0.21	-1.70	-0.61	0.23	W32
21	-0.77	-0.31	0.03	-0.10	-0.38	0.16	-0.01	0.37	0.21	-1.61	-0.61	0.23	W14
21	-0.70	-0.31	0.03	-0.10	-0.38	0.16	-0.01	0.37	0.21	-1.61	-0.61	0.23	W14
21	0.46	-0.94	0.03	-0.10	-0.38	0.16	-1.19	0.37	0.21	-1.74	-0.61	0.23	W05
21	0.58	-0.94	0.03	-0.10	-0.38	0.16	-1.19	0.37	0.21	-1.74	-0.61	0.23	W05
21	0.42	-0.94	0.03	-0.10	-0.38	0.16	-1.19	0.37	0.21	-1.74	-0.61	0.23	W05
21	0.42	-0.94	0.03	-0.10	-0.38	0.16	-1.19	0.37	0.21	-1.74	-0.61	0.23	W05
21	0.42	-0.94	0.03	-0.10	-0.38	0.16	-1.19	0.37	0.21	-1.74	-0.61	0.23	W05
21	0.42	-1.02	0.03	-0.10	-0.38	0.16	-1.19	0.37	0.21	-1.74	-0.61	0.23	W05
22	-0.08	-1.27	0.00	0.00	0.00	-1.04	1.70	0.20	0.00	-1.25	-0.36	0.57	W02
22	0.17	-0.22	0.14	-0.08	-0.15	-0.66	3.73	0.29	0.43	-1.45	-0.36	0.57	W28
22	0.42	1.15	0.14	-0.08	-0.15	-0.66	7.49	0.42	0.43	-1.54	-0.36	0.57	W10
22	0.42	1.15	0.14	-0.08	-0.15	-0.66	7.49	0.42	0.43	-1.54	-0.36	0.57	W10
22	0.42	1.07	0.14	-0.08	-0.15	-0.66	7.49	0.27	0.43	-1.45	-0.36	0.57	W10
22	0.42	1.18	0.14	-0.08	-0.15	-0.66	7.49	0.43	0.43	-1.45	-0.36	0.57	W10
22	0.15	0.72	0.14	-0.08	-0.15	-0.66	5.17	0.43	0.43	-1.45	-0.36	0.57	W01
22	0.08	0.55	0.14	-0.08	-0.15	-0.66	5.34	0.43	0.43	-1.45	-0.36	0.57	W01
22	0.08	0.55	0.14	-0.08	-0.15	-0.66	5.34	0.43	0.43	-1.17	-0.36	0.57	W01
22	0.08	0.48	0.14	-0.08	-0.15	-0.66	5.63	0.43	0.43	-1.39	-0.36	0.57	W01
23	-0.29	-0.05	0.07	-0.08	-0.12	0.20	-3.83	0.49	0.69	-0.98	-0.05	0.46	E08
23	-0.18	-0.16	0.07	-0.08	-0.12	0.20	-4.12	0.49	0.69	-0.88	-0.05	0.46	E08
23	-0.62	0.18	0.07	-0.08	-0.12	0.20	-5.57	0.49	0.69	-0.88	-0.05	0.46	E02
23	-0.62	-0.18	0.07	-0.08	-0.12	0.20	-5.83	0.49	0.69	-1.10	-0.05	0.46	E02
23	-0.62	-0.18	0.07	-0.08	-0.12	0.20	-5.83	0.49	0.69	-1.10	-0.05	0.46	E02
23	-0.62	-0.18	0.07	-0.08	-0.12	0.20	-5.83	0.49	0.69	-1.10	-0.05	0.46	E02
23	-0.62	-0.18	0.07	-0.08	-0.12	0.20	-5.83	0.49	0.69	-1.10	-0.05	0.46	E02
23	-0.49	-0.18	0.07	-0.08	-0.12	0.20	-5.83	0.49	0.69	-1.10	-0.05	0.46	E02
23	-0.49	-0.18	0.07	-0.08	-0.12	0.20	-5.83	0.49	0.69	-1.10	-0.05	0.46	E02
23	-0.65	-0.18	0.07	-0.08	-0.12	0.20	-5.83	0.49	0.69	-1.10	-0.05	0.46	E02
24	-0.76	-0.53	-0.05	-0.03	-0.30	-0.01	0.87	0.46	0.39	-2.42	0.76	0.41	E16
24	0.34	-0.51	-0.05	-0.03	-0.30	0.03	1.18	0.38	0.39	-2.39	0.76	0.41	E20
24	-0.61	-0.49	-0.05	-0.03	-0.30	0.03	1.39	0.38	0.39	-2.37	0.76	0.41	E16
24	-0.61	-0.71	-0.05	-0.03	-0.30	0.03	1.39	0.38	0.39	-2.51	0.76	0.41	E16
24	-6.40	-2.60	-0.05	-0.03	-0.30	0.03	-2.52	0.38	0.39	-2.51	0.76	0.41	E07
24	-6.40	-2.47	-0.05	-0.03	-0.30	0.03	-2.52	0.38	0.39	-2.51	0.76	0.41	E07
24	-6.47	-2.47	-0.05	-0.03	-0.30	0.03	-2.52	0.38	0.39	-2.51	0.76	0.41	E07
24	-6.47	-2.47	-0.05	-0.03	-0.30	0.03	-2.83	0.38	0.39	-2.35	0.76	0.41	E07
24	-6.82	-2.32	-0.05	-0.03	-0.30	0.03	-2.83	0.38	0.39	-2.35	0.76	0.41	E07

24	-6.45	-2.47	-0.05	-0.03	-0.30	0.03	-2.83	0.38	0.39	-2.47	0.76	0.41	E07
25	-0.05	-0.18	-0.12	0.02	-0.02	-2.13	-5.50	0.41	0.24	-1.00	0.34	0.73	N16
25	0.31	0.24	-0.12	0.02	-0.02	-2.18	-0.65	0.41	0.24	-1.50	0.34	0.73	N20
25	-0.24	0.29	-0.12	0.02	-0.02	-2.18	-1.81	0.41	0.24	0.56	0.34	0.73	N02
25	0.30	0.25	-0.12	0.02	-0.02	-2.18	-1.81	0.41	0.24	0.56	0.34	0.73	N02
25	0.24	0.25	-0.12	0.02	-0.02	-2.18	-1.81	0.41	0.24	0.56	0.34	0.73	N02
25	0.34	0.25	-0.12	0.02	-0.02	-2.18	-1.81	0.41	0.24	0.56	0.34	0.73	N02
25	0.27	0.25	-0.12	0.02	-0.02	-2.18	-1.81	0.41	0.24	0.56	0.34	0.73	N02
25	0.27	0.21	-0.12	0.02	-0.02	-2.18	-1.95	0.41	0.24	0.64	0.34	0.73	N02
25	0.27	0.21	-0.12	0.02	-0.02	-2.18	-1.95	0.41	0.24	0.64	0.34	0.73	N02
25	0.23	0.28	-0.12	0.02	-0.02	-2.18	-1.95	0.41	0.24	0.57	0.34	0.73	N02
26	0.28	-0.67	0.08	0.04	-0.45	0.22	-1.81	0.42	1.06	-1.92	2.00	0.00	N14
26	1.29	0.42	0.08	0.04	-0.45	0.20	-1.64	0.42	1.06	-1.94	2.00	0.00	N12
26	1.21	0.34	0.08	0.04	-0.45	0.20	-1.48	0.42	1.06	-1.91	2.00	0.00	N12
26	1.26	0.38	0.08	0.04	-0.45	0.20	-1.48	0.29	1.06	-1.91	2.00	0.00	N12
26	1.26	0.38	0.08	0.04	-0.45	0.20	-1.60	0.41	1.06	-1.91	2.00	0.00	N12
26	1.38	0.38	0.08	0.04	-0.45	0.12	-1.60	0.41	1.06	-1.80	2.00	0.00	N12
26	0.34	-0.44	0.08	0.04	-0.45	0.12	-1.40	0.41	1.06	-1.88	2.00	0.00	N09
26	0.58	-0.44	0.08	0.04	-0.45	0.23	-1.40	0.41	1.06	-1.88	2.00	0.00	N09
26	0.43	-0.44	0.08	0.04	-0.45	0.23	-1.40	0.41	1.06	-1.88	2.00	0.00	N09
26	0.54	-0.40	0.08	0.04	-0.45	0.23	-1.48	0.41	1.06	-1.88	2.00	0.00	N09
27	-1.22	-0.28	-0.02	-0.01	0.36	0.86	8.71	0.21	0.06	-11.14	-0.40	0.46	N08
27	-1.26	-0.34	-0.02	-0.01	0.36	0.79	8.03	0.21	0.06	-11.05	-0.40	0.46	N08
27	-1.30	-0.32	-0.02	-0.01	0.36	0.88	8.24	0.21	0.06	-10.95	-0.40	0.46	N08
27	-1.30	-0.32	-0.02	-0.01	0.36	0.88	8.24	0.21	0.06	-10.95	-0.40	0.46	N08
27	-1.30	-0.32	-0.02	-0.01	0.36	0.88	7.88	0.21	0.06	-10.95	-0.40	0.46	N08
27	-1.14	-0.32	-0.02	-0.01	0.36	0.88	7.88	0.21	0.06	-10.95	-0.40	0.46	N08
27	-1.14	-0.32	-0.02	-0.01	0.36	0.88	8.12	0.21	0.06	-10.95	-0.40	0.46	N08
27	-1.07	-0.41	-0.02	-0.01	0.36	0.88	7.50	0.37	0.06	-15.00	-0.40	0.46	N08
27	-1.25	-0.41	-0.02	-0.01	0.36	2.03	8.00	0.37	0.06	-14.49	-0.40	0.46	N08
27	-1.09	-0.28	-0.02	-0.01	0.36	2.15	8.23	0.37	0.06	-14.89	-0.40	0.46	N08
28	0.63	-0.37	-0.04	0.02	-0.49	0.59	-0.38	0.40	0.40	-0.19	-0.63	0.72	W16
28	0.35	-0.50	-0.04	0.02	-0.49	0.58	2.10	0.30	0.40	0.04	-0.63	0.72	W12
28	0.42	-0.57	-0.04	0.02	-0.49	0.58	1.91	0.30	0.40	-0.07	-0.63	0.72	W12
28	0.42	-0.57	-0.04	0.02	-0.49	0.58	1.91	0.30	0.40	-0.07	-0.63	0.72	W12
28	0.49	-0.24	-0.04	0.02	-0.49	0.58	1.15	0.30	0.40	0.05	-0.63	0.72	W03
28	0.49	-0.24	-0.04	0.02	-0.49	0.58	1.15	0.30	0.40	0.05	-0.63	0.72	W03
28	0.49	-0.24	-0.04	0.02	-0.49	0.58	1.15	0.30	0.40	0.18	-0.63	0.72	W03
28	0.49	-0.24	-0.04	0.02	-0.49	0.58	1.49	0.30	0.40	0.18	-0.63	0.72	W03
28	0.49	-0.24	-0.04	0.02	-0.49	0.58	1.31	0.30	0.40	0.18	-0.63	0.72	W03



## Over-the-top.

row 1 has the full solution and rms using all the data  
 row 2 applies the full solution to the "below-the-top" data only  
 row 3 has the full solution and rms for the "under-the-top" data  
 row 4 applies the restricted solution to all the sources

```

1 -> file : vlax.dec29.93
ant      A6      A7      A2      -A1      E3      E5
                                     RMS
                                     az    el
1 -> file : vlax.dec29.93
1 1      0.9      1.2     -2.6     3.5    -10.1   37.6    0.0    0.0    10.6  11.4
1 1      0.9      1.2     -2.6     3.5    -10.1   37.6    0.0    0.0    8.7  11.2
1 1     -8.8     10.3    -2.7     4.1     21.5   13.3    0.0    0.0    7.7   7.1
1 1     -8.8     10.3    -2.7     4.1     21.5   13.3    0.0    0.0   11.3  20.3

2 1      8.5     -3.7    -3.1     1.5     -0.8   -3.4    0.0    0.0    5.1   5.9
2 1      8.5     -3.7    -3.1     1.5     -0.8   -3.4    0.0    0.0    3.3   6.1
2 1      6.3     -1.6    -2.0     0.7      3.0    -6.0    0.0    0.0    3.1   5.8
2 1      6.3     -1.6    -2.0     0.7      3.0    -6.0    0.0    0.0    5.4   6.2

3 1      5.1     -5.0     1.7    -3.2    -4.7     5.2    0.0    0.0    4.0   7.9
3 1      5.1     -5.0     1.7    -3.2    -4.7     5.2    0.0    0.0    3.3   8.3
3 1      6.5     -6.1     1.2    -3.7     6.5    -3.5    0.0    0.0    3.4   7.5
3 1      6.5     -6.1     1.2    -3.7     6.5    -3.5    0.0    0.0    4.2  10.1

4 1      1.5     -1.9    -1.5    -0.9     0.8     0.0    0.0    0.0    4.3   5.3
4 1      1.5     -1.9    -1.5    -0.9     0.8     0.0    0.0    0.0    4.0   5.3
4 1      1.6     -1.8    -2.6    -0.5     0.5     0.3    0.0    0.0    4.0   5.2
4 1      1.6     -1.8    -2.6    -0.5     0.5     0.3    0.0    0.0    4.5   5.2

5 1     -2.5     -2.9     2.7     1.2     3.7    -2.8    0.0    0.0    3.6   5.3
5 1     -2.5     -2.9     2.7     1.2     3.7    -2.8    0.0    0.0    3.1   5.3
5 1     -1.3     -4.0     1.6     1.9     0.1     0.1    0.0    0.0    3.1   5.1
5 1     -1.3     -4.0     1.6     1.9     0.1     0.1    0.0    0.0    3.8   5.7

7 1      0.9      0.3     2.9     1.2     0.8     7.7    0.0    0.0    5.0  14.6
7 1      0.9      0.3     2.9     1.2     0.8     7.7    0.0    0.0    4.8  15.2
7 1     -0.6     1.5     3.0     1.1    12.4    -1.6    0.0    0.0    4.7  14.8
7 1     -0.6     1.5     3.0     1.1    12.4    -1.6    0.0    0.0    5.1  16.0

8 1    -11.8     4.0     1.8    -0.5     3.8     1.8    0.0    0.0    6.0   5.9
8 1    -11.8     4.0     1.8    -0.5     3.8     1.8    0.0    0.0    5.5   6.0
8 1    -11.0     3.0     0.6     0.4     3.4     2.3    0.0    0.0    5.3   6.0
8 1    -11.0     3.0     0.6     0.4     3.4     2.3    0.0    0.0    6.0   6.1

9 1      7.8     -1.6    -0.5     4.3    -4.2     3.8    0.0    0.0    8.6  12.4
9 1      7.8     -1.6    -0.5     4.3    -4.2     3.8    0.0    0.0    6.9  12.8
9 1      4.0      1.9    -3.8     5.0     8.2    -5.5    0.0    0.0    7.0  11.9
9 1      4.0      1.9    -3.8     5.0     8.2    -5.5    0.0    0.0    9.3  13.9

10 1     14.2    -4.0     3.7     0.9     0.9     2.3    0.0    0.0    4.7   7.8
10 1     14.2    -4.0     3.7     0.9     0.9     2.3    0.0    0.0    4.0   7.9
10 1     12.4    -1.9     2.6     1.4     6.9    -2.2    0.0    0.0    3.8   7.7
10 1     12.4    -1.9     2.6     1.4     6.9    -2.2    0.0    0.0    4.7   8.6

11 1     -9.0      2.7     6.3    -2.8     5.0     4.9    0.0    0.0    4.6   8.8
11 1     -9.0      2.7     6.3    -2.8     5.0     4.9    0.0    0.0    3.6   9.0
11 1     -6.0     -0.5     5.1    -2.8    14.0    -1.5    0.0    0.0    3.1   8.6
11 1     -6.0     -0.5     5.1    -2.8    14.0    -1.5    0.0    0.0    4.9  10.1

12 1     -1.8     -0.8    -3.8    -1.0     4.6    -9.6    0.0    0.0    4.0  11.9
12 1     -1.8     -0.8    -3.8    -1.0     4.6    -9.6    0.0    0.0    3.8  11.4
12 1     -2.2     -0.8    -4.5     1.2    37.3   -34.7    0.0    0.0    3.5   7.2
12 1     -2.2     -0.8    -4.5     1.2    37.3   -34.7    0.0    0.0    3.8  21.1

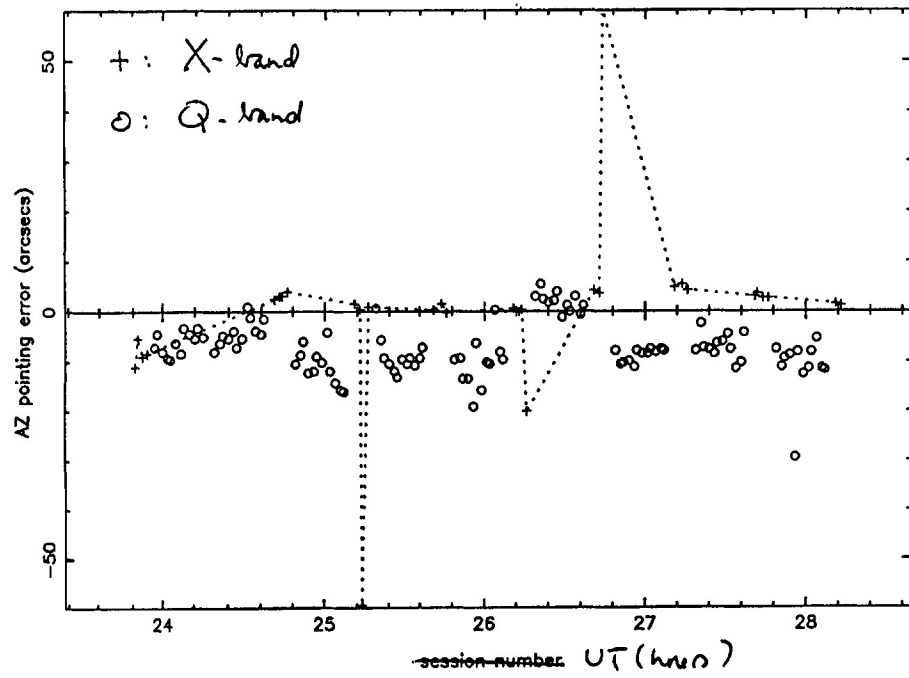
```

13	1	-1.6	4.0	0.4	2.9	-2.5	1.9	0.0	0.0	4.1	8.5
13	1	-1.6	4.0	0.4	2.9	-2.5	1.9	0.0	0.0	4.0	8.7
13	1	-3.1	5.3	-1.4	4.6	5.8	-4.2	0.0	0.0	4.1	8.2
13	1	-3.1	5.3	-1.4	4.6	5.8	-4.2	0.0	0.0	4.4	9.5
14	1	-22.9	2.1	0.0	0.7	-2.1	7.8	0.0	0.0	5.6	9.8
14	1	-22.9	2.1	0.0	0.7	-2.1	7.8	0.0	0.0	4.7	10.0
14	1	-16.5	-4.4	-0.5	1.5	1.4	5.2	0.0	0.0	3.9	9.9
14	1	-16.5	-4.4	-0.5	1.5	1.4	5.2	0.0	0.0	6.4	10.0
15	1	-4.2	6.1	-0.8	1.8	-4.7	-12.8	0.0	0.0	8.9	8.7
15	1	-4.2	6.1	-0.8	1.8	-4.7	-12.8	0.0	0.0	7.9	8.5
15	1	-1.1	2.5	-4.0	3.2	-3.9	-13.5	0.0	0.0	7.3	8.2
15	1	-1.1	2.5	-4.0	3.2	-3.9	-13.5	0.0	0.0	9.4	9.0
16	1	4.8	-5.2	2.8	0.9	1.5	3.7	0.0	0.0	5.3	6.6
16	1	4.8	-5.2	2.8	0.9	1.5	3.7	0.0	0.0	4.2	6.2
16	1	0.4	-1.7	3.0	0.8	3.1	1.8	0.0	0.0	3.8	6.0
16	1	0.4	-1.7	3.0	0.8	3.1	1.8	0.0	0.0	5.5	6.9
17	1	-12.4	2.8	1.2	0.0	-2.7	4.8	0.0	0.0	8.1	7.7
17	1	-12.4	2.8	1.2	0.0	-2.7	4.8	0.0	0.0	6.8	7.4
17	1	-5.7	-2.9	2.9	-0.8	-6.8	8.0	0.0	0.0	6.7	7.1
17	1	-5.7	-2.9	2.9	-0.8	-6.8	8.0	0.0	0.0	8.7	7.9
18	1	-109.4	34.0	1.1	-0.7	-0.2	-0.6	0.0	0.0	20.7	11.9
18	1	-109.4	34.0	1.1	-0.7	-0.2	-0.6	0.0	0.0	14.8	12.0
18	1	-77.9	3.9	3.7	-3.9	8.0	-7.4	0.0	0.0	9.3	11.2
18	1	-77.9	3.9	3.7	-3.9	8.0	-7.4	0.0	0.0	25.1	13.1
19	1	4.7	-1.6	0.1	1.5	0.7	1.4	0.0	0.0	3.5	6.8
19	1	4.7	-1.6	0.1	1.5	0.7	1.4	0.0	0.0	3.2	6.7
19	1	1.7	1.0	-1.6	2.8	2.5	0.3	0.0	0.0	3.0	6.6
19	1	1.7	1.0	-1.6	2.8	2.5	0.3	0.0	0.0	3.5	7.0
20	1	-8.9	5.5	3.2	4.9	2.6	2.1	0.0	0.0	4.6	5.9
20	1	-8.9	5.5	3.2	4.9	2.6	2.1	0.0	0.0	4.7	6.0
20	1	-12.1	8.0	3.8	5.1	7.8	-1.9	0.0	0.0	4.6	5.8
20	1	-12.1	8.0	3.8	5.1	7.8	-1.9	0.0	0.0	4.8	6.6
21	1	-1.8	-2.0	-0.1	1.9	7.8	-1.9	0.0	0.0	4.5	8.0
21	1	-1.8	-2.0	-0.1	1.9	7.8	-1.9	0.0	0.0	4.2	8.6
21	1	-2.5	-1.0	-0.2	2.8	12.4	-5.5	0.0	0.0	4.1	8.5
21	1	-2.5	-1.0	-0.2	2.8	12.4	-5.5	0.0	0.0	4.5	8.4
22	1	0.7	0.6	5.4	-2.1	-8.2	11.1	0.0	0.0	5.6	6.5
22	1	0.7	0.6	5.4	-2.1	-8.2	11.1	0.0	0.0	5.4	6.6
22	1	2.0	0.0	6.2	-2.5	-3.2	7.2	0.0	0.0	5.3	6.3
22	1	2.0	0.0	6.2	-2.5	-3.2	7.2	0.0	0.0	5.7	7.2
23	1	-15.4	2.2	6.9	-2.7	3.1	9.8	0.0	0.0	10.5	14.2
23	1	-15.4	2.2	6.9	-2.7	3.1	9.8	0.0	0.0	9.0	13.4
23	1	-6.7	-4.8	12.8	-5.2	18.6	-2.3	0.0	0.0	8.9	11.4
23	1	-6.7	-4.8	12.8	-5.2	18.6	-2.3	0.0	0.0	11.7	17.4
24	1	-1.8	0.4	4.0	0.6	3.0	2.1	0.0	0.0	6.1	8.4
24	1	-1.8	0.4	4.0	0.6	3.0	2.1	0.0	0.0	4.6	8.4
24	1	-1.3	0.9	5.7	1.2	18.7	-10.1	0.0	0.0	4.4	7.1
24	1	-1.3	0.9	5.7	1.2	18.7	-10.1	0.0	0.0	6.4	11.9
25	1	5.9	-2.5	0.7	3.1	2.7	1.8	0.0	0.0	3.7	6.6
25	1	5.9	-2.5	0.7	3.1	2.7	1.8	0.0	0.0	3.7	6.6
25	1	4.6	-0.9	-0.9	4.5	7.3	-1.6	0.0	0.0	3.7	6.3
25	1	4.6	-0.9	-0.9	4.5	7.3	-1.6	0.0	0.0	3.9	7.1
26	1	-0.3	-3.7	0.9	1.1	3.4	0.5	0.0	0.0	3.9	6.8
26	1	-0.3	-3.7	0.9	1.1	3.4	0.5	0.0	0.0	3.9	7.0
26	1	-3.6	-0.5	-0.3	2.3	4.3	0.2	0.0	0.0	3.9	6.8
26	1	-3.6	-0.5	-0.3	2.3	4.3	0.2	0.0	0.0	4.3	6.9

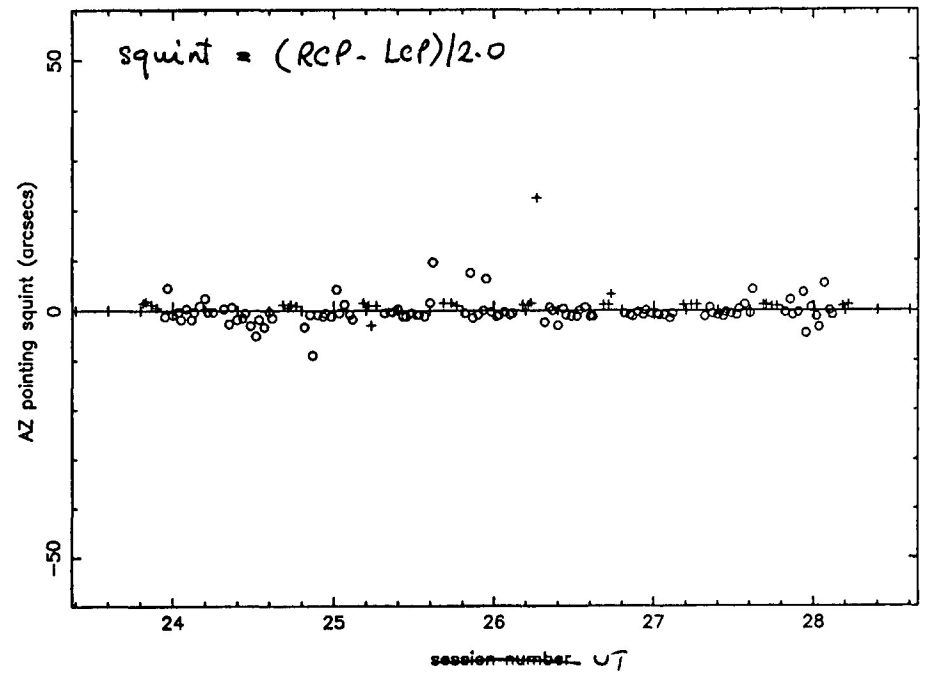


27	1	-0.6	-1.3	-2.6	2.2	-2.9	3.9	0.0	0.0	5.1	8.6
27	1	-0.6	-1.3	-2.6	2.2	-2.9	3.9	0.0	0.0	4.7	9.2
27	1	-1.3	-0.9	-4.9	3.6	2.9	-0.4	0.0	0.0	4.9	8.7
27	1	-1.3	-0.9	-4.9	3.6	2.9	-0.4	0.0	0.0	5.5	9.1
28	1	-18.2	1.5	4.4	0.7	-5.6	1.3	0.0	0.0	6.0	8.8
28	1	-18.2	1.5	4.4	0.7	-5.6	1.3	0.0	0.0	4.4	8.2
28	1	-13.3	-3.2	6.5	-2.0	5.9	-7.0	0.0	0.0	4.1	6.9
28	1	-13.3	-3.2	6.5	-2.0	5.9	-7.0	0.0	0.0	6.6	11.0





Pointing, NOV 30, ant 4



Pointing, NOV 30, ant 4

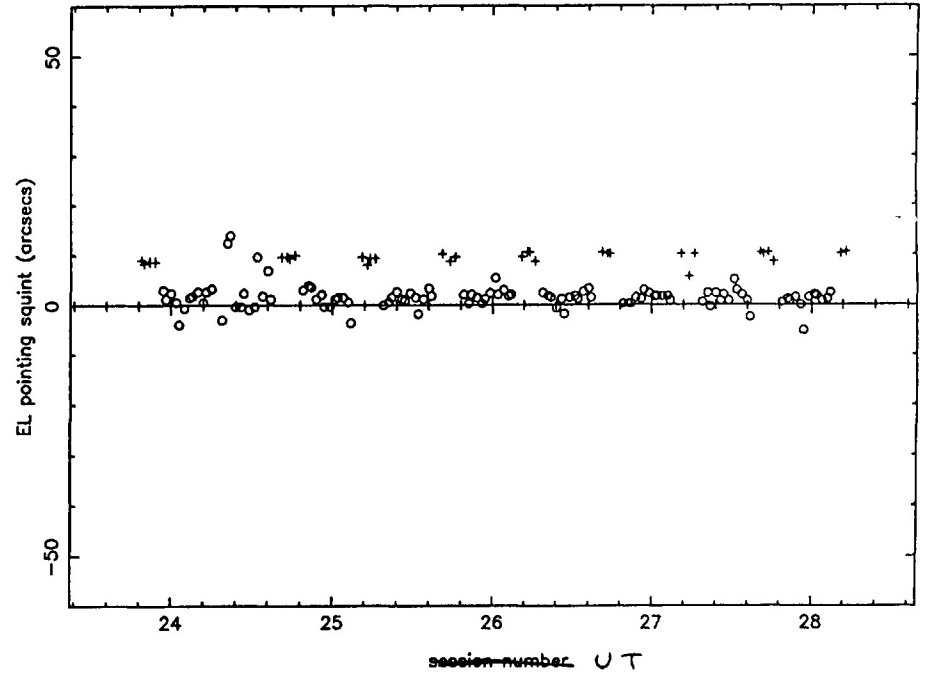
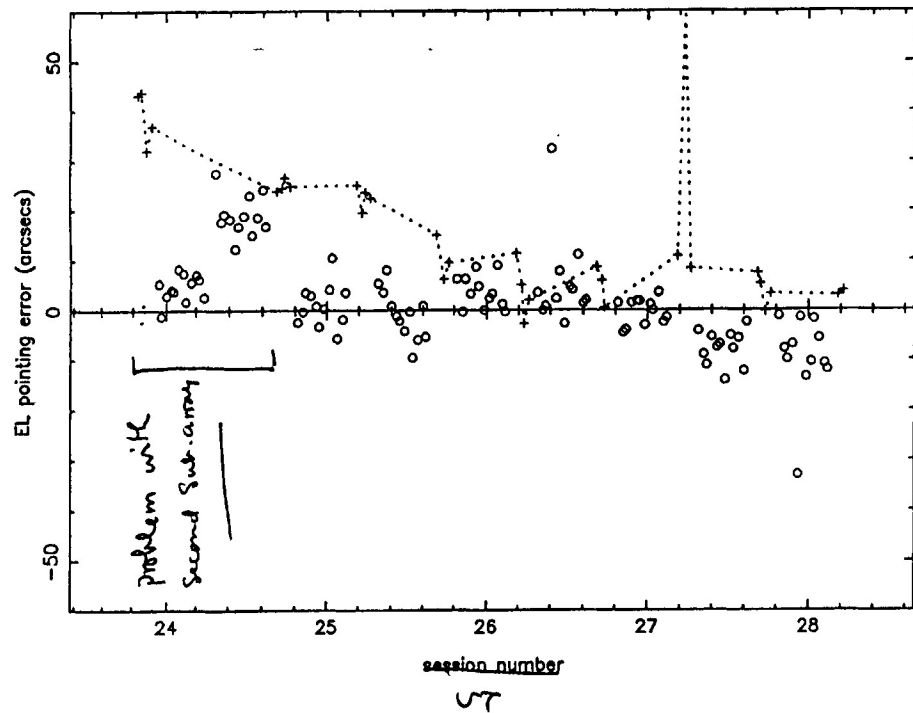
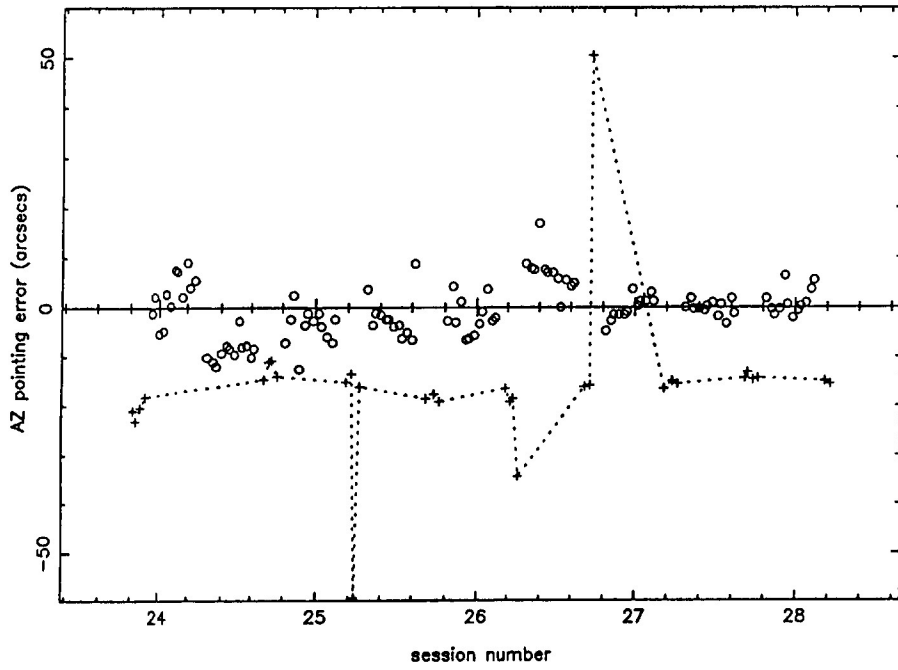
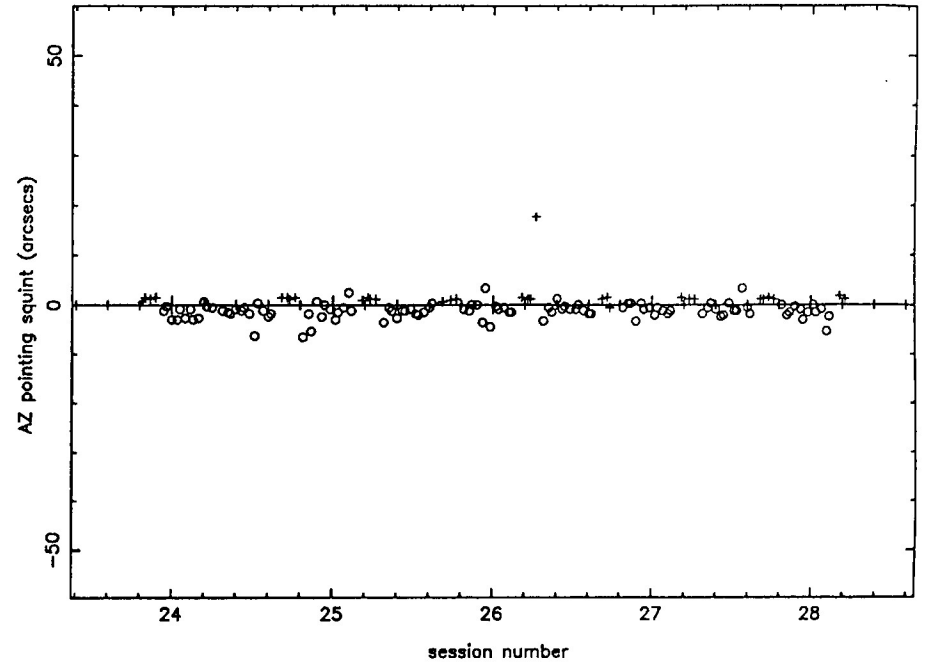


Fig 1

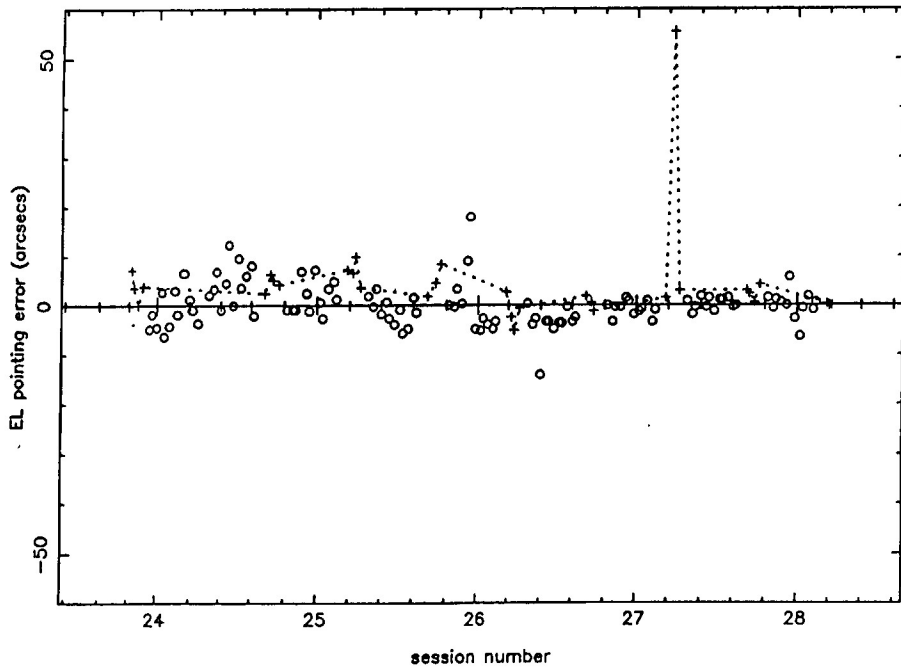
Pointing, NOV 30, ant 8



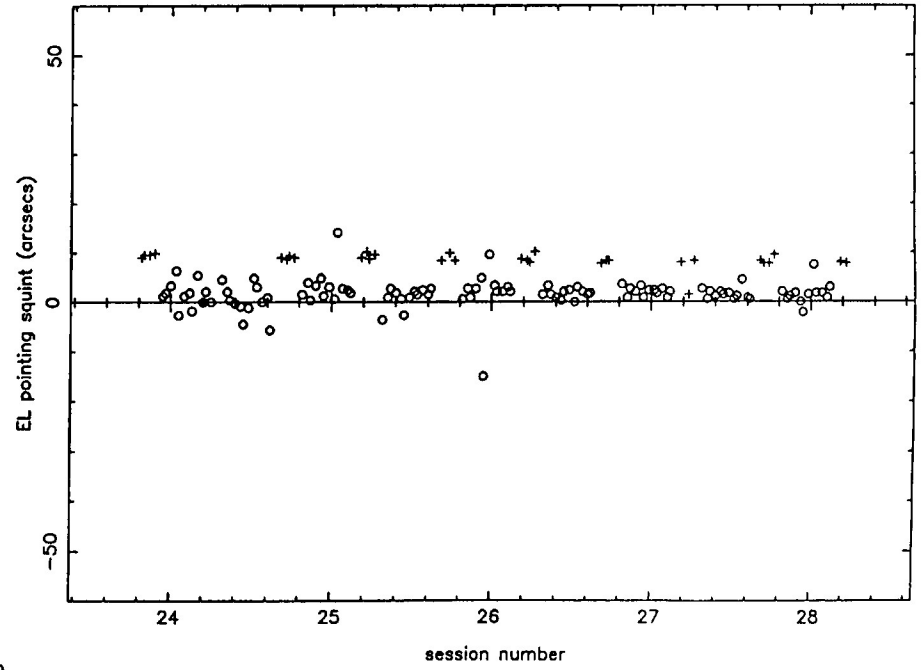
Pointing, NOV 30, ant 8



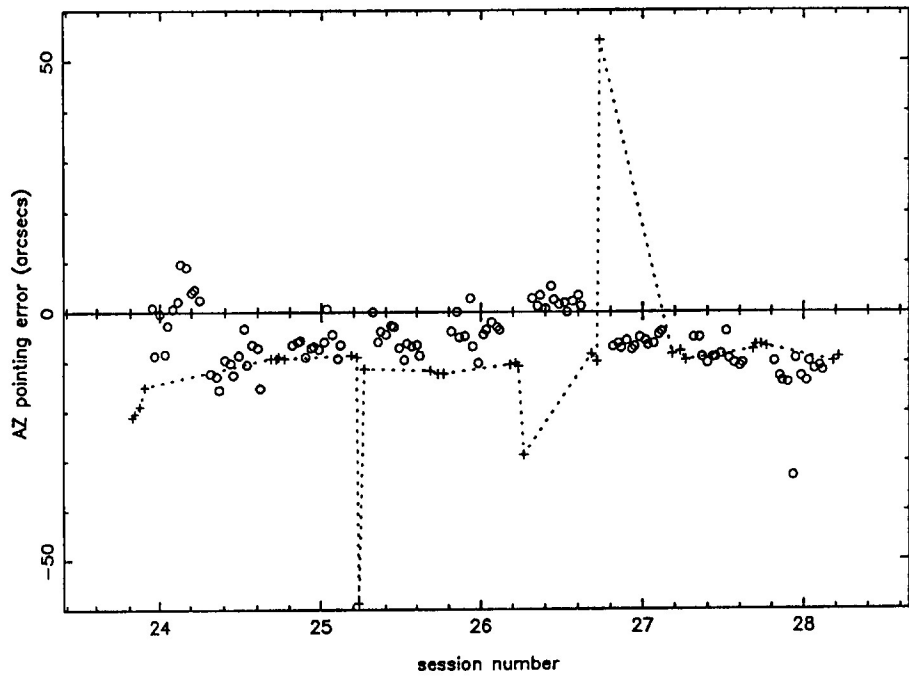
Pointing, NOV 30, ant 8



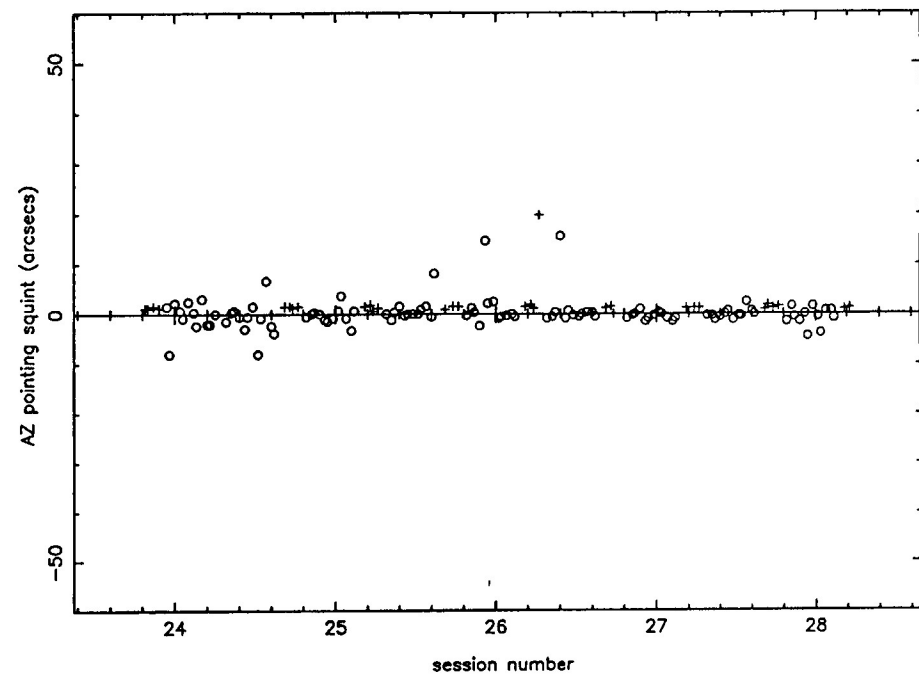
Pointing, NOV 30, ant 8



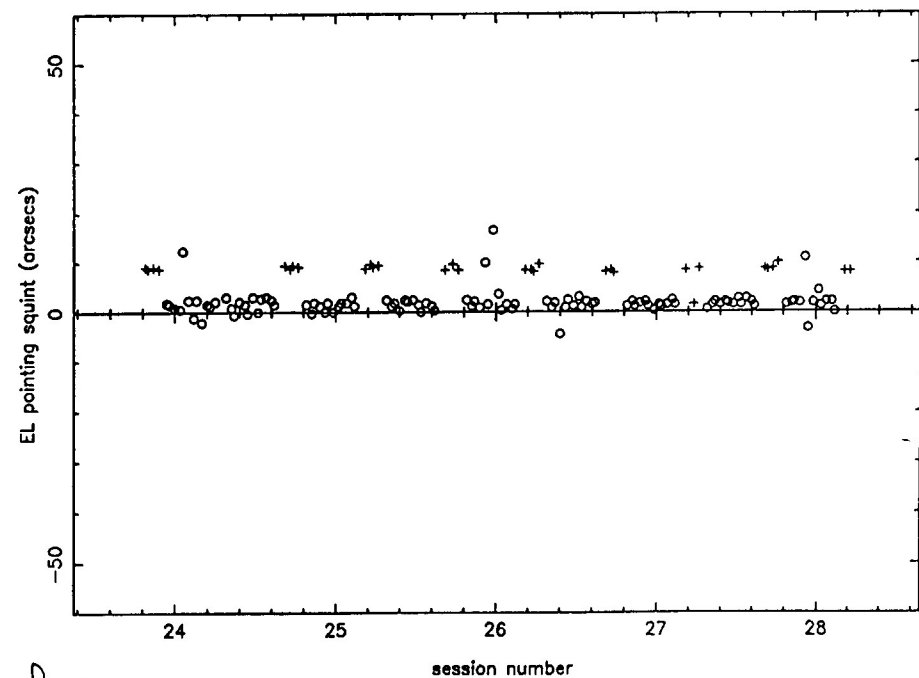
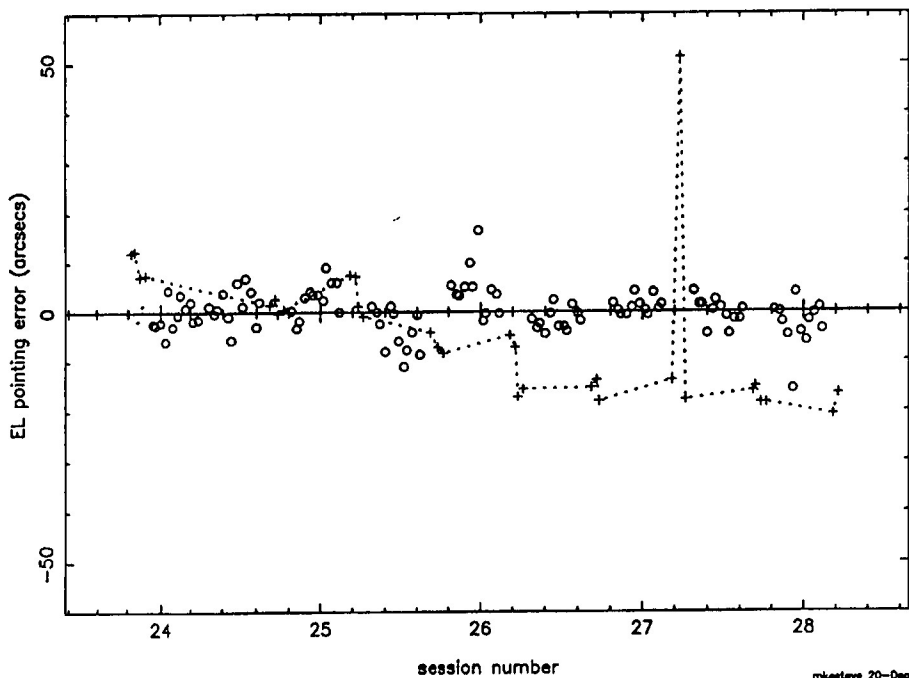
R2



Pointing, NOV 30, ant 12

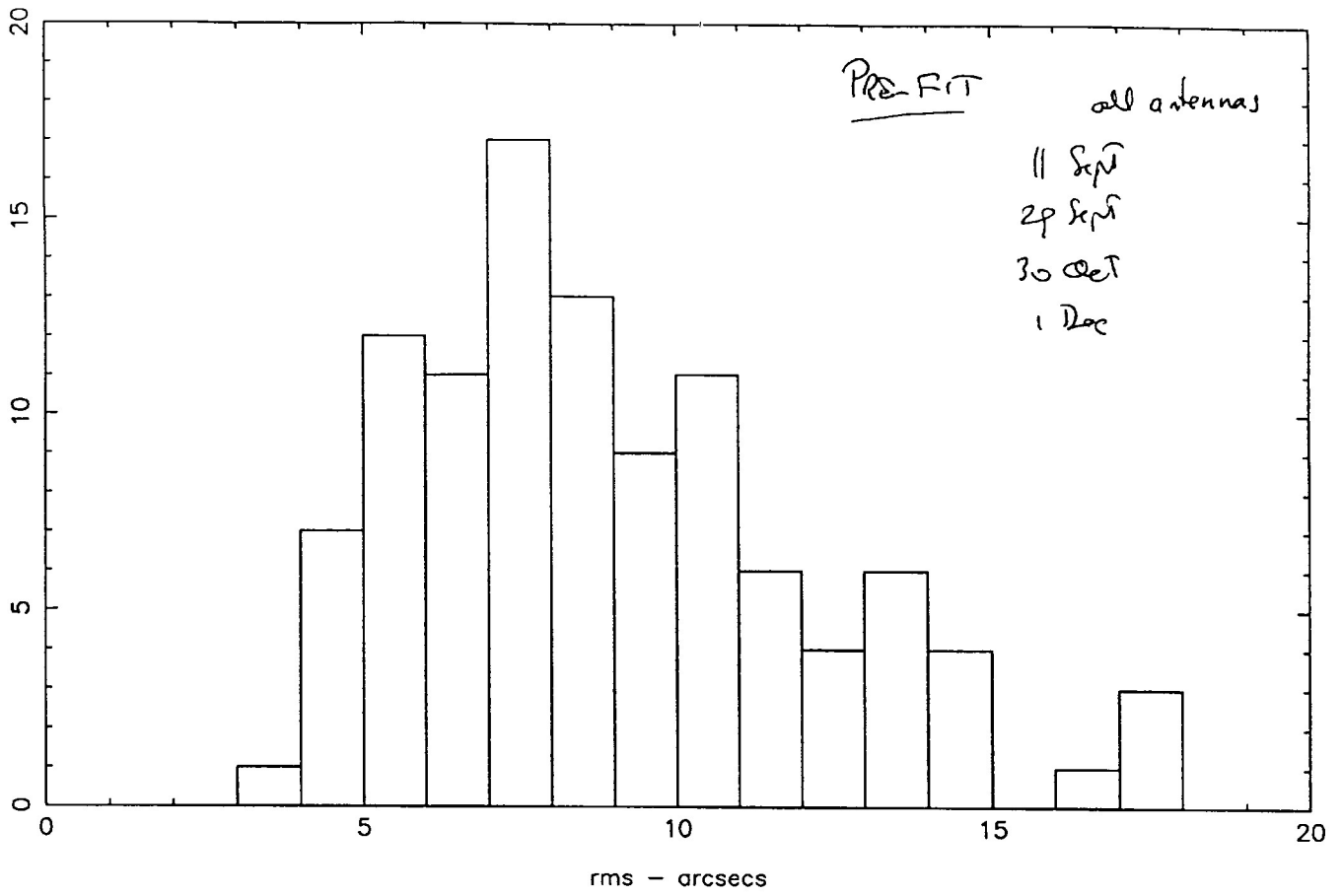


Pointing, NOV 30, ant 12

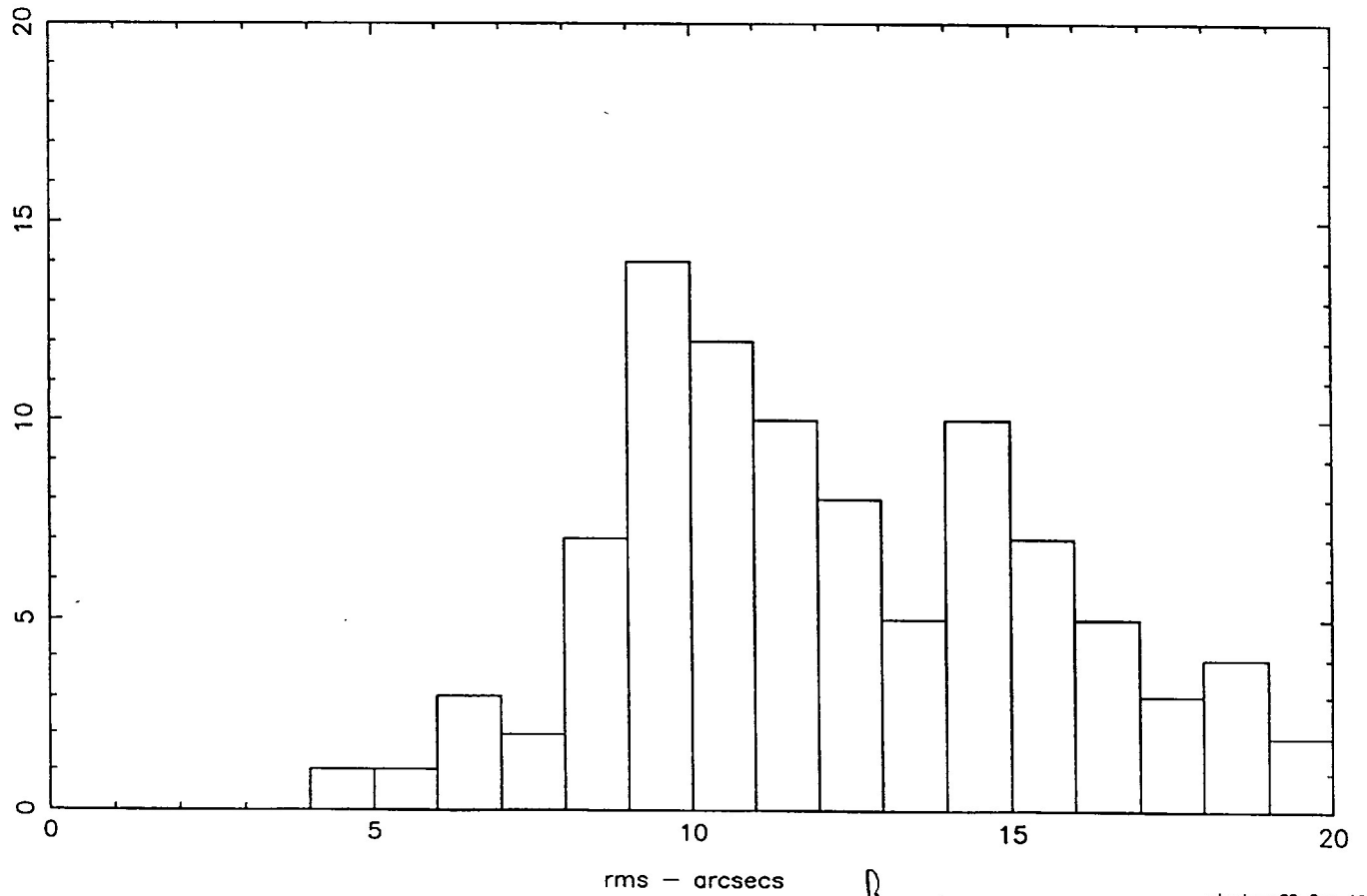


*LS* 3

azimuth pointing rms

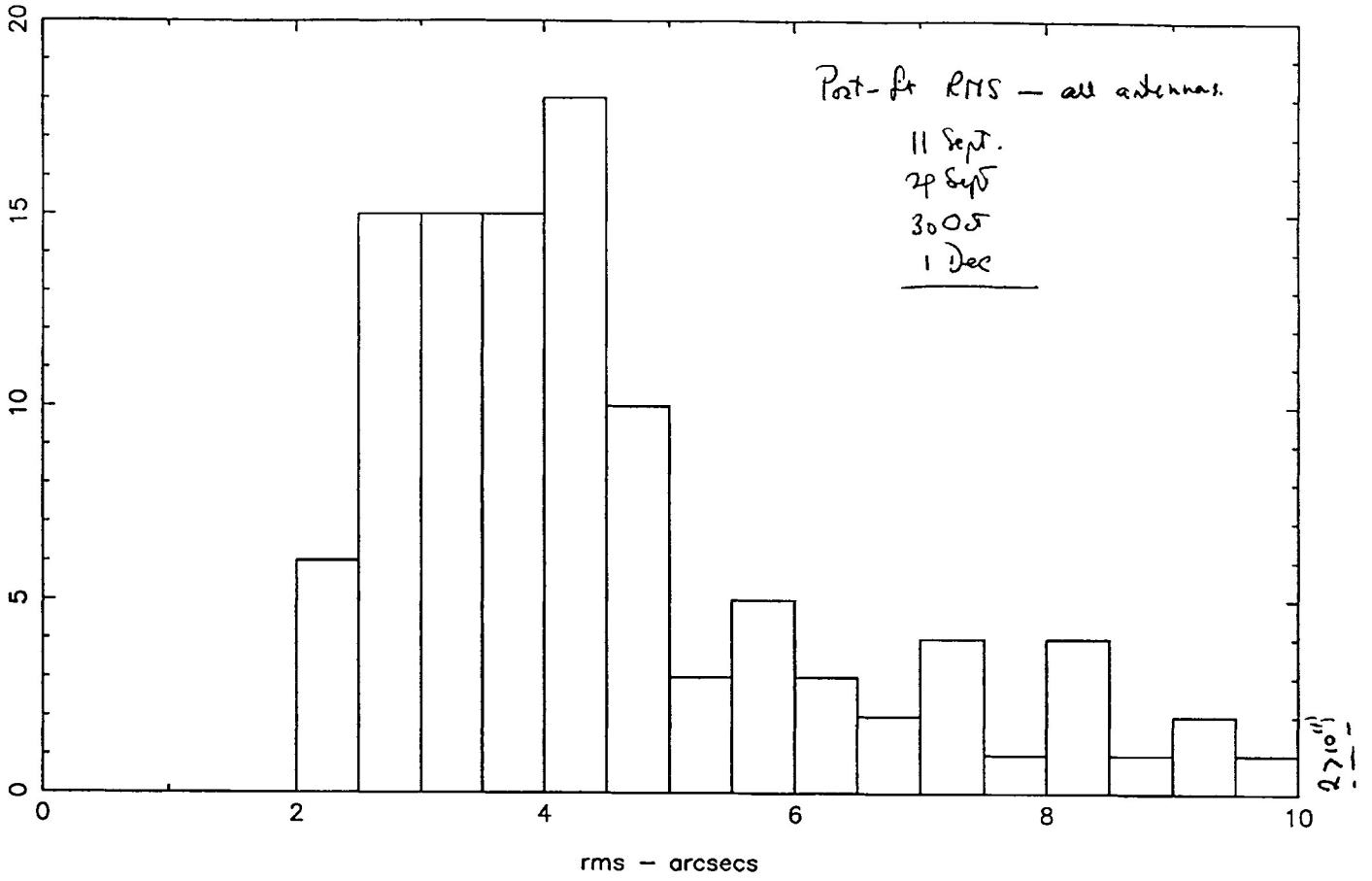


elevation pointing rms



pg 4

azimuth pointing rms



elevation pointing rms

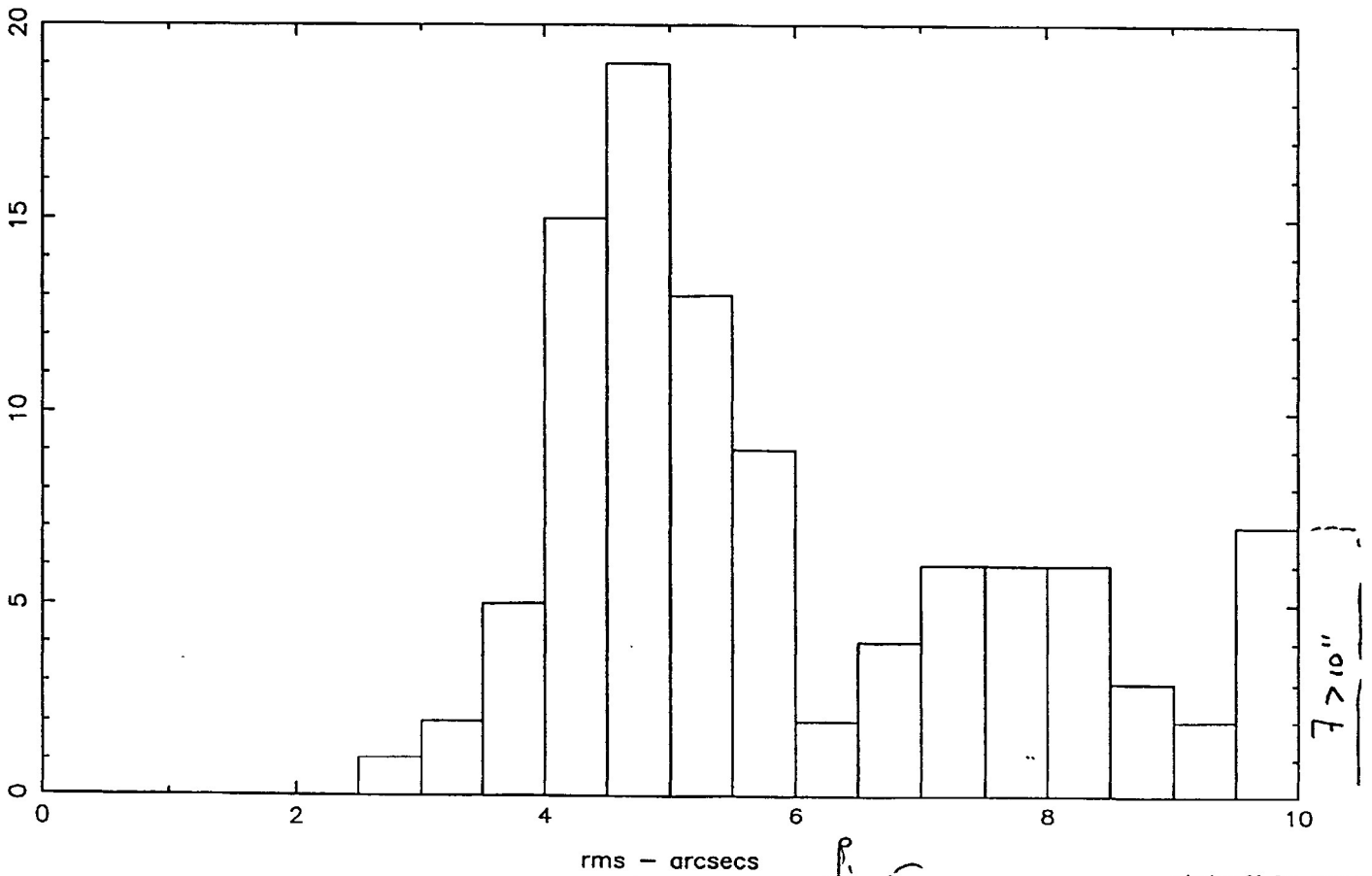


Fig 5

PRE-FIT

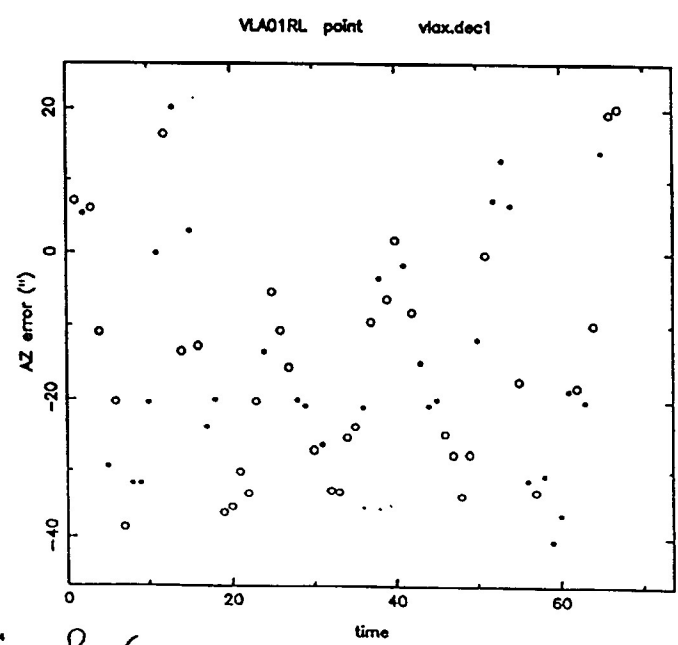
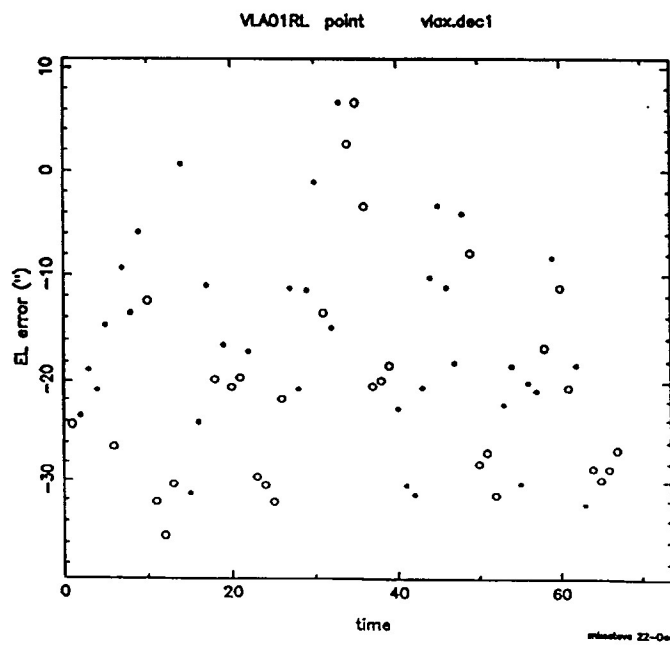
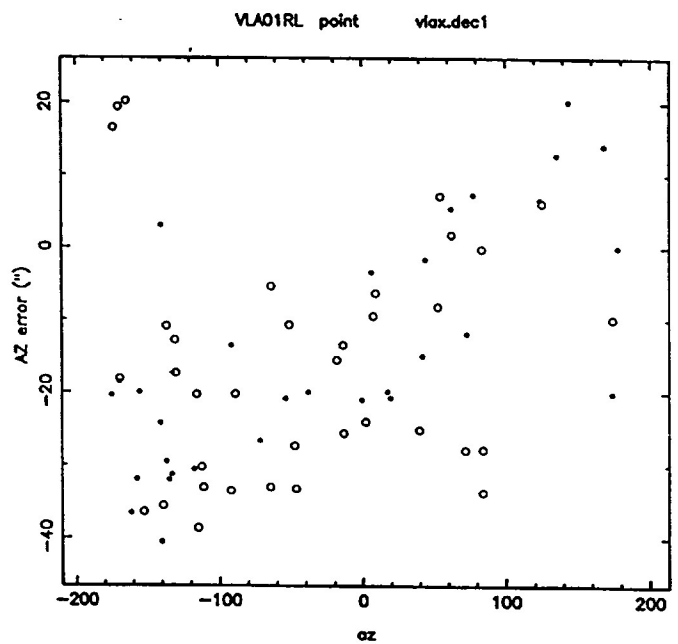
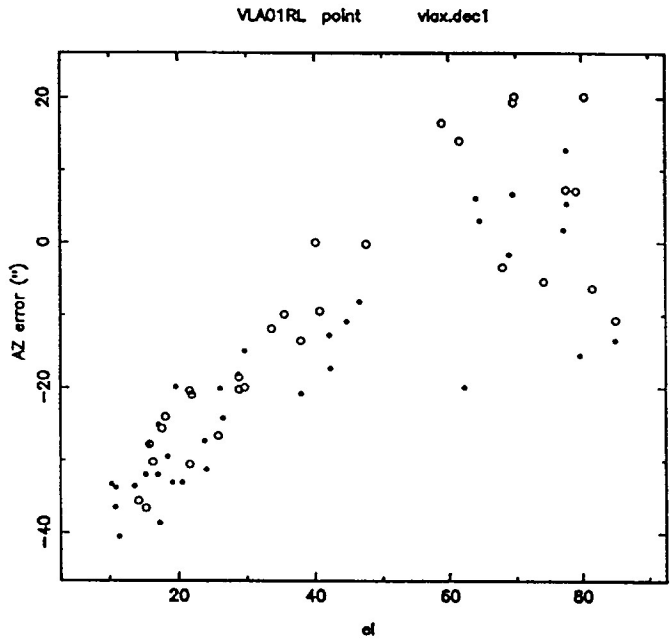
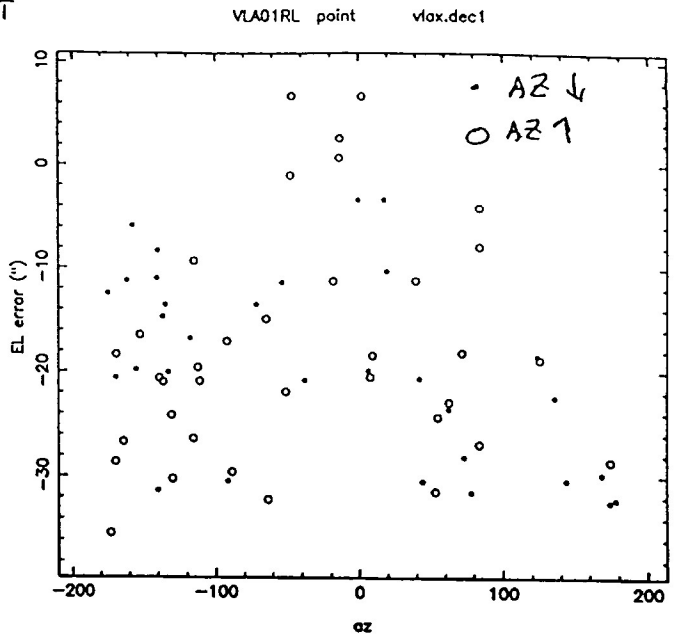
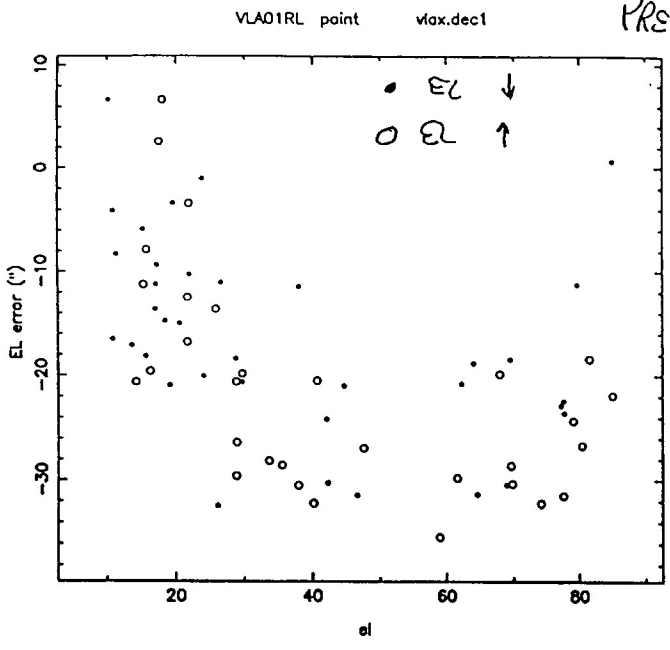
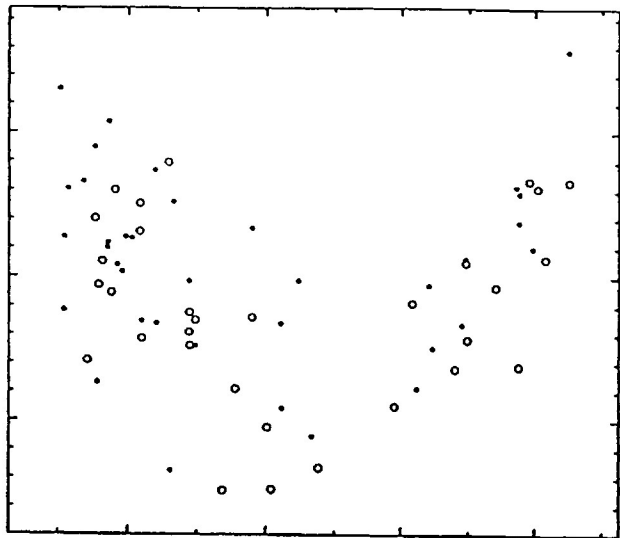


Fig 6 a



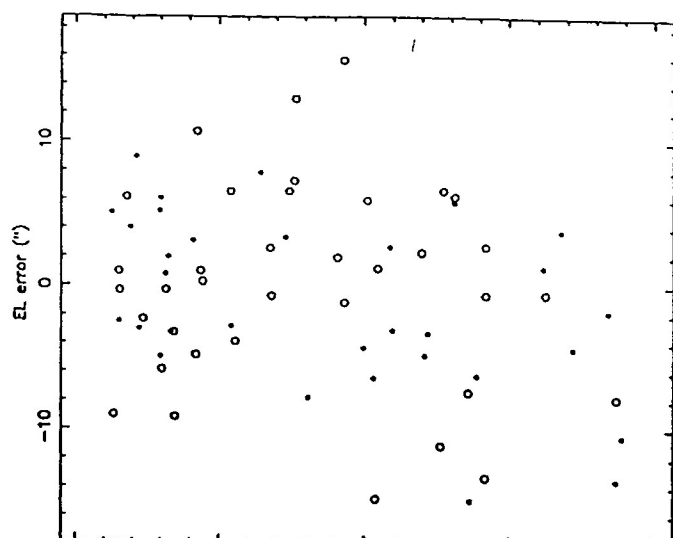
Post-Fit

VLA01RL point vlx.dec1



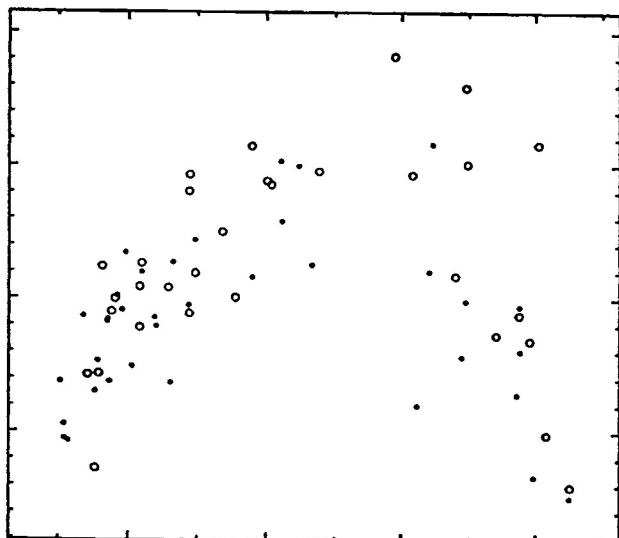
el

VLA01RL point vlx.dec1



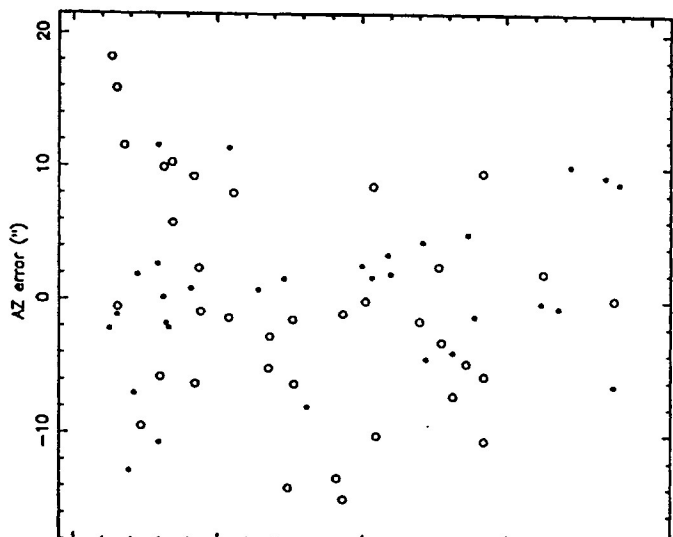
az

VLA01RL point vlx.dec1



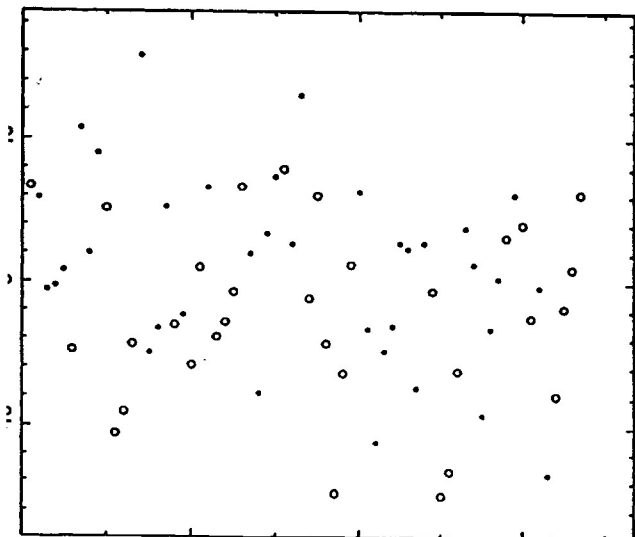
el

VLA01RL point vlx.dec1



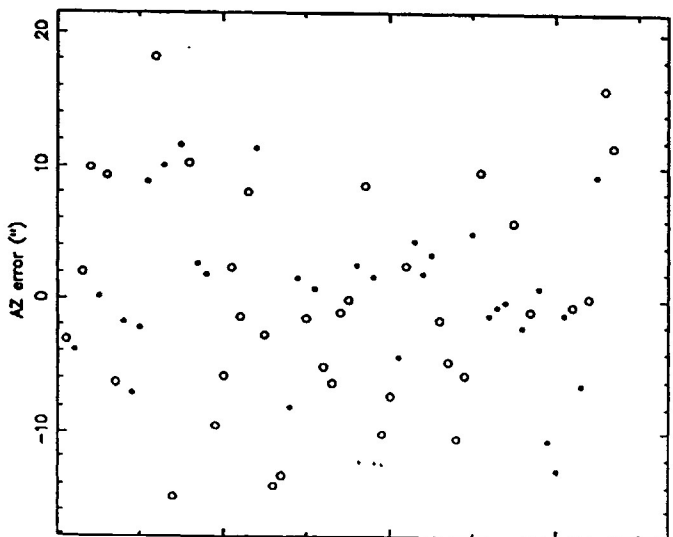
az

VLA01RL point vlx.dec1



time

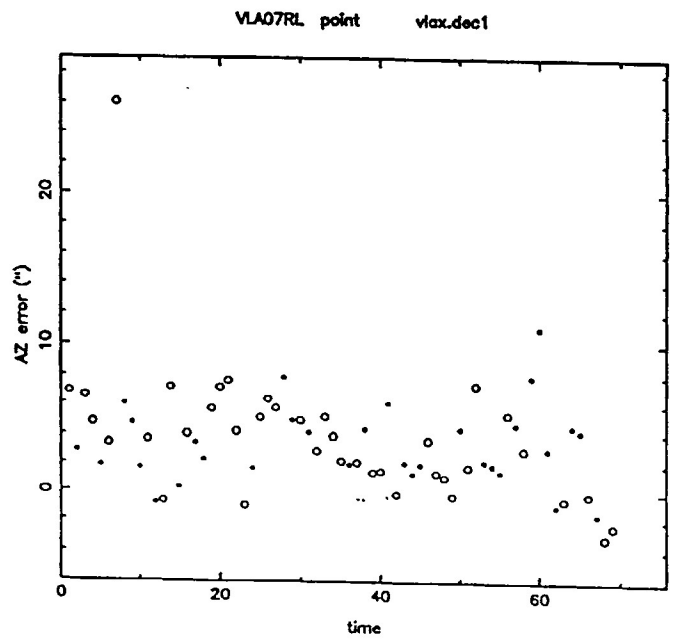
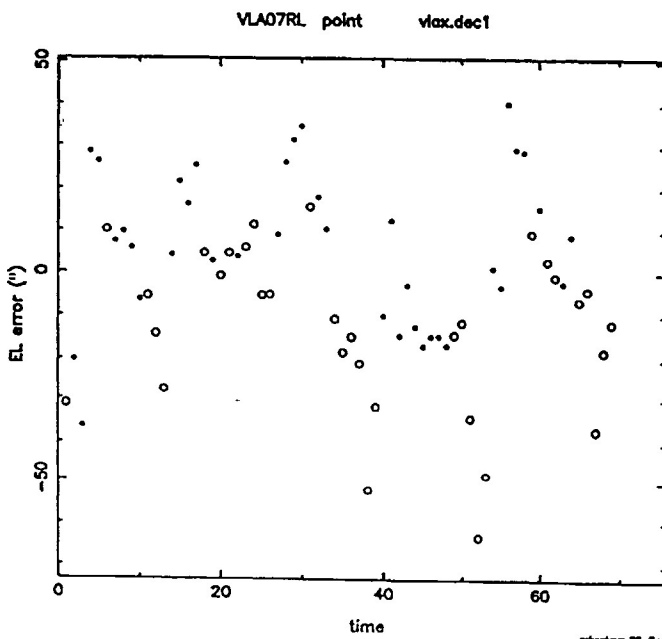
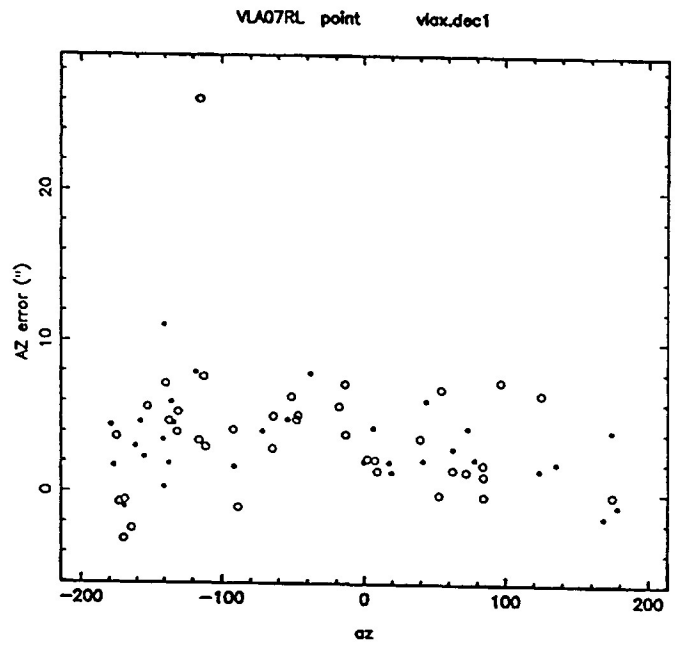
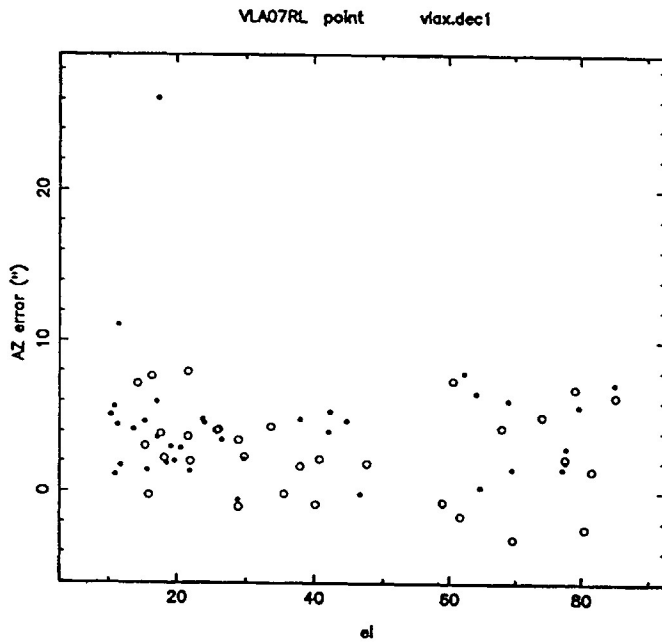
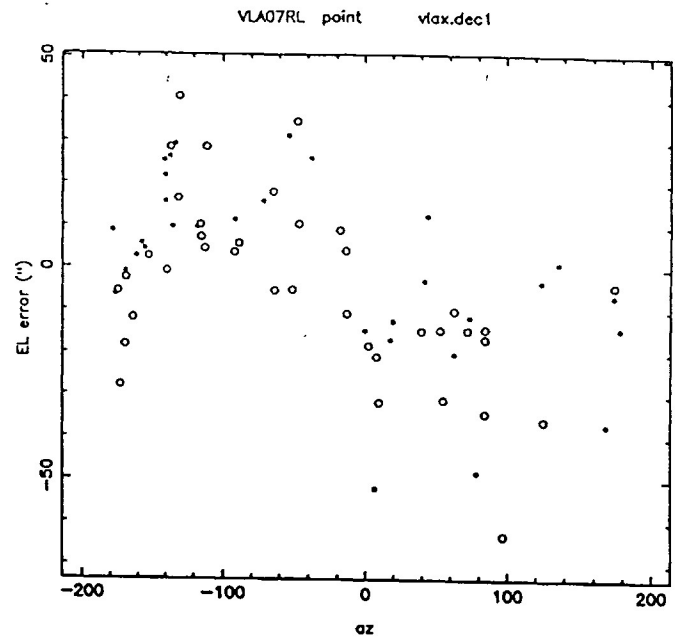
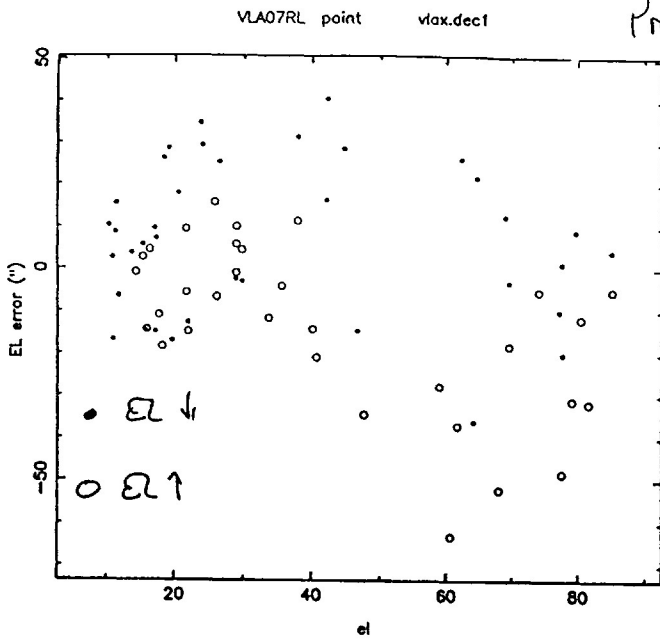
VLA01RL point vlx.dec1



time

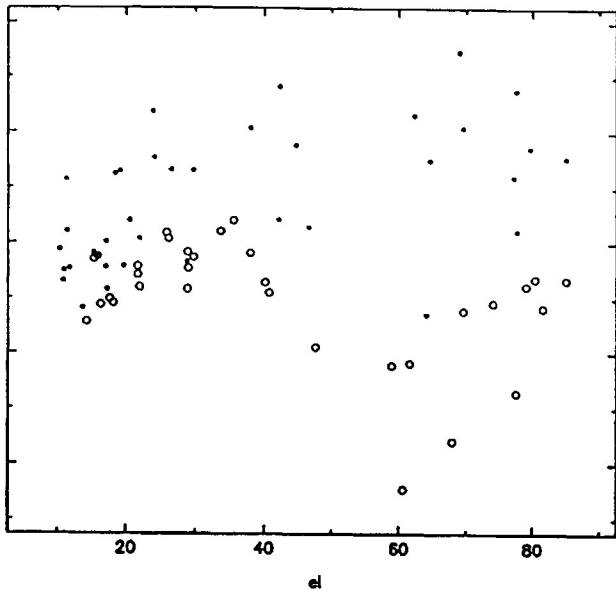
Fig 6h

Plot

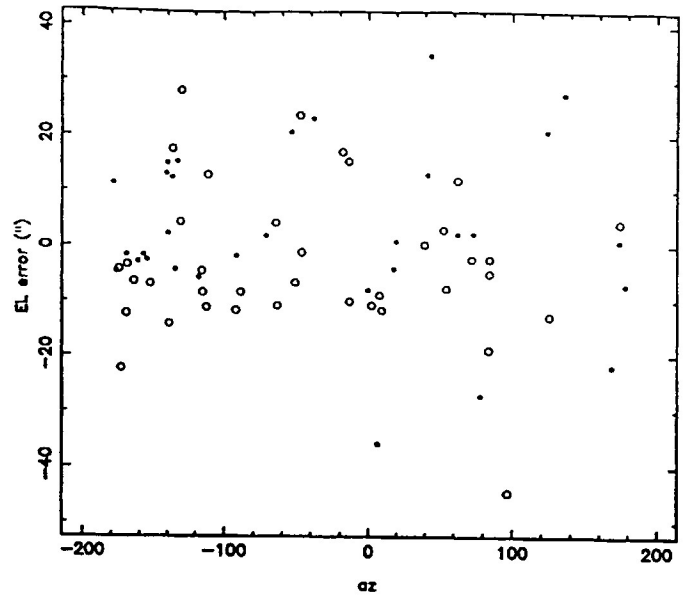


Post-fit

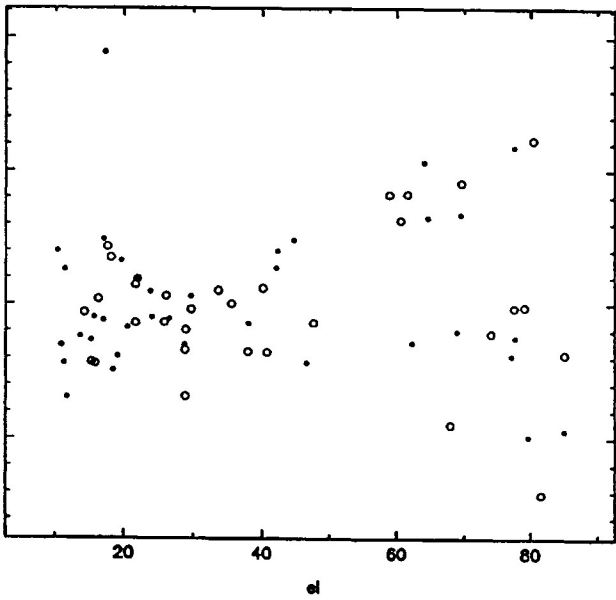
VLA07RL point vlx.dec1



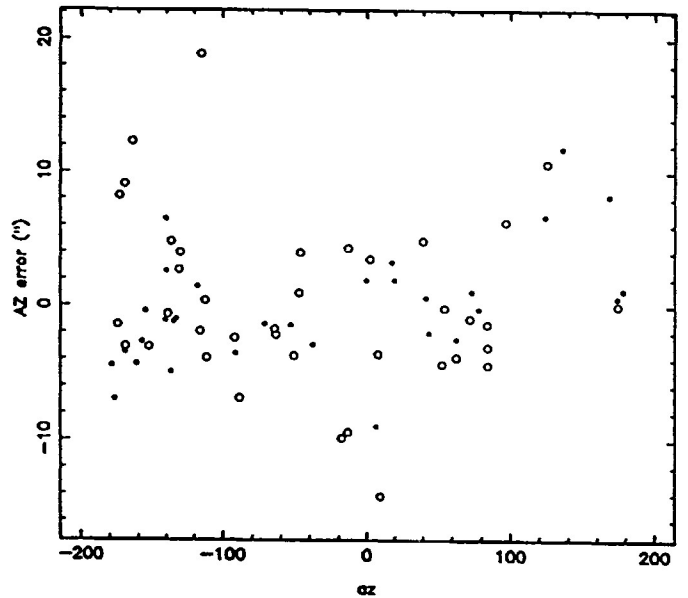
VLA07RL point vlx.dec1



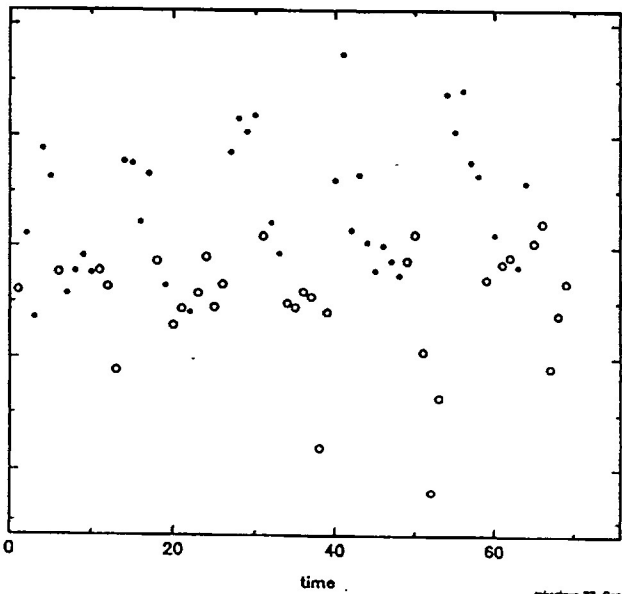
VLA07RL point vlx.dec1



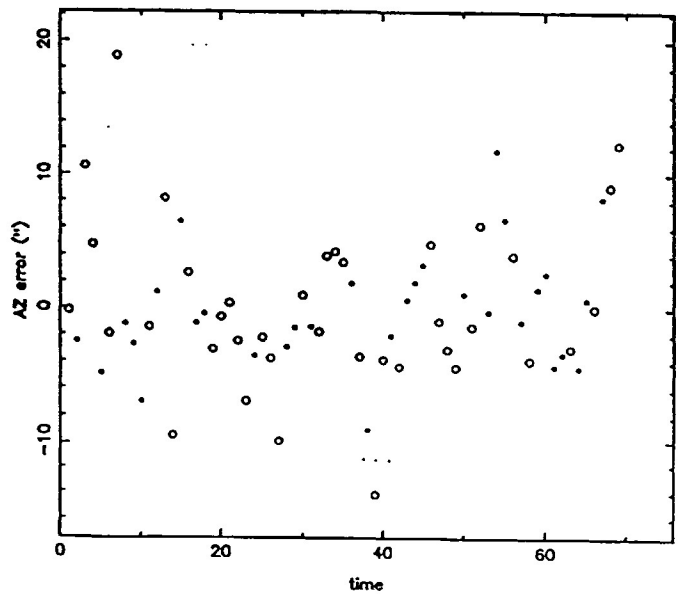
VLA07RL point vlx.dec1



VLA07RL point vlx.dec1



VLA07RL point vlx.dec1



Pre-f

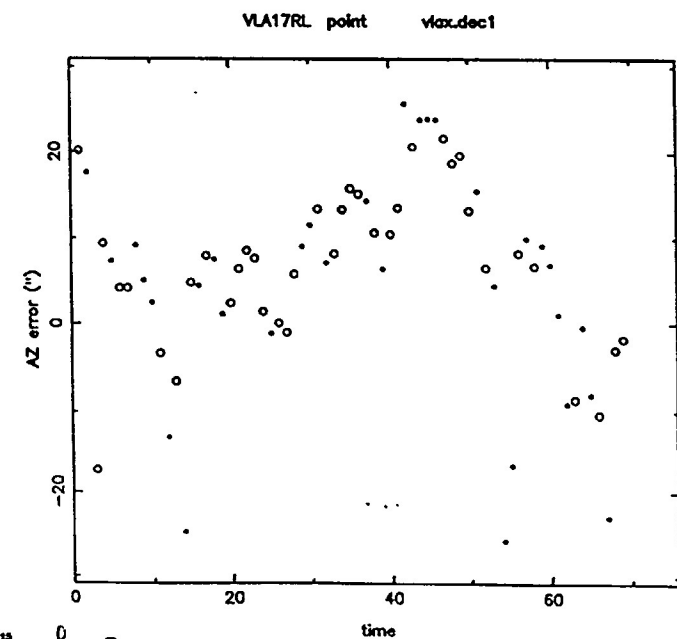
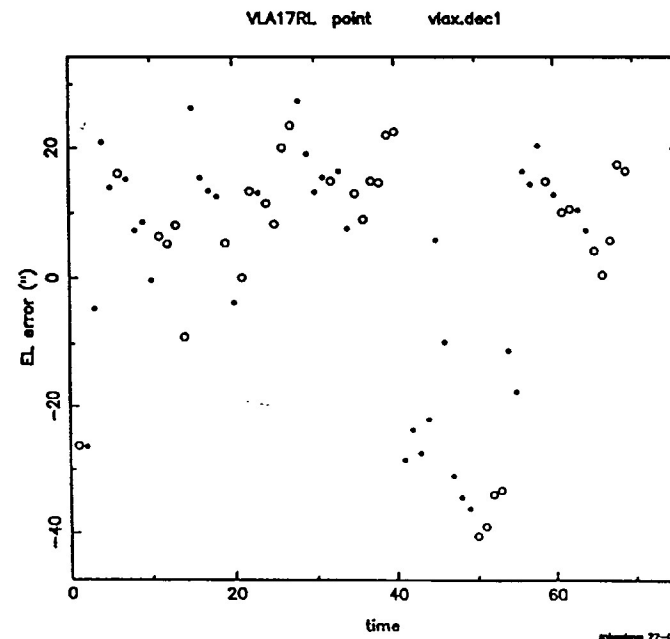
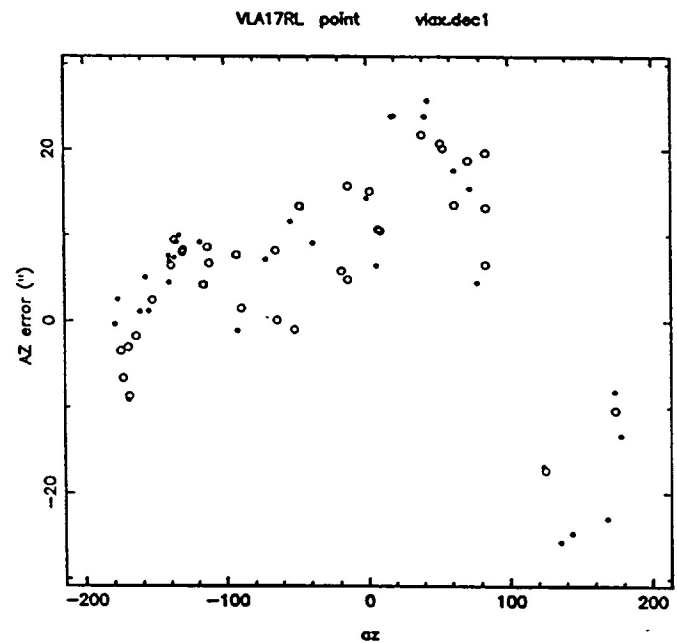
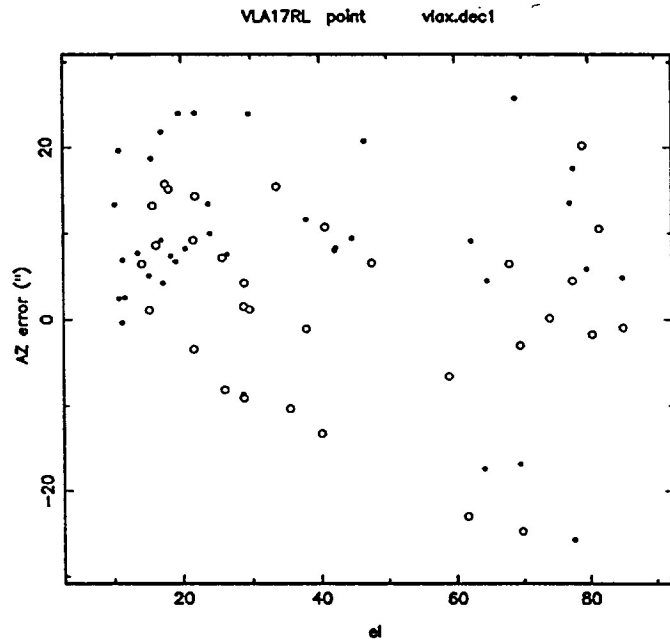
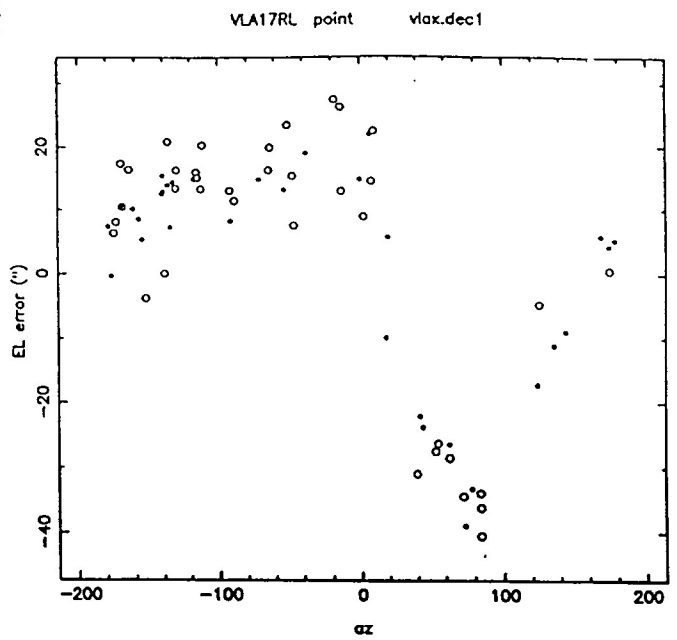
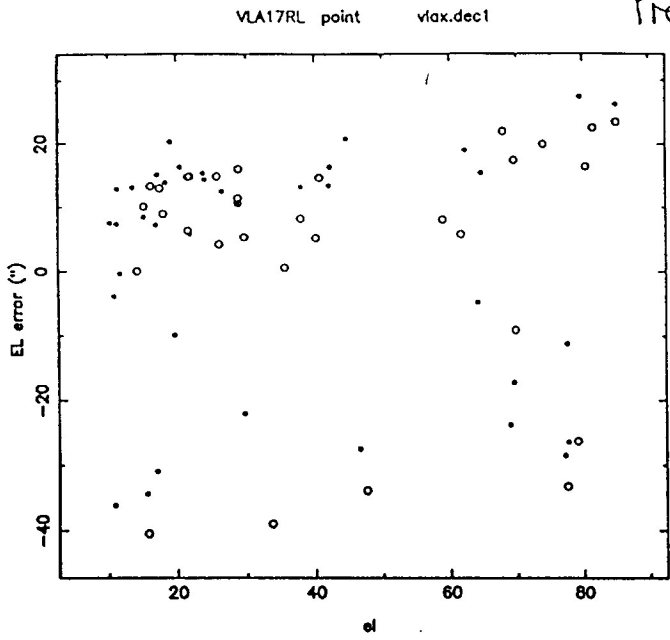
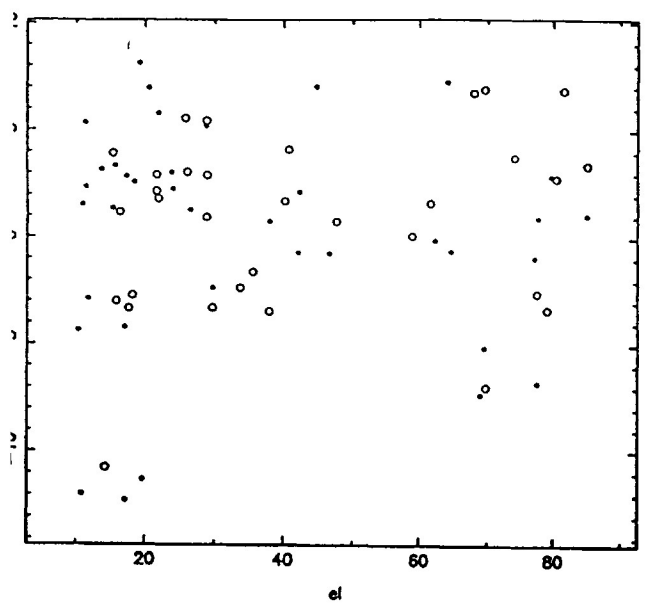


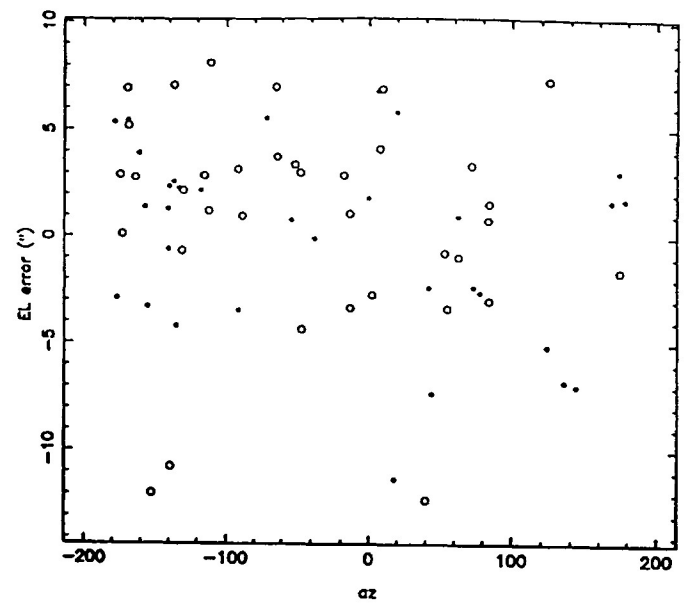
Fig 8a

*Post-Dr*

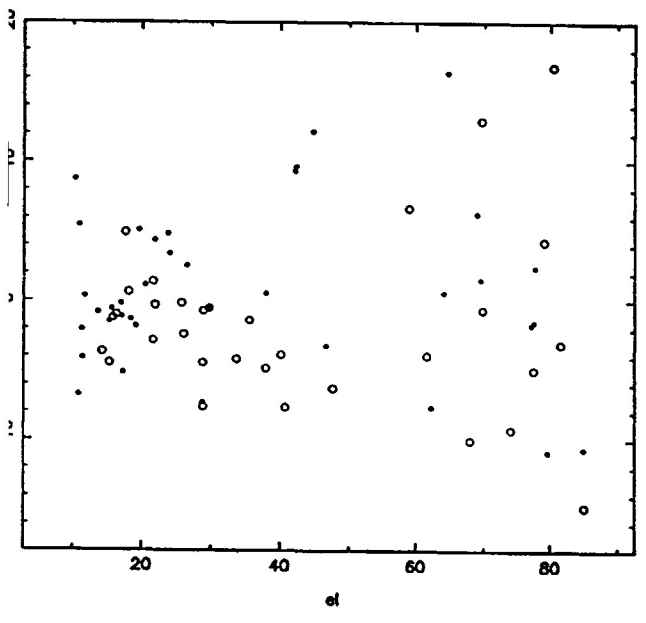
VLA17RL point vax.dec1



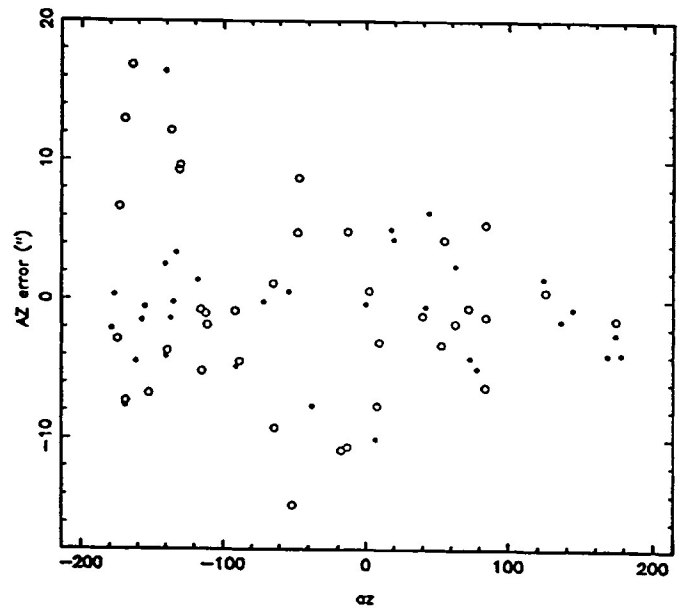
VLA17RL point vax.dec1



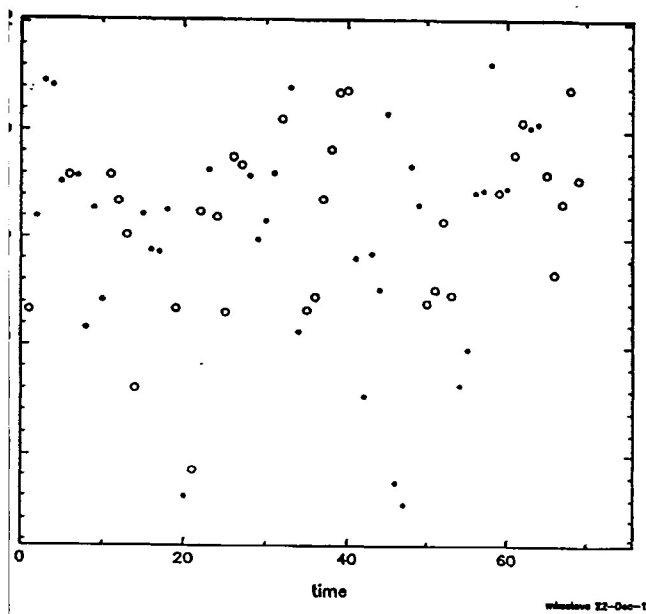
VLA17RL point vax.dec1



VLA17RL point vax.dec1



VLA17RL point vax.dec1



VLA17RL point vax.dec1

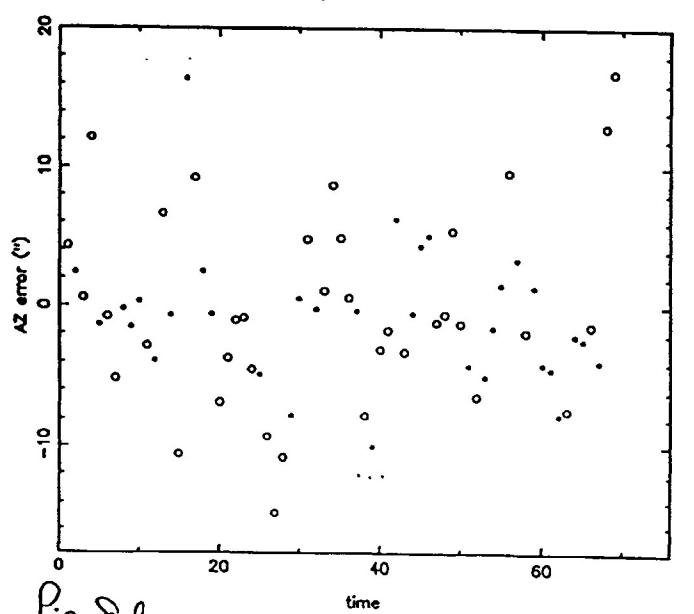
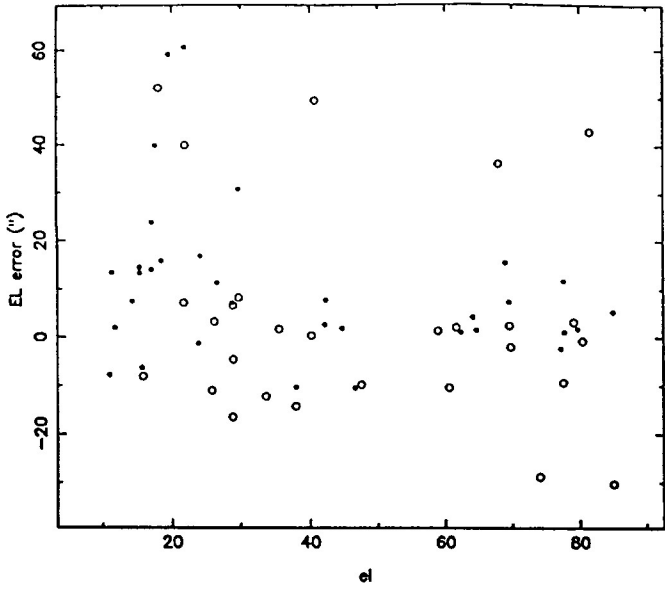


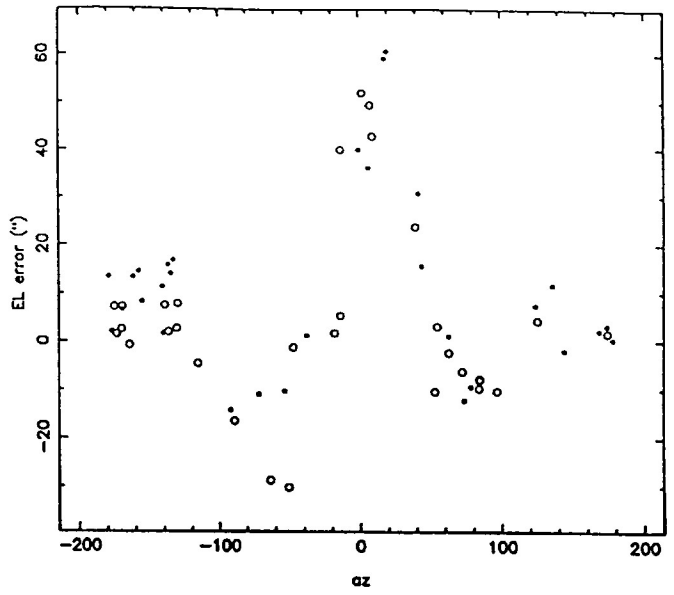
*Fig 8e*

Pre-fit

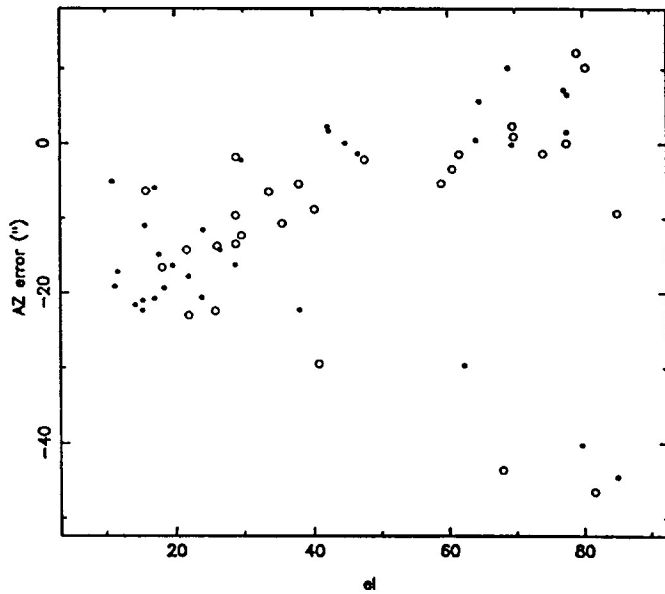
VLA23RL point v1ax.dec1



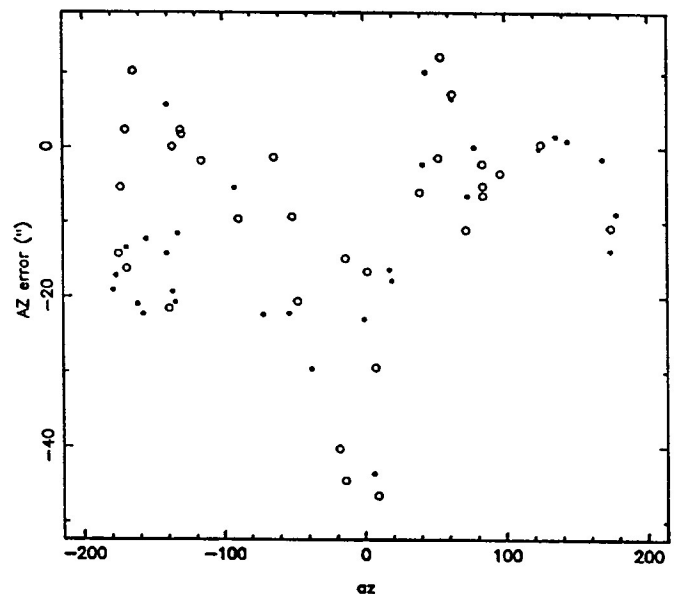
VLA23RL point v1ax.dec1



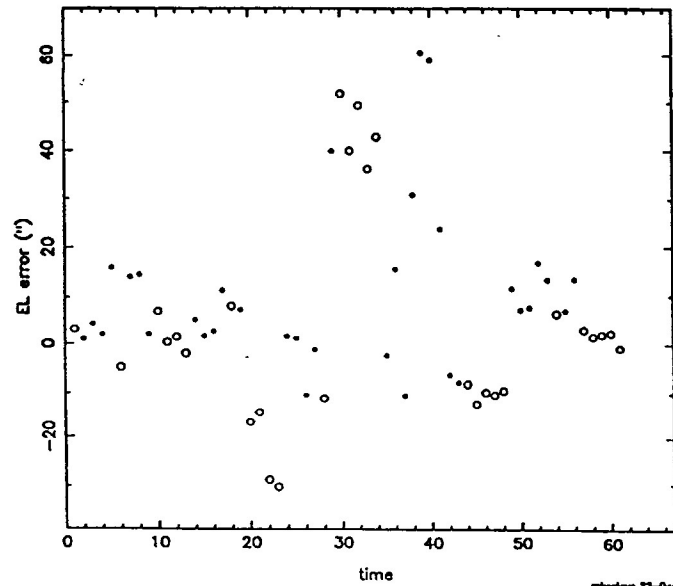
VLA23RL point v1ax.dec1



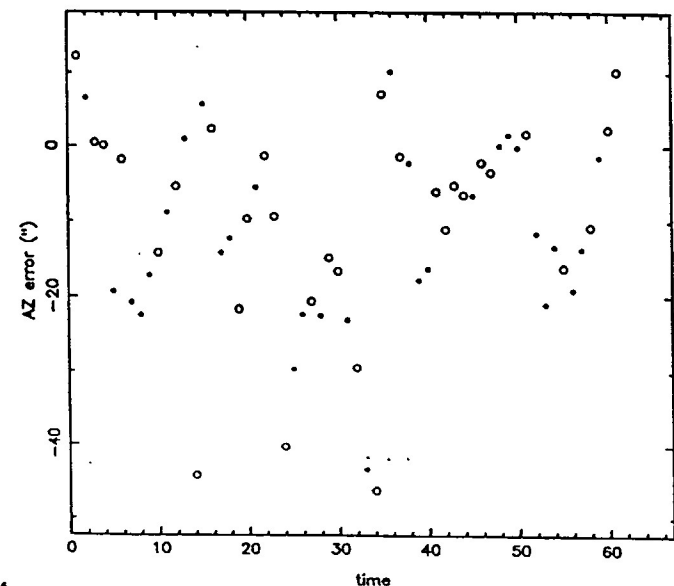
VLA23RL point v1ax.dec1



VLA23RL point v1ax.dec1



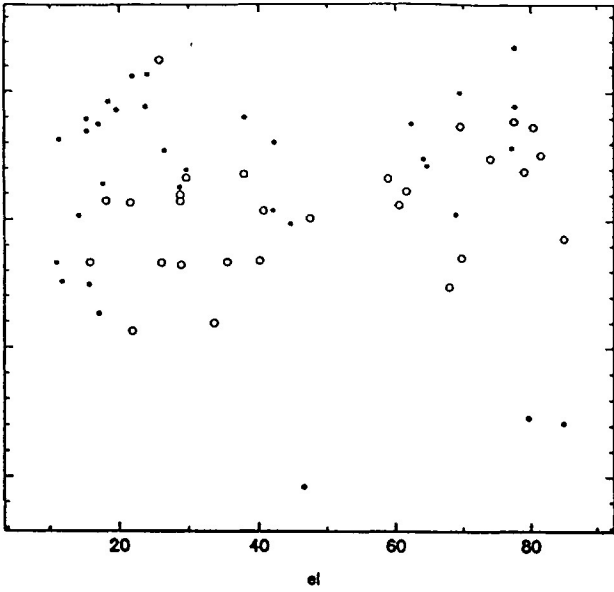
VLA23RL point v1ax.dec1



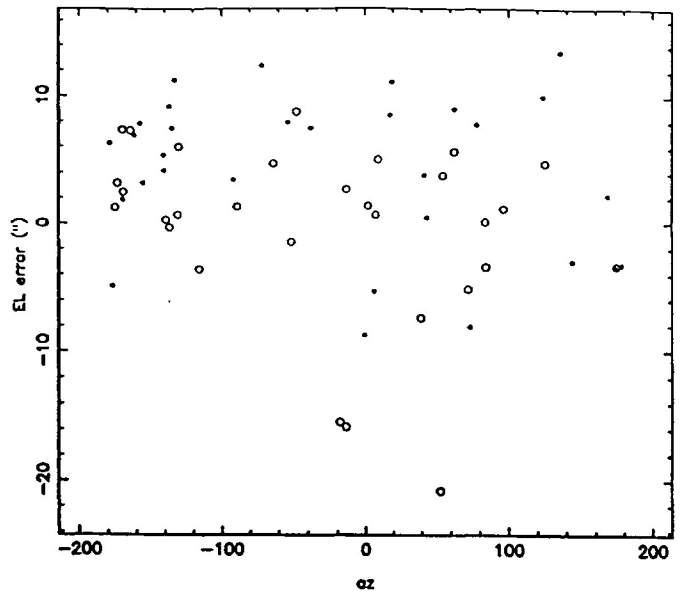
AS 9a

Post-fs

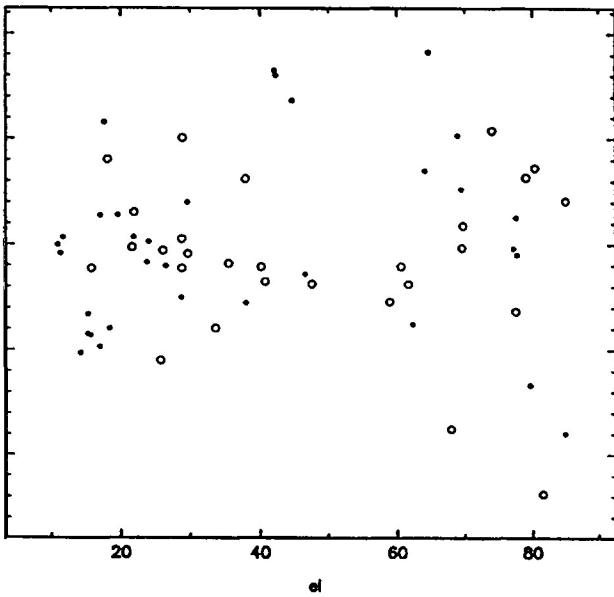
VLA23RL point vax.dec1



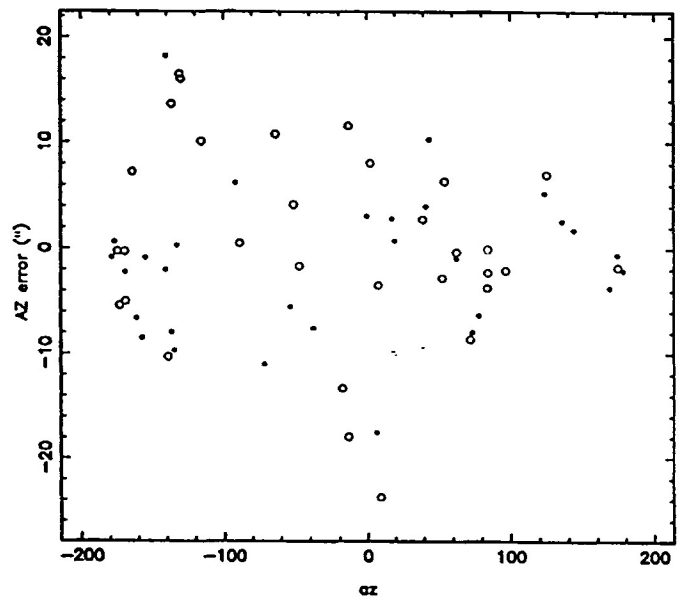
VLA23RL point vax.dec1



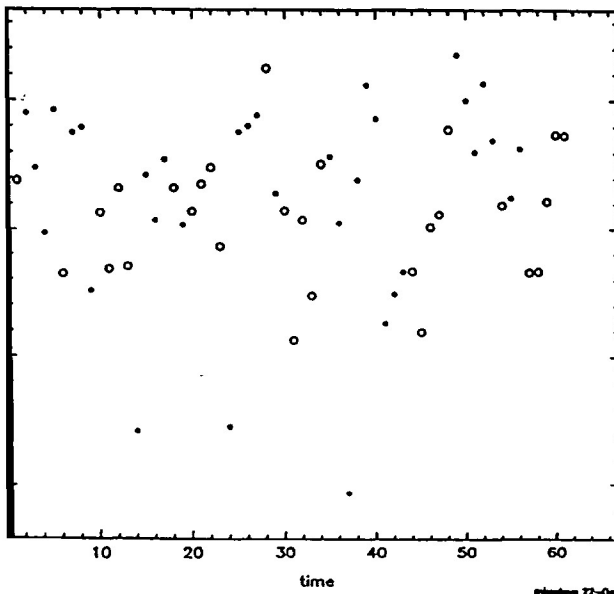
VLA23RL point vax.dec1



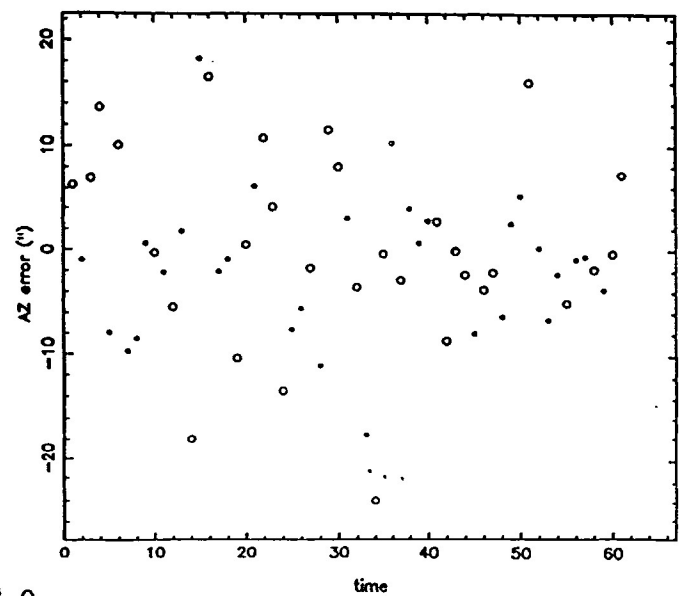
VLA23RL point vax.dec1



VLA23RL point vax.dec1

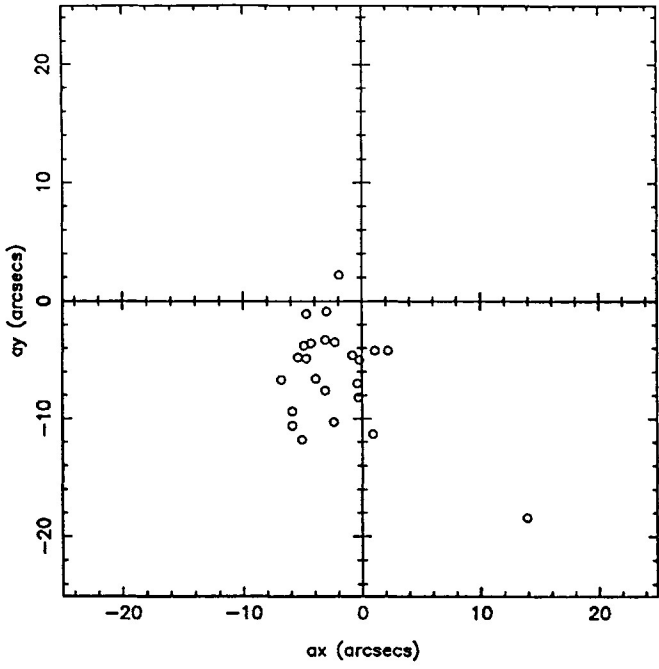


VLA23RL point vax.dec1

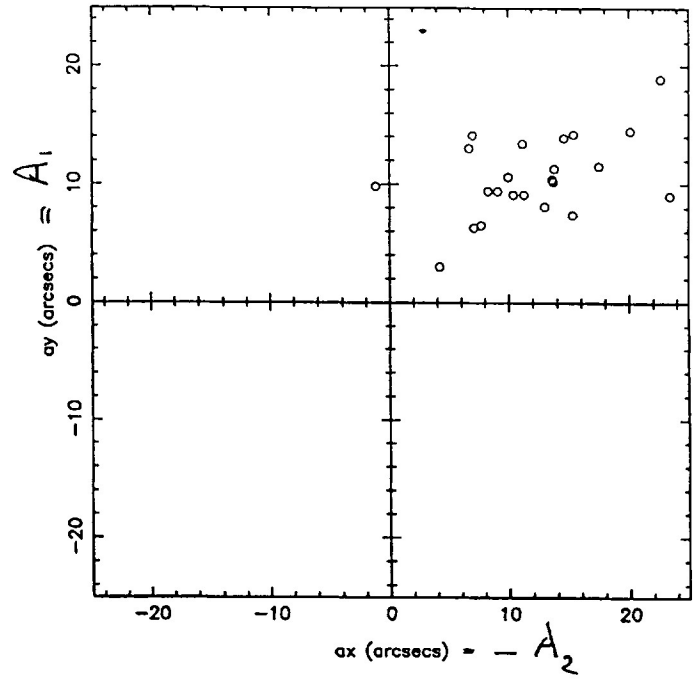


fs 7h

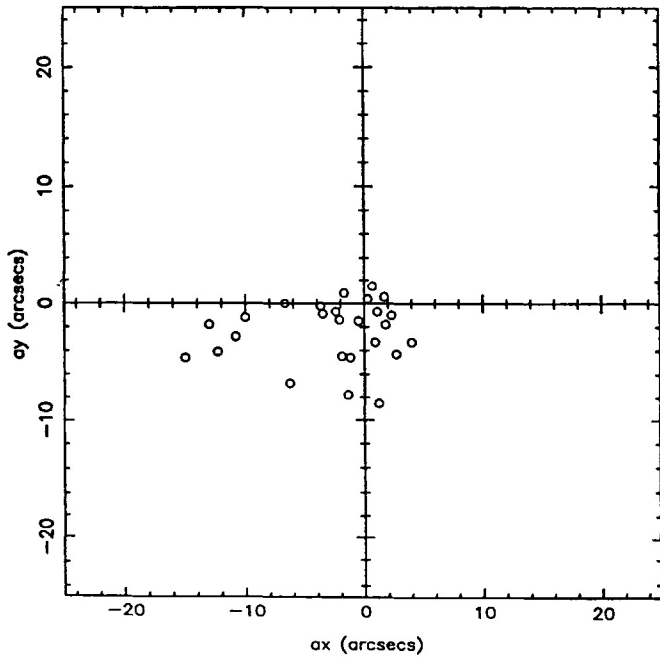
file : vlax.apr17.92



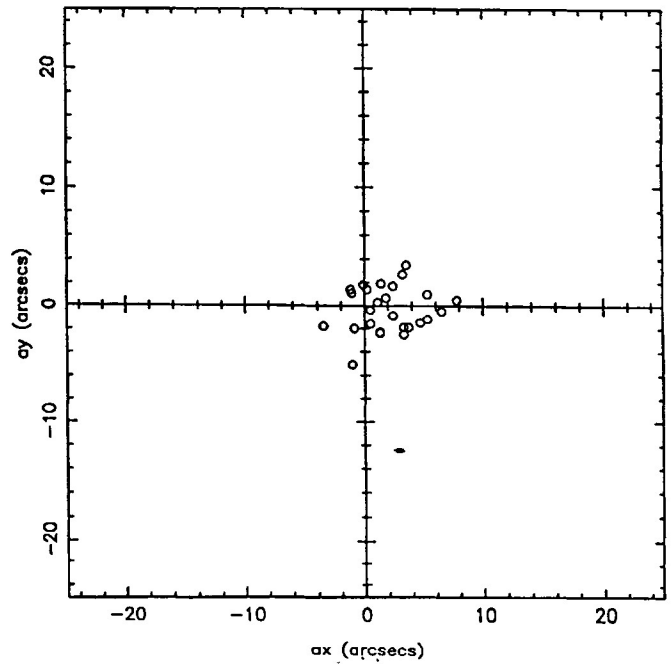
file : vlax.feb20.93



file : vlax.jun29.93

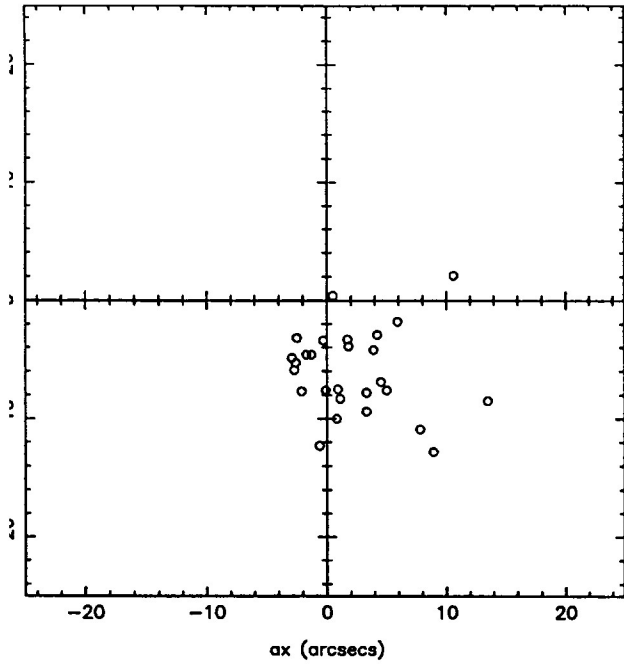


file : vlax.jul21.93

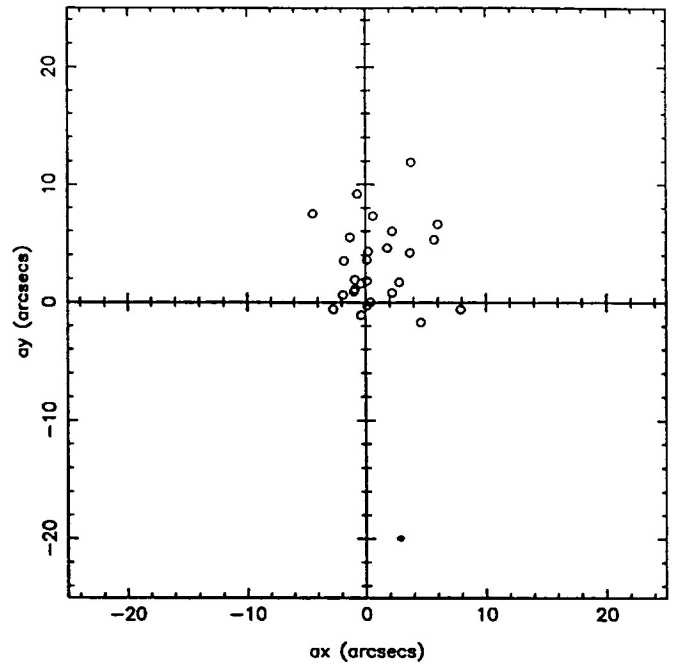




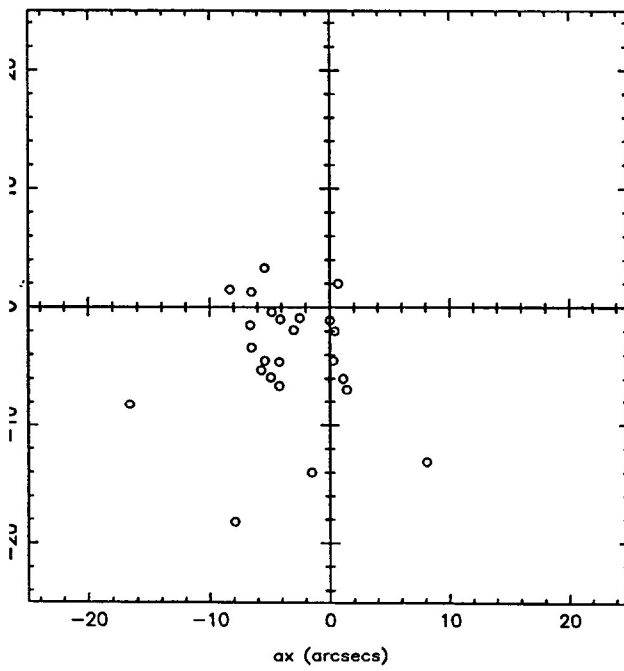
file : vlax.sep11.93



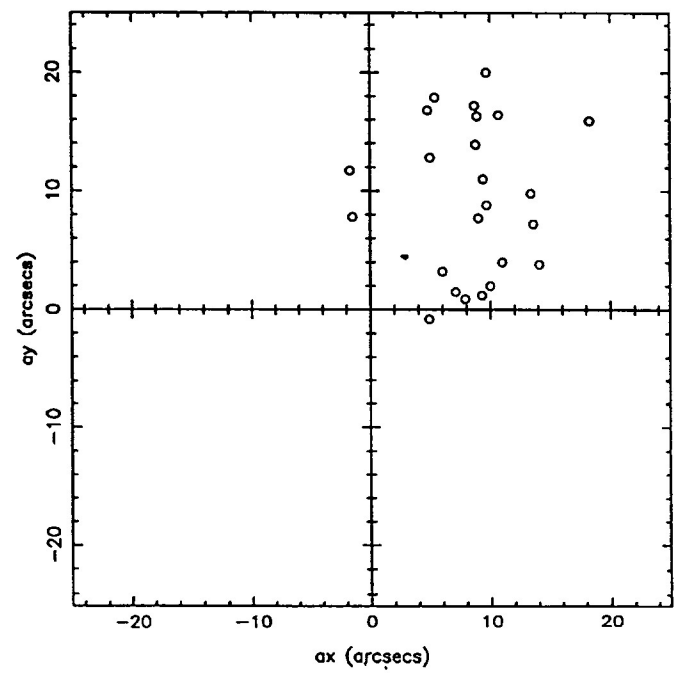
file : vlax.sep29.93



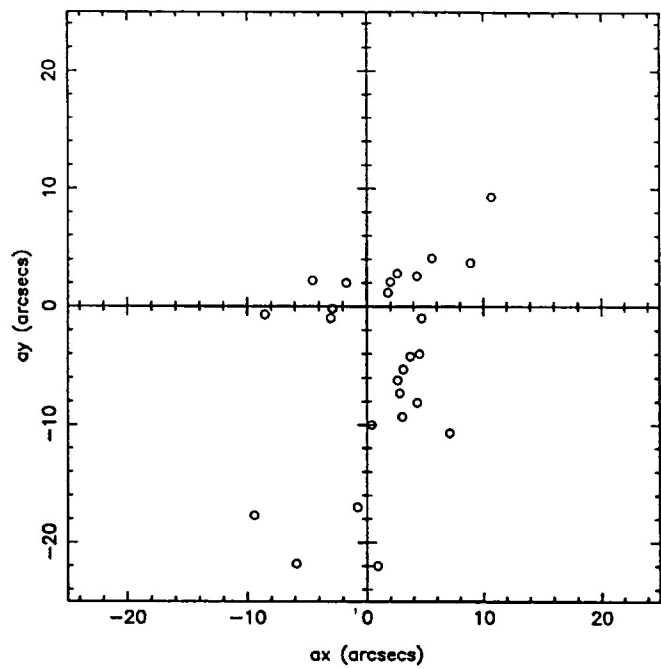
file : vlax.oct30.93



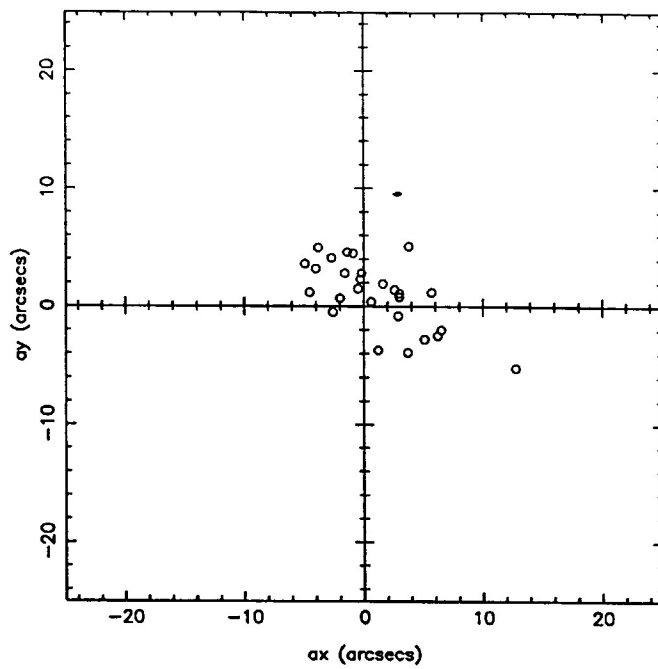
file : vlax.nov14.93



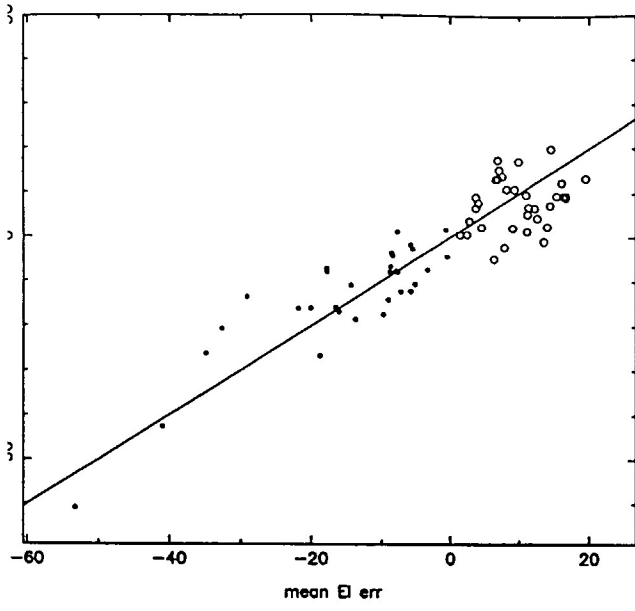
file : vlax.dec1.93



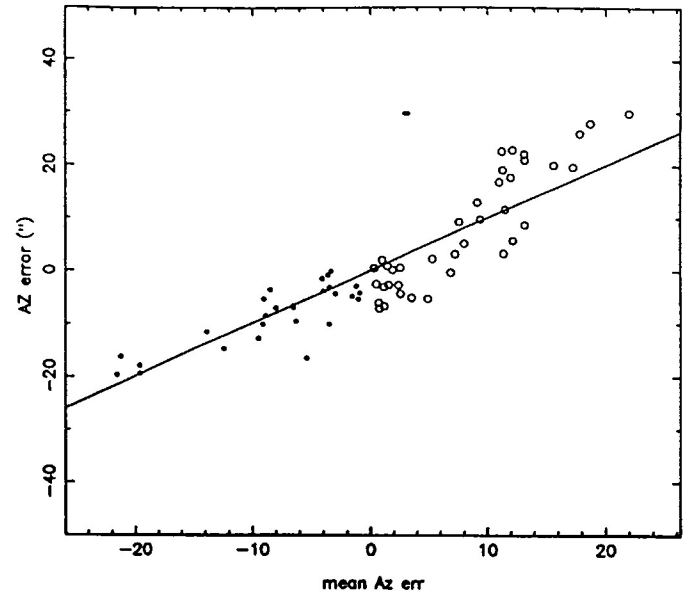
file : vlax.dec29.93



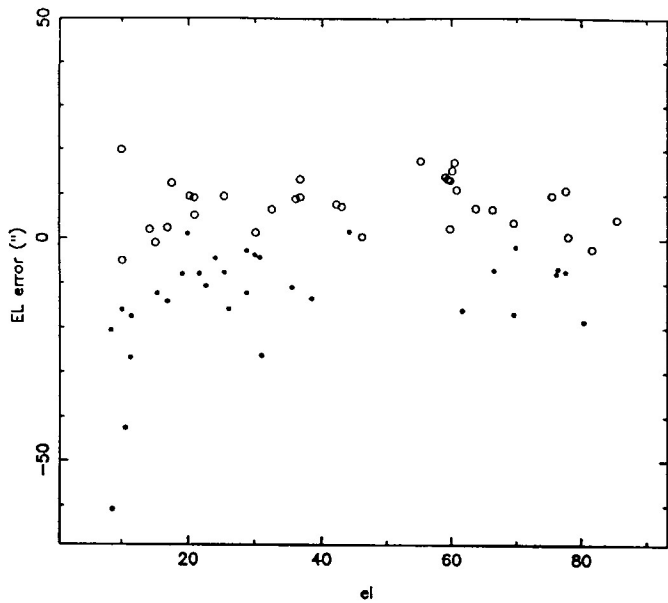
VLA04RL point vlx.feb20.93



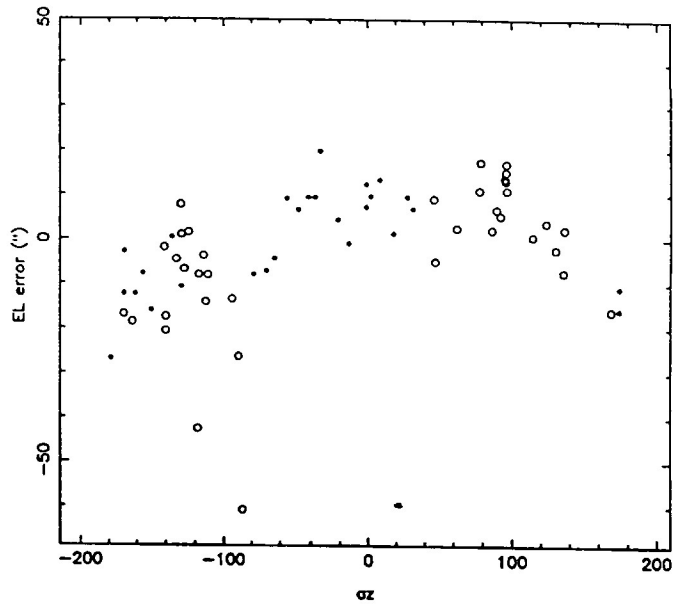
VLA04RL point vlx.feb20.93



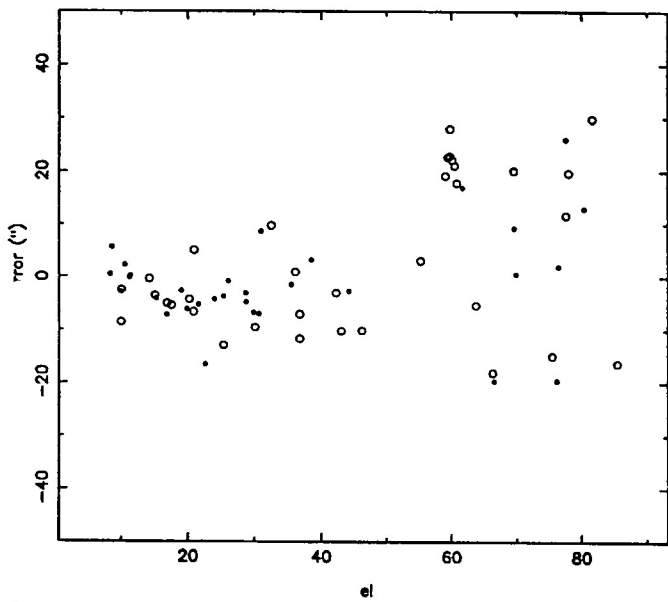
VLA04RL point v1ax.feb20.93



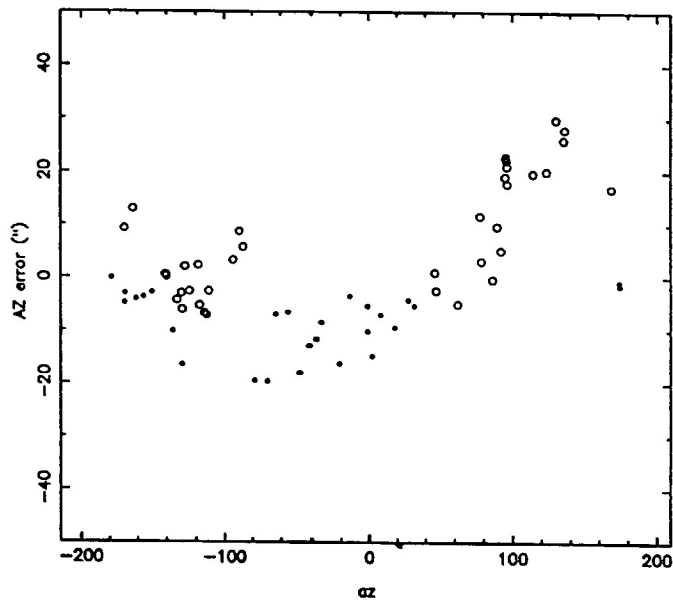
VLA04RL point v1ax.feb20.93



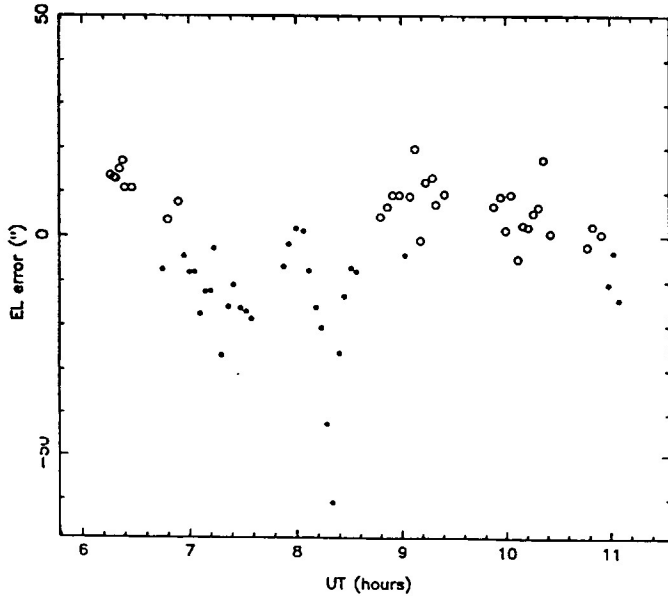
VLA04RL point v1ax.feb20.93



VLA04RL point v1ax.feb20.93



VLA04RL point v1ax.feb20.93



VLA04RL point v1ax.feb20.93

